

**DETERMINATION OF HEAT CAPACITIES AT CONSTANT VOLUME FROM  
EXPERIMENTAL (*P-RHO-T*) DATA**

A Thesis

by

ANDREA DEL PILAR TIBADUIZA RINCON

Submitted to the Office of Graduate and Professional Studies of  
Texas A&M University  
in partial fulfillment of the requirements for the degree of

MASTER OF SCIENCE

Chair of Committee,	Kenneth R. Hall
Co-Chair of Committee,	James C. Holste
Committee Members,	Ioannis Economou
	Maria Barrufet
Head of Department,	M. Nazmul Karim

August 2015

Major Subject: Chemical Engineering

Copyright 2015 Andrea Del Pilar Tibaduiza Rincon

## ABSTRACT

This work examines the uncertainty in the determination of the heat capacity at constant volume from experimental volumetric data. The proposed methodology uses the experimental ( $P$ - $\rho$ - $T$ ) data for a ternary mixture of methane, ethane and propane measured over a range of temperatures from 140 to 500 K at pressures up to 200 MPa. The resulting approach determines truly isochoric data and calculates isochoric densities with a maximum deviation of  $\pm 0.5$  % from the predictions of GERG 2008 EoS. Values for the first and second derivative of the pressure with respect to temperature at constant density needed for determining the caloric properties come from a fit of the ( $P$ - $\rho$ - $T$ ) data using a rational equation and also from numerical techniques. By transformation of the data, it is possible to calculate the residual and absolute heat capacities at constant volume with a maximum uncertainty of 1.5% that results from comparing the differences in the predictions using analytical and numerical approaches, which reflects the uncertainty of the experimental ( $P$ - $\rho$ - $T$ ) data.

## **DEDICATION**

Armando, Esther, Camilo, Jackeline

and

Our Families

## ACKNOWLEDGMENTS

I hereby want to thank Dr. Kenneth R. Hall for his guidance and advice on this research project. He honored me with the opportunity to join the Thermodynamics Research Group in College Station, TX and this opened to door to develop my professional path to obtain my Master Degree at Texas A&M University. I appreciate his patience and understanding during the challenging times, especially during the transition to Doha, Qatar. I am grateful to Dr. Hall for financially supporting me for the last four years and for his support both professional and personal.

I would like to thank Dr. James Holste for his invaluable contributions and rigorous scientific knowledge that enhanced the accuracy and applicability of this research project. Dr. Holste was my supervisor during the experimental stage of this work and other projects with the oil and gas industry developed in the Thermodynamics Research Group in College Station, TX. I would like to gratefully acknowledge my advisory committee members, Dr. Ioannis Economou and Dr. Maria Barrufet for their time, advices and suggestions.

I had one of the most fruitful time in College Station, TX thanks to my colleagues in our research group. I appreciate the help I received from Dr. Diego Cristancho and Dr. Ivan Mantilla during the early stages of my lab experience. I feel very lucky to continue my professional development working hand by hand in challenging projects with Mr. Martin Gomez and Mr. Robert Browne in the same research group. I would like to thank them for their cooperation, time and friendship.

I would like to acknowledge the guidance and support received from the faculty members and administrative staff of Texas A&M University at Qatar. Special thanks to Dr. Ioannis Economou, professor of the Chemical Engineering Department who besides to integrate my Committee of graduation was a fundamental support in my professional and personal decisions. I am very blessed and happy to have discovered and experienced the Middle East culture and the friendship found in Qatar. I also want to acknowledge Qatar Foundation for the financial support throughout my Master program.

Above all, I am very indebted and grateful to my parents Armando Tibaduiza and Esther Rincon for their unconditional love, support and understanding. I send thanks to my whole family and friends in Colombia and to my brother and sister, Camilo and Jackeline, they are my driving force and my motivation to continue learning and growing every day.

## NOMENCLATURE

$n$	Total number of moles (mol)
$\rho$	Density (kg/m <sup>3</sup> )
$V$	Volume (m <sup>3</sup> )
$T$	Temperature (K)
$P$	Pressure (MPa)
$C_P$	Heat capacity at constant pressure (kJ/kmol)
$C_V$	Heat capacity at constant volume (kJ/kmol)
$R$	Universal gas constant: 8.3144621 (kJ/kmol-K)
$U$	Uncertainty (%)
$k$	Ratio of heat capacities

### *Superscripts*

*	Reference condition
°	Calibration condition
'	True isochore condition
<i>ig</i>	Ideal gas state
<i>r</i>	Residual property

### ***Subscripts***

<i>c</i>	Cell
<i>l</i>	Transmission line
<i>t</i>	Pressure Transducer

### ***Greek letters***

$\alpha$	Thermal expansion coefficient ( $K^{-1}$ )
$\beta$	Isothermal compressibility coefficient ( $MPa^{-1}$ )

### ***Abbreviations***

MSD	Magnetic Suspension Densimeter
LPI	Low Pressure Isochoric Apparatus
HPI	High Pressure Isochoric Apparatus
EoS	Equation of State
Eq	Equation
OD	External Diameter
ID	Internal Diameter
PT30K	30,000 psi Range Pressure Transducer
Cu-Be	Beryllium Cooper 175 Alloy
Iso	Isochore
Rms	Root mean square

## TABLE OF CONTENTS

	Page
ABSTRACT .....	ii
DEDICATION .....	iii
ACKNOWLEDGMENTS.....	iv
NOMENCLATURE.....	vi
TABLE OF CONTENTS .....	viii
LIST OF FIGURES.....	x
LIST OF TABLES .....	xiii
1. INTRODUCTION.....	1
1.1 Economic Impact of Natural Gas .....	1
1.2. Literature Review of Calorimetric Measurements .....	5
1.2.1 Adiabatic Calorimeter for Heat Capacities Measurements <sup>16</sup> .....	6
1.2.2 Flow Calorimeters for Constant Pressure Heat Capacities Measurements .....	7
1.2.3 Caloric Properties for Natural Gas Mixtures <sup>12</sup> .....	8
1.3 Research Proposal and Objectives of the Study.....	9
2. EXPERIMENTAL CHARACTERIZATION OF NATURAL GAS MIXTURES .....	11
2.1 Magnetic Suspension Densimeter (MSD) <sup>8,9</sup> .....	11
2.2 Low and High Pressure Isochoric Apparatus <sup>6,9,30</sup> .....	14
3. HEAT CAPACITIES FROM EXPERIMENTAL ( <i>P-RHO-T</i> ) DATA.....	17
3.1 Stage 1. Experimental Data Acquisition .....	17
3.2 Stage 2. Isochoric Corrections .....	20
3.2.1 Definition of Reference State .....	21
3.2.2 Isochoric Density Determination.....	23
3.2.3 True Isochores Determination .....	35
3.3 Stage 3. Derivative Determination .....	37
3.4 Stage 4. Residual and Absolute Properties .....	55
3.5 Stage 5. Uncertainty Analysis .....	64



4. CONCLUSIONS .....	71
REFERENCES .....	75
APPENDIX A. EXPERIMENTAL ISOTHERMAL AND ISOCHORIC DATA .....	79
APPENDIX B. ISOCHORIC DENSITY AND TRULY ISOCHORIC DATA .....	89
APPENDIX C. REGRESSION RESULTS OF FIT P VS T.....	96
APPENDIX D. FIRST AND SECOND DERIVATIVES .....	97
APPENDIX E. EXPRESSION OF RESIDUAL HEAT CAPACITY .....	104
APPENDIX F. REGRESSION RESULTS OF INTEGRAND FUNCTION .....	106
APPENDIX G. IDEAL GAS HEAT CAPACITY DIPPR PROJECT .....	110
APPENDIX H. RESIDUAL AND ABSOLUTE HEAT CAPACITY .....	111
APPENDIX I. INTEGRAND FUNCTION OF NUMERICAL DERIVATIVES .....	118
APPENDIX J. MATLAB CODE.....	120

## LIST OF FIGURES

	Page
Figure 1. Distribution in consumption of natural gas in U.S. 2013 <sup>2</sup> .....	2
Figure 2. Gas demand in American market <sup>3</sup> .....	3
Figure 3. US generation from coal, gas-fired plants and renewable energies <sup>3</sup> .....	3
Figure 4. (a) Basic scheme for the MSD <sup>25</sup> (b) Operating modes of the MSD <sup>25</sup> .....	12
Figure 5. Schematic diagram of the isochoric experiment <sup>30</sup> .....	14
Figure 6. Isochoric cell cut view for the high pressure equipment <sup>6</sup> .....	15
Figure 7. Methodology to determine ( $C_v$ ) from experimental ( $P$ - $\rho$ - $T$ ) data .....	17
Figure 8. Experimental data of residual gas sample.....	19
Figure 9. Noxious volume in isochoric apparatus.....	20
Figure 10. Percentage deviation of density values from MSD.....	22
Figure 11. Per cent deviation of isochoric densities in the LPI.....	29
Figure 12 Layout of high pressure isochoric cell .....	32
Figure 13. Percentage of deviation of isochoric densities from HPI.....	34
Figure 14. True isochores diagram.....	36
Figure 15. Strategy to calculate numerical and analytical derivatives .....	37
Figure 16 Residuals in pressure for isochores 1 to 3 using Eq. 25 .....	42
Figure 17 Residuals in pressure for isochores 1 to 3 using Eq. 30 .....	42
Figure 18 Residuals in pressure for isochores 4 and 5 using Eq. 25.....	43
Figure 19 Residuals in pressure for isochores 4 and 5 using Eq. 30.....	43
Figure 20 Residuals in pressure for isochores 6 to 10 using Eq. 25 .....	44

Figure 21 Residuals in pressure for isochores 6 to 10 using Eq. 30 .....	44
Figure 22 First derivative for isochore 1 .....	45
Figure 23 Second derivative for isochore 1 .....	45
Figure 24 First derivative for isochore 2 .....	46
Figure 25 Second derivative for isochore 2 .....	46
Figure 26 First derivative for isochore 3 .....	47
Figure 27 Second derivative for isochore 3 .....	47
Figure 28 First derivative for isochore 4 .....	48
Figure 29 Second derivative for isochore 4 .....	48
Figure 30 First derivative for isochore 5 .....	49
Figure 31 Second derivative for isochore 5 .....	49
Figure 32 First derivative for isochore 6 .....	50
Figure 33 Second derivative for isochore 6 .....	50
Figure 34 First derivative for isochore 7 .....	51
Figure 35 Second derivative for isochore 7 .....	51
Figure 36 First derivative for isochore 8 .....	52
Figure 37 Second derivative for isochore 8 .....	52
Figure 38 First derivative for isochore 9 .....	53
Figure 39 Second derivative for isochore 9 .....	53
Figure 40 First derivative for isochore 10 .....	54
Figure 41 Second derivative for isochore 10 .....	54
Figure 42. Integrand function of $(C_v^r)$ equation for subset 1 .....	57
Figure 43. Integrand function of $(C_v^r)$ equation for subset 2 .....	57
Figure 44. Integrand function of $(C_v^r)$ equation for subset 3 .....	58

Figure 45. ( $C_v'$ ) for subset 1. (220 – 300 K).....	59
Figure 46. ( $C_v'$ ) for subset 2. (310 – 390 K).....	59
Figure 47. ( $C_v'$ ) for subset 3. (400 – 450 K).....	60
Figure 48. ( $C_v$ ) for subset 1. Temperatures 220 – 300 K .....	63
Figure 49. ( $C_v$ ) for subset 2. Temperatures 310 – 390 K .....	63
Figure 50. ( $C_v$ ) for subset 3. Temperatures 400 – 450 K .....	64
Figure 51. Integrand function of Eq. 34 using numerical derivatives.....	65
Figure 52. Integrand function of Eq. 34 using analytical derivatives .....	66
Figure 53. Integrand function predicted. T = 280 K .....	67
Figure 54. Percentage of residual heat capacity .....	70
Figure 55. Integrand function of Eq. 34 for subset 1 using numerical derivatives .....	118
Figure 56. Integrand function of Eq. 34 for subset 2 using numerical derivatives .....	118
Figure 57. Integrand function of Eq. 34 for subset 3 using numerical derivatives .....	119

## LIST OF TABLES

	Page
Table 1. Natural gas demand 2010 - 2018 (bcm) <sup>3</sup> .....	2
Table 2. Relative uncertainty in ( $C_v$ ) experimental values for mixtures and pure fluids measured with adiabatic calorimeter <sup>16</sup> .....	7
Table 3. MSD specifications .....	13
Table 4. Experimental measurements of density taken in the MSD of TAMU .....	13
Table 5. Low pressure apparatus (LPI) specifications <sup>30</sup> .....	16
Table 6. High pressure apparatus (HPI) specifications <sup>6</sup> .....	16
Table 7. Experimental measurements taken in the LPI of TAMU.....	16
Table 8. ( $P$ - $\rho$ - $T$ ) reference values for each isochore. EoS values from GERG-2008 .....	23
Table 9. Thermal expansion and isothermal compressibility coefficients .....	25
Table 10. Volumes for LPI.....	26
Table 11. LPI values to calculate distortion parameters for stainless steel.....	27
Table 12. Parameters for stainless steel .....	28
Table 13 Lengths for noxious volume estimation in the HPI.....	30
Table 14 Technical specifications for high pressure cross and valve in the HIP .....	30
Table 15 Volumes for HPI .....	31
Table 16. HPI values to calculate distortion parameters for Cu-Be.....	33
Table 17. Parameters for Cu-Be .....	33
Table 18. Pseudo points in the isochoric experiment.....	38
Table 19. Outliers in the isochoric experiment .....	39
Table 20. Subset of temperatures for integral of residual heat capacity .....	56

Table 21. Ideal gas heat capacities at constant volume.....	62
Table 22. Regression results using numerical derivatives. T = 280 K.....	65
Table 23. Regression results using analytical derivatives. T = 280 K .....	66
Table 24. Residual heat capacity at T = 280 K from numerical derivatives .....	68
Table 25. Residual heat capacity at T = 280 K from analytical derivatives .....	68
Table 26. Absolute heat capacity and global uncertainty at T = 280K .....	69
Table 27. MSD measurements and compared to values predicted by GERG 2008.....	79
Table 28. High pressure isochoric apparatus measurements. EoS: GERG 2008 .....	82
Table 29. Low pressure isochoric apparatus measurements. EoS: GERG 2008.....	85
Table 30. Isochoric density and ( $P$ '- $\rho$ *- $T$ ) data .....	89
Table 31. Coefficients, standard error, rms and number of points per isochore (n) for regression analysis using Eq. 30.....	96
Table 32. First and second derivatives for set 1 .....	97
Table 33. First and second derivatives for set 2 .....	100
Table 34. First and second derivatives for set 3 .....	102
Table 35. Regression results of Eq. 35 for set 1 .....	106
Table 36. Regression results of Eq. 35 for set 2.....	107
Table 37. Regression results of Eq. 35 for set 3.....	109
Table 38. Parameters for Eq. 49 .....	110
Table 39. Residual and absolute heat capacity for set 1.....	111
Table 40. Residual and absolute heat capacity for set 2.....	114
Table 41. Residual and absolute heat capacity for set 3.....	116

## 1. INTRODUCTION

### 1.1 Economic Impact of Natural Gas

Natural gas is a mixture of several hydrocarbons, its composition depends upon the source and it is considered as the greenest fossil fuel. Natural gases can be classified as: “wet” when they include significant amount of hydrocarbons other than methane such as: ethane, propane, butane and pentane; “dry” when the composition is almost pure methane, and “sour” when it contains significant amount of hydrogen sulfide<sup>1</sup>. Natural gas is a major energy source in the United States with consumption of 740 billion cubic meters (bcm)<sup>2</sup> and a global demand estimated at 3,500 bcm<sup>1</sup> in 2013, up 1.2% from 2012 levels.

The global demand for natural gases depends upon the interactions among fuel supply and all the sectors in the custody chain of transfer, geopolitical and governmental policies, market forces, and companies’ decisions and investments. These factors play a role in determining the availability and competitiveness of natural gas in traditional sectors and its expansion into new ones. The forecast for global gas demand is 3,962 bcm in 2018 as it is shown in Table 1<sup>3</sup>.

Natural gas is mainly a fuel used to produce steel, glass, paper, clothing, electricity and to heat buildings and water. It is also a raw material for fertilizers, plastics, antifreeze, medicines and explosives<sup>2</sup>. Figure 2 exhibits the distributions for consumption of natural gas in the U.S. in 2013.

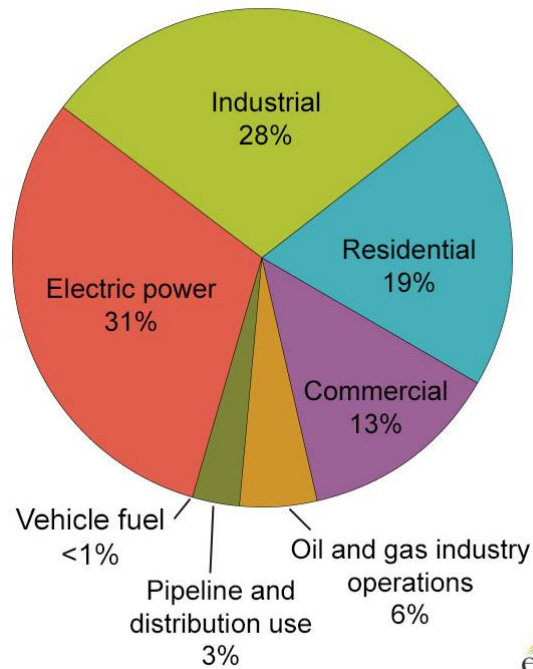
**Table 1.** Natural gas demand 2010 - 2018 (bcm)<sup>3</sup>

	2010	2012	2014	2016	2018	2018/12 (%)
Europe	567	513	506	518	525	0.4
Americas	850	893	903	942	977	1.5
Asia Oceania	198	229	238	248	261	2.2
Africa	105	113	133	146	154	5.3
Asia	283	286	299	333	360	3.9
China*	109	149	189	237	295	12.1
FSU/non-OECD Europe	681	677	688	699	709	0.8
Latin America	152	160	166	178	190	2.9
Middle East	370	407	433	458	492	3.2
<b>Total</b>	<b>3 315</b>	<b>3 427</b>	<b>3 555</b>	<b>3 759</b>	<b>3 962</b>	<b>2.4</b>

Note: detailed demand data by country and by sector are available in Tables 30 and 31 in the Chapter The Essentials.

\* China includes Hong Kong.

**Natural gas use, 2013**



Source: U.S. Energy Information Administration, *Natural Gas Annual* (October 31, 2014)

**Figure 1.** Distribution in consumption of natural gas in U.S. 2013<sup>2</sup>



Americas is the largest natural gas market with a growth rate of 1.5% per year in terms of volume. Around 53% of this growth comes from the power generation sector alone (Figure 2) in which the switch from coal to gas continues (Figure 3)<sup>3</sup>.

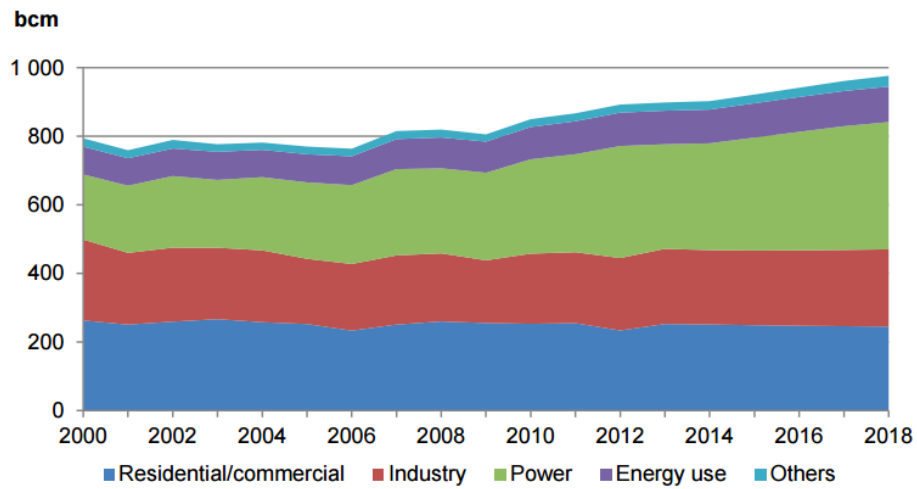


**Figure 2.** Gas demand in American market<sup>3</sup>

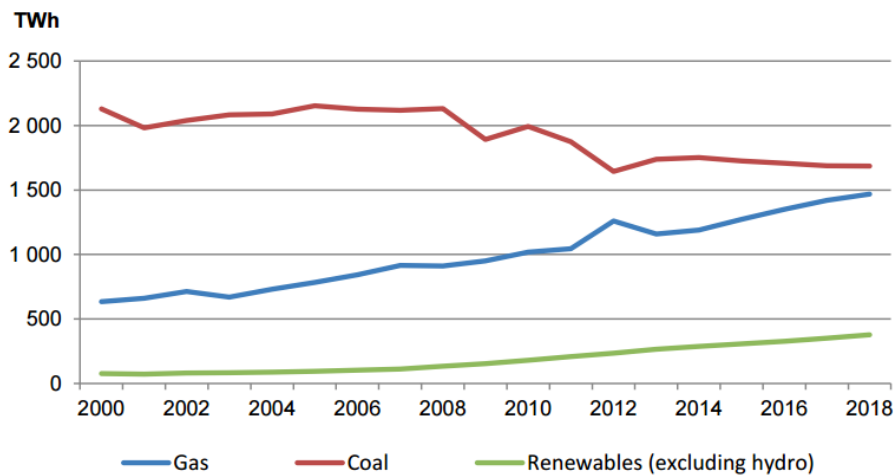


**Figure 3.** US generation from coal, gas-fired plants and renewable energies<sup>3</sup>

In terms of reserves of natural gas, the estimate is that about 190 trillion cubic meters (tcm)<sup>1</sup> of natural gas reserves exist worldwide in conventional sources<sup>4</sup> (geological formations that do not require specialized technologies to unlock their potential). However the reserves from recoverable gas sources (assuming technology becomes available to produce them) are estimated about 440 tcm<sup>1</sup>. On the other hand, estimated recoverable unconventional resources such as Shale Gas<sup>5</sup>, trapped in reservoirs with low permeability are around 240 tcm<sup>1</sup>. Altogether, this would last around 220 years, based upon current rates of gas consumption<sup>1,3</sup>.

The forecast of demand suggests that study and research of the properties of natural gas and a holistic analysis of all the factors that determine its price is crucial. When natural gas enters to the custody transfer chain, the price is calculated from<sup>6</sup>:

$$\frac{\$}{day} = \left( \frac{m^3}{day} \right) \left( \frac{kg}{m^3} \right) \left( \frac{J}{kg} \right) \left( \frac{\$}{J} \right) \quad (1)$$

The first factor on the right-hand side of Eq. 1 is the volumetric flow rate determined by flow meters (e.g. orifice meters<sup>7</sup>), the second factor is the density that is available with high accuracy from volumetric measurements<sup>8-10</sup>. The third factor is the heating value that is available from calorimetric measurements. The final factor is the price of the natural gas on an energy basis. From Eq. 1 is clear that the caloric and volumetric properties for natural gas mixtures are essential information for the gas processing industry. Several Equations of State (EoS), such as AGA8-DC92<sup>11</sup> and GERG-2008<sup>12</sup>, can

predict the thermodynamic properties of natural gas. The experimental data for energies, entropies and heat capacities are useful in developing new EoS, for empirical correlations needed to determine the energy content of the hydrocarbon gas streams, and for use in conjunction with other sets of experimental data, such as volumetric data ( $P$ - $\rho$ - $T$ ), for developing thermodynamic models<sup>13</sup>. On the other hand, knowledge of the experimental derivatives such as  $(\partial P/\partial T)_\rho$  and  $(\partial^2 P/\partial T^2)_\rho$  help in evaluating the thermodynamic consistency of EoS and the impact of using numerical and analytical derivatives during its development.

An important physical property of the gases is the ratio of the heat capacities at constant pressure ( $C_P$ ) and heat capacities at constant volume ( $C_V$ ) defined as:

$$k = \frac{C_P}{C_V} \quad (2)$$

The factor  $k$  in Eq. 2 appears in the design of components and evaluation of the overall performance of compressors<sup>14,15</sup>.

## 1.2. Literature Review of Calorimetric Measurements

The most popular method for determining caloric properties is via calorimetric measurements, however those properties also can result from using thermodynamic relationships and volumetric data. This section presents a review of the procedures and

current state of art for calorimetric measurements as well as the specifications and accuracy for apparatus used to acquire volumetric data.

### ***1.2.1 Adiabatic Calorimeter for Heat Capacities Measurements***<sup>16</sup>

The National Institute of Standards and Technology (NIST) has used the adiabatic method to measure heat capacities of liquid and gas mixtures and pure fluids. The adiabatic calorimeter consists of a twin-bomb arrangement, which allows accurate energy measurements. It minimizes the heat loss caused by gradients in temperature and radiation fluxes by an automatic adjustment of the temperature of a cooper case that surrounds the bomb. The range of temperature is from 20 to 700 K at pressures up to 35 MPa. According to NIST the heat capacity at constant volume ( $C_v$ ) is determined from:

$$C_v = \frac{(\Delta Q - \Delta Q_o)}{m\Delta T} \quad (3)$$

In Eq. 3,  $\Delta Q$  is the value of the energy absorbed by the fluid,  $\Delta Q_o$  is the energy difference between the empty sample bomb and the reference,  $\Delta T$  is the rise in temperature caused by the energy absorbed by a fluid of mass  $m$  contained in the bomb. Typical values of the relative uncertainty for the measured heat capacities at constant volume appear in Table 2.

**Table 2.** Relative uncertainty in ( $C_v$ ) experimental values for mixtures and pure fluids measured with adiabatic calorimeter<sup>16</sup>

Fluid / Mixture	Phase	Range	Relative Uncertainty ( $C_v$ )
Twice Distilled Water	Liquid	Temperature: 300-420 K. Pressure: up to 20 MPa	0.48% <sup>16</sup>
Hydrocarbon Mixture (C <sub>3</sub> H <sub>8</sub> ) and (i-C <sub>4</sub> H <sub>10</sub> )	Liquid	Temperature: 203-342 K. Pressure: up to 35 MPa	0.7% <sup>17</sup>
Isobutane	Vapor	Temperature: 114-345 K. Pressure: up to 35 MPa	0.7% <sup>18</sup>
Propane	Vapor	Temperature: 85-345 K. Pressure: up to 35 MPa	0.7% <sup>19</sup>
Nitrogen	Vapor and Liquid	Temperature: 85-345 K. Pressure: up to 35 MPa	2% in vapor <sup>20</sup> 0.5% in liquid
Mixture CO <sub>2</sub> and C <sub>2</sub> H <sub>6</sub>	Vapor and Liquid	Temperature: 220-340 K. Pressure: up to 35 MPa	2% in vapor <sup>21</sup> 0.5% in liquid

### *1.2.2 Flow Calorimeters for Constant Pressure Heat Capacities Measurements*

Ernest et al.<sup>22</sup> constructed a flow calorimeter that accounts for the differences between the International Practical Temperature Scale 1968 (IPTS-68) and the Thermodynamic Temperature Scale (TTS) derived from the differences between accurate values of the isobaric heat capacity using these corresponding scales. The design of the calorimeter is a U-shaped tube isolated by vacuum, and a radiation shield with platinum resistance thermometer (PRT) wires that contact the electrically heated flowing gas. The apparatus operates continuously by recycling the gas that flows to a condenser after the calorimeter stage followed by heating the condenser to push the liquid into a two-phase container where the gas flow that goes to the calorimeter results at constant pressure by evaporating the liquid. The range of operation in temperature is from -20 to 200 °C with

pressures up to 1.5 MPa. The experimental heat capacity at constant pressure ( $C_p$ ) is calculated from:

$$C_p = \frac{P}{m \left( (T_2 - T_1)_m - ((T_2 - T_1)_b) \right)} \quad (4)$$

In Eq. 4 the mass flow rate  $m$  results from weighing the condensate and noting the collection time. The  $C_p$  value results from using the difference between a main experiment (with heating) and a blank experiment (without heating),  $P$  is the heating power in Watts. Use of the blank experiment is convenient because it includes the effect of Joule-Thompson cooling and changes in potential and kinetic energy, therefore improving the accuracy of the  $C_p$ .

Measurements of specific heat capacity for Xenon in the gas phase from -20 to 100 °C and at pressures up to 0.4 MPa yield an uncertainty value for  $C_p$  of  $\pm 0.05$  %. Other applications of flow calorimeters include the determination of enthalpies of absorption<sup>23</sup> and enthalpy differences<sup>24</sup>.

### ***1.2.3 Caloric Properties for Natural Gas Mixtures***<sup>12</sup>

The GERG-2008 EoS<sup>12</sup> for the thermodynamic properties of natural gases is explicit in the Helmholtz free energy as a function of temperature, density and composition. This EoS has a database of more than 125 000 experimental data points for thermal and caloric properties of binary mixtures, natural gases and multicomponent mixtures. Just 9 % of the database presents caloric properties with a relative uncertainty

ranging from 1 to 2% for isochoric and isobaric heat capacities and relative uncertainty from 0.2 to 0.5% for enthalpy differences.

The caloric experimental data cover a range in temperature from 250 to 350 K at pressures up to 20 MPa. However, compared to  $(P-\rho-T)$  data sets, measurements for caloric properties of natural gases are scarce, especially for mixtures of nitrogen – carbon dioxide and carbon dioxide – propane. The GERG-2008 EoS reports a percentage deviation of  $\pm 5\%$  in the values of isobaric heat capacities for ternary and quaternary mixtures of methane, nitrogen, propane and ethane when compared to experimental isobaric heat capacities with uncertainty in measurements of 2.5%. No values of percentage deviation for isochoric heat capacities appear in GERG-2008.

### **1.3 Research Proposal and Objectives of the Study**

After the analysis of the economic impact of natural gas, the importance of experimental data for fluids and mixtures in modeling EoS is apparent. The lack of accurate measurements for heat capacities at constant volume directly from calorimetric measurements, requires alternatives for determining caloric properties. This research project proposes to expand the scope of the volumetric measurements by applying thermodynamic principles to provide accurate values of heat capacities at constant volume.

The main objective of this work is to use  $(P-\rho-T)$  experimental data for a ternary mixture collected in the apparatus of the Thermodynamics Research Group of Texas A&M University for calculating the first and second derivatives of pressure with respect to

temperature needed for determination of the caloric properties: energies, entropies and heat capacities. This project seeks to accomplish the following specific objectives:

1. To propose a methodology that integrates the experimental data from three different apparatus to correct the experimental errors and provide reliable values for the distortion coefficients for Beryllium Cooper 175 Alloy.
2. To analyze the difference between the numerical and analytical methods for the repeatability of the results of the second derivatives of pressure with respect to temperature at constant density  $\left(\partial^2 P^* / \partial T^2\right)_\rho$ .
3. To calculate residual and absolute heat capacities from experimental  $(P-\rho-T)$  data and to claim a value for the global uncertainty.
4. To identify a new, strategic way to develop experimental designs and data acquisition techniques that allow building a complete thermodynamic characterization of fluids.

The following sections present the description of the apparatus used for the experimental characterization of gas mixtures as well as the methodology and results obtained during the execution of this work.



## 2. EXPERIMENTAL CHARACTERIZATION OF NATURAL GAS MIXTURES

Experimental determination of thermodynamic properties for natural gas mixtures is essential information for the gas processing industry and the development and optimization of equations of state. The volumetric ( $P$ - $\rho$ - $T$ ) data along with empirical correlations can determine the energy content of hydrocarbon gas streams and their caloric properties<sup>13</sup>. This work expands the initial scope of the ( $P$ - $\rho$ - $T$ ) measurements by providing a technique to obtain uncertainties for caloric properties.

The experimental data used in this work all were acquired using apparatus located in the Thermodynamic Research Laboratory at Texas A&M University in College Station, TX, USA. The equipment explained in this section provides accurate ( $P$ - $\rho$ - $T$ ) measurements of fluids over broad ranges of pressure and temperature.

### 2.1 Magnetic Suspension Densimeter (MSD)<sup>8,9</sup>

The MSD uses Archimedes' principle, which states that the upward buoyancy force exerted on a body immersed in a fluid is equal to the weight of the fluid that the body displaces. In this apparatus the buoyant force is related to the density of the fluid measured by weighing a sinker in vacuum and then in the presence of a fluid under pressure. The significant feature of the apparatus is that the balance and the sinker have a magnetic coupling (Figure 4a), thus the apparent mass measurement of the sinker occurs while it is levitated via a suspension coupling in the pressure cell at a fixed temperature and pressure.

The system uses two compensation weights made from titanium (Ti) and tantalum (Ta) to correct for nonlinearity and the effect of air buoyancy on the balance (Figure 4b).

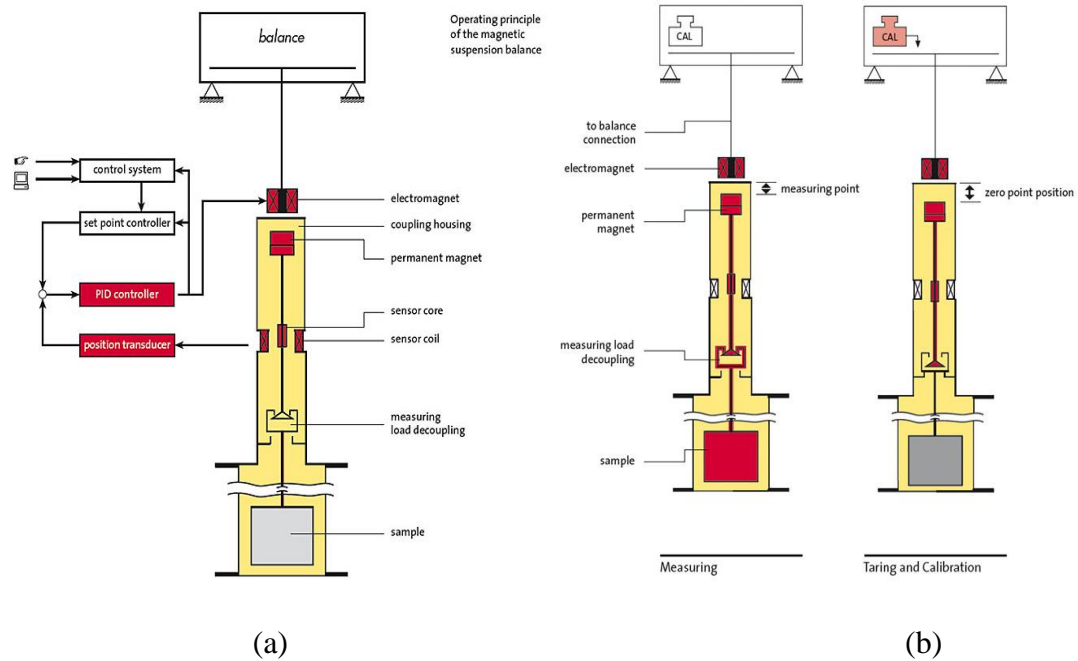


**Figure 4.** (a) Basic scheme for the MSD<sup>25</sup> (b) Operating modes of the MSD<sup>25</sup>

Eq. 5 is used to determine the density of the fluid inside the pressure vessel<sup>6</sup>, in which  $m_v$  is the mass of the sinker in vacuum,  $m_a$  is the apparent mass of the sinker in the fluid, while  $m_{Ti}$  and  $m_{Ta}$  are the masses of the external weights. The volume of the sinker ( $V_s$ ) is a function of temperature and pressure. The specifications and accuracy of the MSD appear in Table 3. The measurements using the MSD for determining the densities of pure fluids and mixtures along with the uncertainties appear in Table 4.

$$\rho = \frac{(m_v + m_{Ti} - m_{Ta}) - (m_a + m_{Ti} - m_{Ta})}{V_s} \quad (5)$$

**Table 3.** MSD specifications

<b>Magnetic Suspension Densimeter (MSD)</b>	Uncertainty in density: 0.0005 kg/m <sup>3</sup> Range of Density: 0- 2000 kg/m <sup>3</sup> Material of the cell: Beryllium- Copper. Range of Temperature: 193.15 – 523.15 K Stability in Temperature: ± 5 mK Pressure Range: 0-200 MPa Uncertainty in pressure: 0.01% of full scale
<b>Sinker (Titanium Cylinder). Conditions measured at 293.15K and 1 bar by Rubotherm.</b>	Volume: 6.74083 ± 0.00034 cm <sup>3</sup> Uncertainty in volume: ±0.05% Mass: 30.39157 g
<b>Analytical balance (Mettler Toledo AT 261)</b>	Range: 0-62 g Uncertainty: 0.03 mg

**Table 4.** Experimental measurements of density taken in the MSD of TAMU

<b>Fluid /Mixture</b>	<b>Range of temperature</b>	<b>Uncertainty in Density</b>
SNG 1 <sup>9</sup>	250 - 450 K	≤ 0.1 %
SNG (2-4) <sup>10</sup>	250 - 450 K	≤ 0.2 %
Ternary 1 (Methane, Ethane, Propane) <sup>8</sup>	300 - 400 K	≤ 0.3 %
Ethane <sup>26</sup>	298 - 450 K	≤ 0.03 %
Carbon Dioxide <sup>27</sup>	310 - 450 K	≤ 0.1 %
Methane <sup>28</sup>	300 - 450 K	≤ 0.03 %
Nitrogen <sup>29</sup>	265 - 400 K	≤ 0.05 %

## 2.2 Low and High Pressure Isochoric Apparatus<sup>6,9,30</sup>

In an isochoric experiment the amount of fluid inside the cell remains constant while varying both temperature and pressure. Slight changes in the volume caused by expansion and contraction of the cell material when changing temperature and pressures along with the effect of mass transport between the cell and the pressure transducer require correction to determine the density of the fluid. The typical arrangement of an isochoric apparatus includes temperature and pressure controller systems, vacuum pump and radiation shields (Figure 5). The arrangement of the radiation shields and the positions of the thermopiles on the isochoric cell ensure rapid stability in temperature and gradients of temperature at equilibrium of 0.005 mK<sup>6,30</sup>.

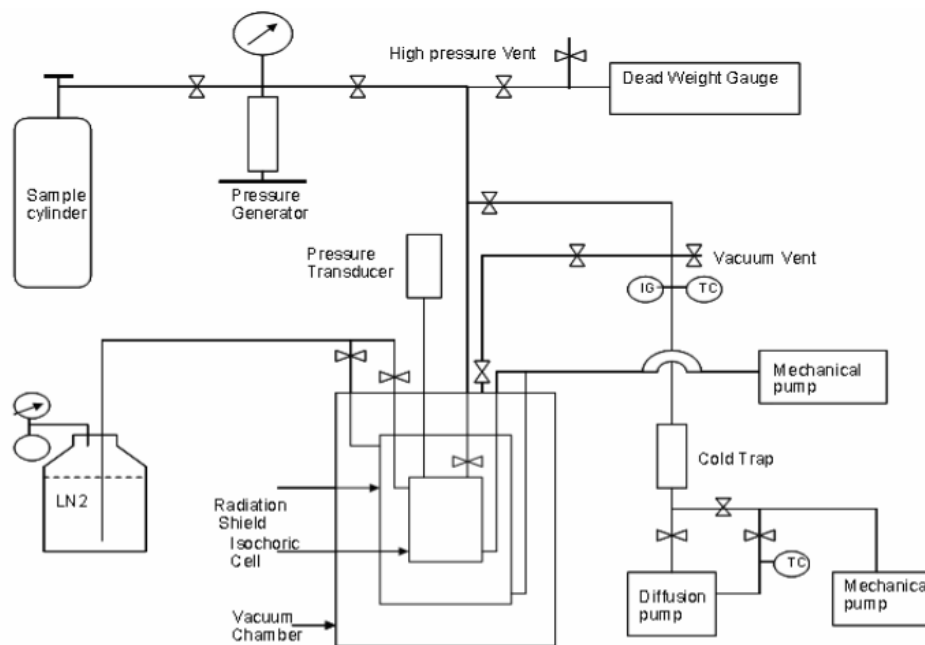


**Figure 5.** Schematic diagram of the isochoric experiment<sup>30</sup>

Figure 6 presents a general overview of the isochoric cell for the high-pressure isochoric apparatus. The specifications of the materials, properties and accuracy of the low and high pressure isochoric apparatus appear in Tables 5 and 6.

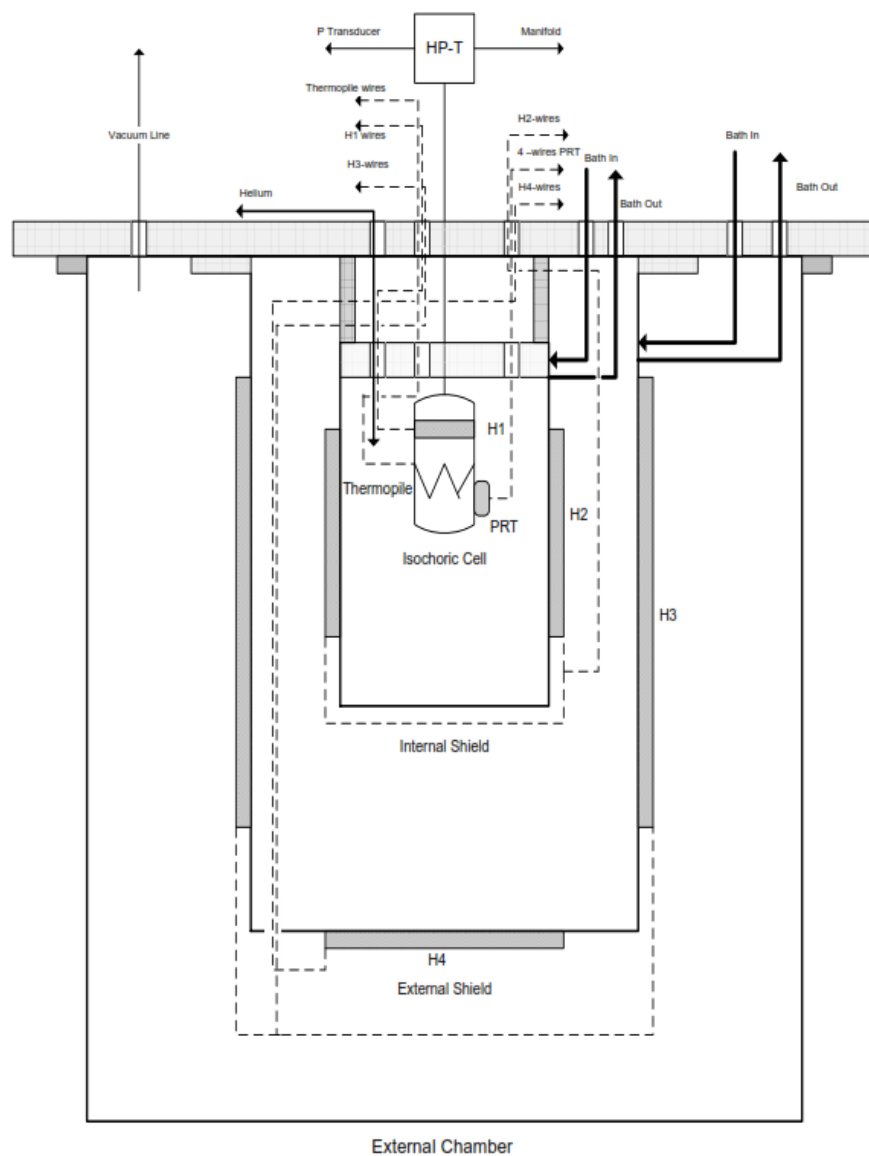


**Figure 6.** Isochoric cell cut view for the high pressure equipment<sup>6</sup>

**Table 5.** Low pressure apparatus (LPI) specifications<sup>30</sup>

<b>Low Pressure Isochoric Apparatus (LPI)</b>	
Material of the cell, connection line and pressure transducer: Stainless Steel Temperature: 100 – 500 K. Stability in temperature: $\pm 5$ mK Pressure: Up to 20 MPa. Uncertainty in pressure: 0.01% of full scale	
<b>Calibration values</b>	$V_c^o = 6.01 \cdot 10^{-5} \text{ m}^3$ . $V_l^o = 7.32 \cdot 10^{-9} \text{ m}^3$ . $V_i^o = 2.05 \cdot 10^{-7} \text{ m}^3$ $T_o = 298.15 \text{ K}$ . $P_o = 0.101325 \text{ MPa}$
<b>Coefficients</b> <sup>9</sup>	Stainless Steel: $\alpha = 4.86 \cdot 10^{-5} \text{ K}^{-1}$ . $\beta = 2.53 \cdot 10^{-5} \text{ MPa}^{-1}$

**Table 6.** High pressure apparatus (HPI) specifications<sup>6</sup>

<b>High Pressure Isochoric Apparatus (HPI)</b>	
Material of the cell: Beryllium- Copper. Material of connection line and pressure transducer: Stainless Steel Temperature: 100 – 500 K. Stability in temperature: $\pm 10$ mK Pressure: Up to 200 MPa. Uncertainty in pressure: 0.01% of full scale	
<b>Calibration values</b>	$V_c^o = 1.05 \cdot 10^{-5} \text{ m}^3$ . $V_l^o = 1.02 \cdot 10^{-7} \text{ m}^3$ . $V_i^o = 1.42 \cdot 10^{-7} \text{ m}^3$ $T_o = 298.15 \text{ K}$ . $P_o = 0.101325 \text{ MPa}$
<b>Coefficients</b> <sup>31</sup>	Beryllium Cooper: $\alpha = 5.215 \cdot 10^{-5} \text{ K}^{-1}$ . $\beta = 3.471 \cdot 10^{-5} \text{ MPa}^{-1}$ Stainless Steel: $\alpha = 4.86 \cdot 10^{-5} \text{ K}^{-1}$ . $\beta = 2.53 \cdot 10^{-5} \text{ MPa}^{-1}$

The experimental data taken with the low pressure apparatus appear in Table 7. The data presented in the following section represent the first reliable ( $P$ - $T$ ) data taken with the high-pressure isochoric apparatus.

**Table 7.** Experimental measurements taken in the LPI of TAMU

<b>Fluid /Mixture</b>	<b>Range of temperature</b>	<b>Range of pressure</b>
SNG 1 <sup>9</sup>	257 - 343 K	up to 20 MPa
SNG (2-4) <sup>10</sup>	250 - 350 K	up to 20 MPa
Ternary 1 (Methane, Ethane, Propane) <sup>8</sup>	220 - 320 K	up to 20 MPa

### 3. HEAT CAPACITIES FROM EXPERIMENTAL ( $P$ - $\rho$ - $T$ ) DATA

The methodology for determining the heat capacity at constant volume from experimental data has five stages illustrated in Figure 7.

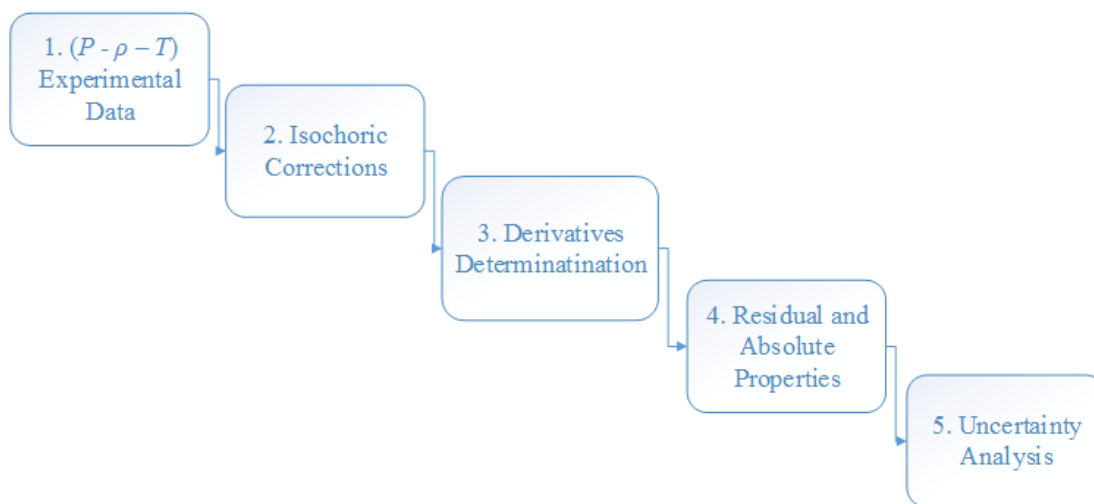


**Figure 7.** Methodology to determine ( $C_v$ ) from experimental ( $P$ - $\rho$ - $T$ ) data

#### 3.1 Stage 1. Experimental Data Acquisition

This work applies the methodology from Figure 7 to a ternary mixture with a composition similar to a residual gas sample. DCG PARTNERSHIP Inc<sup>32</sup> prepared the mixture gravimetrically with mole fractions of 0.95014 methane, 0.03969 ethane and 0.01017 propane with an estimated gravimetric uncertainty of  $\pm 0.04\%$  NIST- Traceable by weight. Measurements of temperature, pressure and density of the sample occurred in the MSD, LPI and HPI apparatus of the TAMU Thermodynamics Group. The set of data

appears in Figure 8 and Appendix A. It contains 10 isochores and 5 isotherms covering a range of temperature from 140 to 500 K at pressures up to 200 MPa.

A statistical analysis of the properties measured over 20 minutes of stability for each experiment indicates the set of data with the lowest standard deviation to define the ( $P$ - $T$ ) points for each isochore and isotherm.



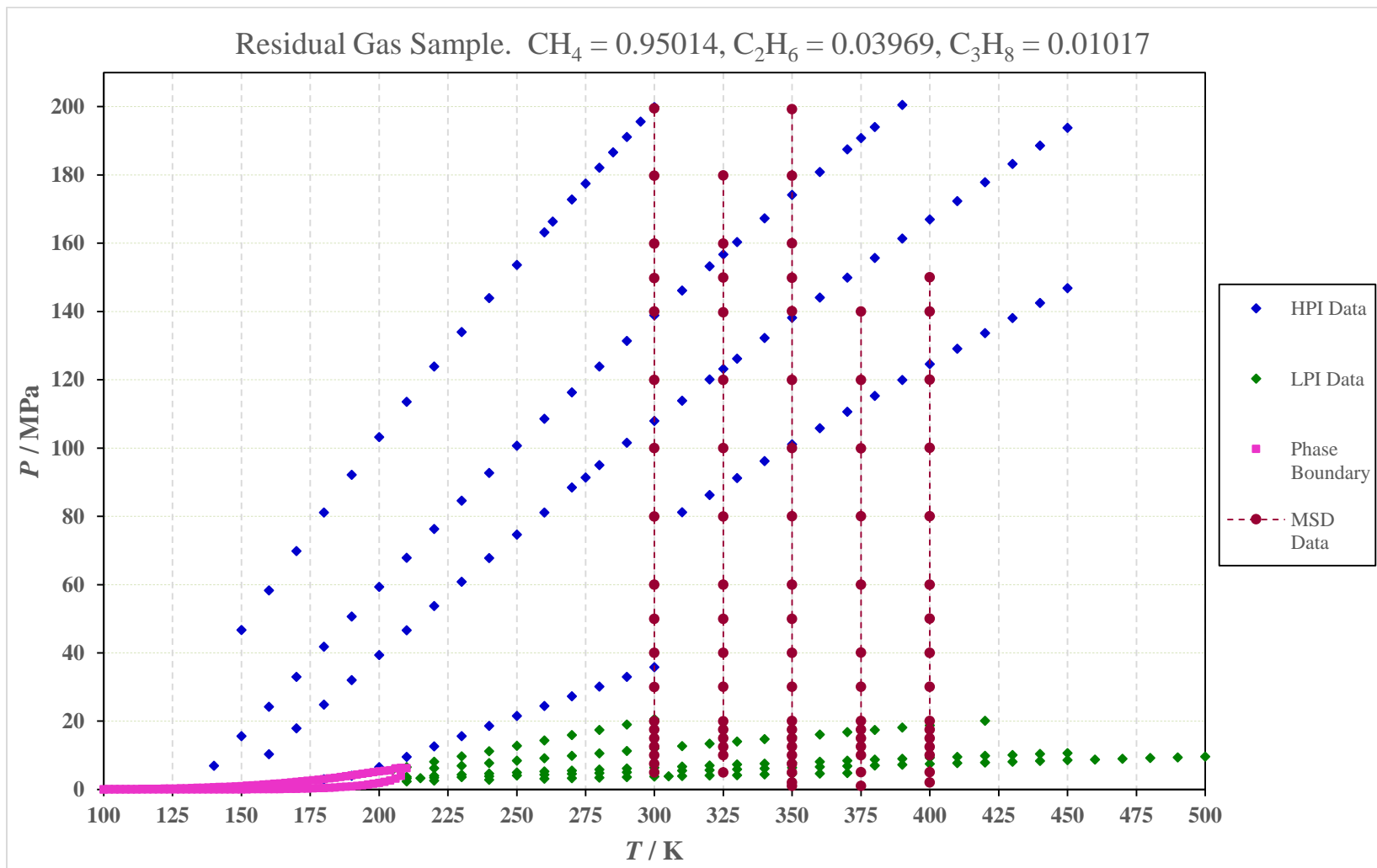


**Figure 8.** Experimental data of residual gas sample

### 3.2 Stage 2. Isochoric Corrections

At this stage, it is necessary to consider factors that cause slight changes in density along the experimental path. First, the volume of the cell varies with temperature and pressure, and second, part of the volume occupied by the fluid is external to the cell and at a different temperature. The external volume is “noxious volume” and corresponds to the amount of gas located in the transmission line and the pressure transducer as shown in Figure 9.

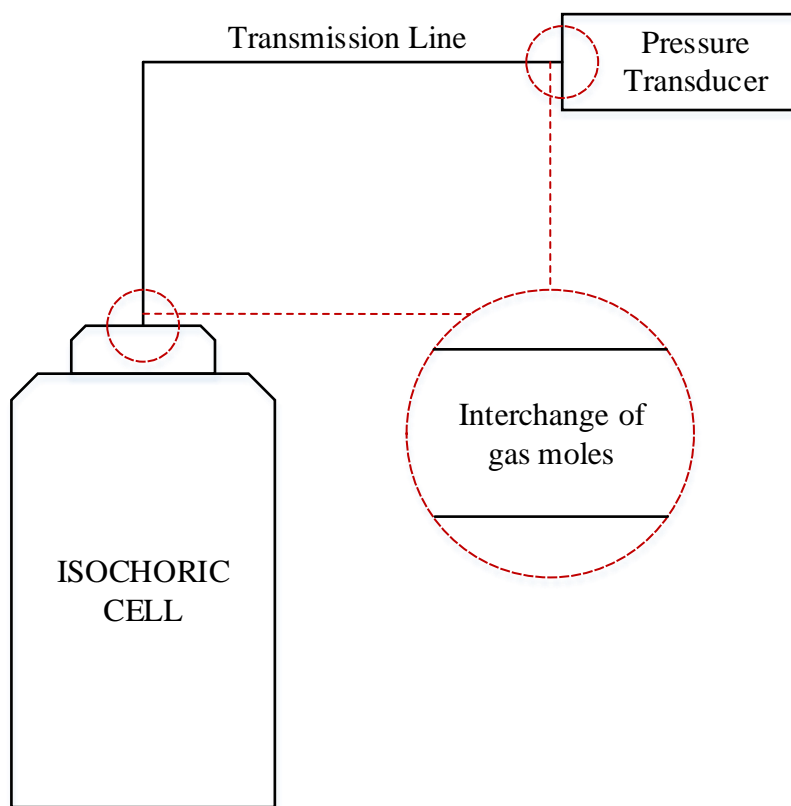


**Figure 9.** Noxious volume in isochoric apparatus

### 3.2.1 Definition of Reference State

Along the “isochoric” path the values of density differ because of changes in temperature and pressure, however the total number of moles for an isochoric line must be constant, in the absence of leaks, in a closed system as shown in Figure 9. Section 3.2.2 describes the determination of the isochoric density based upon the total number of moles in an isochore being constant and defined as:

$$n = n_c + n_l + n_t \quad (6)$$

$$\rho V = \rho_c V_c + \rho_l V_l + \rho_t V_t \quad (7)$$

The subscripts  $c$ ,  $l$  and  $t$  in Eqs. 6 and 7 and throughout this thesis, correspond to the cell, connection line and pressure transducer respectively.

Determination of the density on the left-hand side of Eq. 7 requires a reference state. Using the data from the MSD, it is possible to determine a  $(P-\rho-T)$  value that corresponds to a  $(P-T)$  point on an isochore. The reference state, denoted by  $(P^*-\rho^*-T^*)$  for each isochore is the starting point for determining the isochoric density for each  $(P-T)$  pair on its isochoric line.

The reference density results from using the percentage deviation in density values from the MSD:

$$\% \text{ deviation}_\rho = 100 \cdot \left( \frac{\rho_{MSD} - \rho_{EoS}}{\rho_{MSD}} \right) \quad (8)$$

The Equation of State (EoS) used in Eq. 8 is GERG-2008 because it appears to provide accurate values for densities of natural gas mixtures. Figure 10 shows the % deviation of density for the five isotherms measured in the MSD for the residual gas sample.

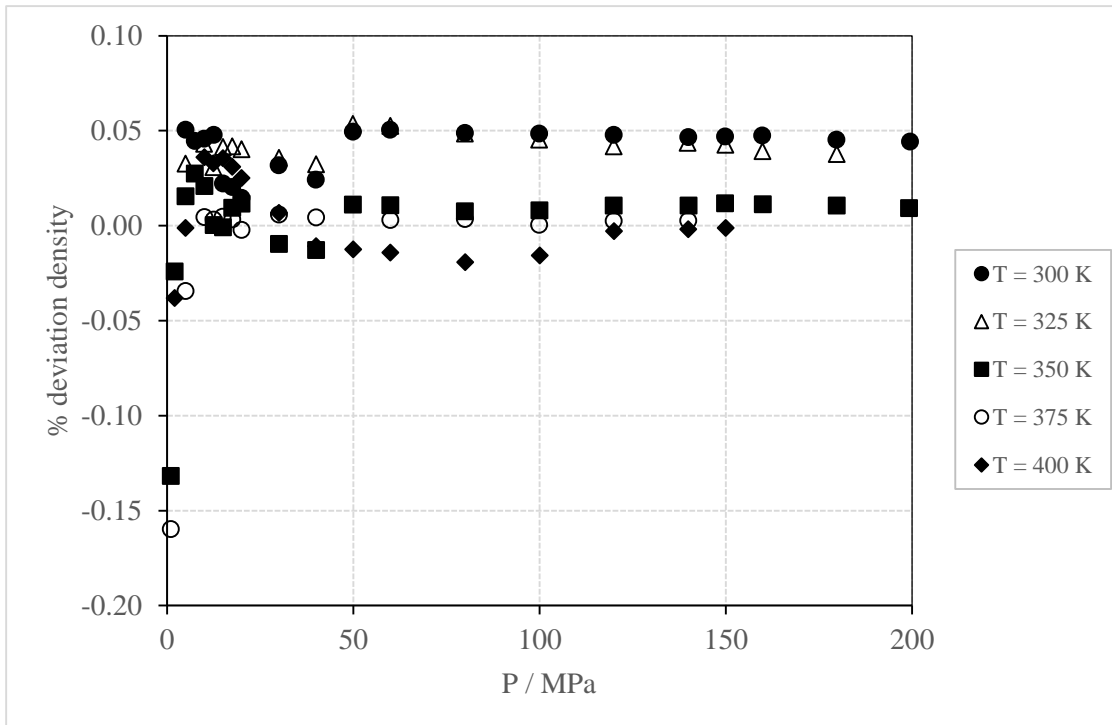


**Figure 10.** Percentage deviation of density values from MSD

From Figure 10, the % deviation in density has a maximum value of  $\pm 0.05\%$  from 20 to 200 MPa, this information along with Eq. 8 enable calculation of the reference density ( $\rho^*$ ):

$$\rho^* = \frac{100 \cdot \rho_{EoS}}{100 - \% \text{ deviation}_\rho} \quad (9)$$

Table 8 summarizes the reference condition values for the ten isochores measured in the high and low pressure isochoric apparatus for the residual gas sample.

**Table 8.** ( $P$ - $\rho$ - $T$ ) reference values for each isochore. EoS values from GERG-2008

Isochore	T* (K)	P* (MPa)	% deviation $\rho$	$P_{EoS}$ (kg/m <sup>3</sup> )	$\rho^*$ (kg/m <sup>3</sup> )
1	300.00	199.871	0.044	418.852	419.037
2	350.00	174.109	0.011	382.630	382.671
3	350.00	138.193	0.011	359.043	359.081
4	350.00	101.041	0.008	326.413	326.439
5	300.00	35.793	0.028	248.113	248.183
6	300.00	20.567	0.015	172.917	172.942
7	350.00	15.446	-0.001	99.564	99.563
8	350.00	7.871	0.027	49.116	49.129
9	350.00	6.383	0.022	39.374	39.383
10	350.00	4.534	0.016	27.522	27.526

### 3.2.2 Isochoric Density Determination

This section shows the algebraic arrangements, assumption and equations needed to determine the isochoric density, which is the density of gas inside the isochoric cell when at equilibrium conditions in ( $P$ - $T$ ). The isomolar characteristic of the isochoric experiment and the reference state can correct for the noxious volume effect when calculating the isochoric density.

From Eq. 6, the number of moles in the cell is

$$n_c = n - n_l - n_t \quad (10)$$

Replacing the total number of moles at reference conditions:

$$n_c = (n_c^* + n_l^* + n_t^*) - n_l - n_t \quad (11)$$

Organizing the terms in Eq. 11 for the line and pressure transducer

$$n_c = n_c^* + (n_l^* - n_l) + (n_t^* - n_t) \quad (12)$$

Dividing Eq. 12 by the moles of the cell at reference conditions

$$\frac{n_c}{n_c^*} = 1 + \frac{(n_l^* - n_l)}{n_c^*} + \frac{(n_t^* - n_t)}{n_c^*} \quad (13)$$

Writing Eq. 13 in terms of density

$$\frac{\rho_c V_c}{\rho_c^* V_c^*} = 1 + \frac{(\rho_l^* V_l^* - \rho_l V_l)}{\rho_c^* V_c^*} + \frac{(\rho_t^* V_t^* - \rho_t V_t)}{\rho_c^* V_c^*} \quad (14)$$

The assumption in the determination of isochoric density is that the main contribution to the mass transport in the system is the expansion and contraction of the volume of the cell when varying temperature and pressure. Furthermore, the temperature of the connection line and pressure transducer are constant during the isochoric experiment. Therefore, the changes in the external volume is meaningless compared to the changes in the volume of the cell, and Eq. 14 becomes:

$$\frac{\rho_c V_c}{\rho_c^* V_c^*} = 1 + \frac{V_l(\rho_l^* - \rho_l)}{\rho_c^* V_c^*} + \frac{V_t(\rho_t^* - \rho_t)}{\rho_c^* V_c^*} \quad (15)$$

Solving for the isochoric density of the cell ( $\rho_c$ )

$$\rho_c = \frac{V_c^*}{V_c} \rho_c^* + \frac{V_l}{V_c} (\rho_l^* - \rho_l) + \frac{V_t}{V_c} (\rho_t^* - \rho_t) \quad (16)$$

The volume for each subsystem in Eq. 16 has the general form

$$V = V^* \exp(\alpha(T - T^*) + \beta(P - P^*)) \quad (17)$$

The distortion parameters  $\alpha$  and  $\beta$  in Eq. 17 are the thermal expansion and isothermal compressibility coefficients respectively<sup>33</sup>. Table 9 contains the values of  $\alpha$  and  $\beta$  for stainless steel and Cu-Be.

$$\alpha = \frac{1}{V} \left( \frac{\partial V}{\partial T} \right)_P \quad (18)$$

$$\beta = -\frac{1}{V} \left( \frac{\partial V}{\partial P} \right)_T \quad (19)$$

**Table 9.** Thermal expansion and isothermal compressibility coefficients

Parameter	Stainless Steel		Beryllium Cooper	
	Stouffer <sup>34</sup>	Lau <sup>31</sup>	Cristancho <sup>6</sup>	
$\alpha$ (K <sup>-1</sup> )	4.86E-05	1.85E-06	1.60E-04	
$\beta$ (MPa <sup>-1</sup> )	2.53E-05	3.37E-05	2.53E-05	

Eqs. 16 and 17 are the key equations to determine the isochoric density. Because of the different design specifications for the isochoric apparatus, the effect of the noxious volume in the isochoric determination is analyzed separately in the following sections.

### 3.2.2.1 Isochoric Density for Low Pressure Isochores

The noxious volume in the LPI is mostly the volume of the pressure transducer. The assumption is that the effect of the change in the volume of the gas when it passes through the transmission line is negligible because the line is at the same constant temperature as the pressure transducer, and its volume is small compared to those of the cell and pressure transducer. Using information from Table 10, it is possible to calculate the noxious volume for the LPI which is 0.34% of the volume of the cell. Therefore, calculation of the densities for isochores 6 to 10 follows from:

$$\rho_c = \frac{V_c^*}{V_c} \rho_c^* + \frac{V_t}{V_c} (\rho_t^* - \rho_t) \quad (20)$$

**Table 10.** Volumes for LPI

<b>Low Pressure Isochoric Apparatus (LPI)</b>	
Cell	Material: Stainless Steel
	Volume: $6.01 \cdot 10^{-5} \text{ m}^3$
	Temperature of operation: 200 - 500 K
Transmission Line	Material: Stainless Steel
	Volume: $7.32 \cdot 10^{-9} \text{ m}^3$
	Temperature of operation: 350.45 K
Pressure Transducer (43K - 101)	Material: Stainless Steel
	Volume: $2.05 \cdot 10^{-7} \text{ m}^3$
	Temperature of operation: 350.45 K



This research work requires validation of the parameters  $\alpha$  and  $\beta$  reported in Table 9. This requires two assumptions: the total number of moles for a single isochore is constant, and values from the MSD and GERG 2008 can provide the density in the cell and in the pressure transducer, respectively. A system of three equations with three unknowns ( $n$ ,  $\alpha$  and  $\beta$ ) results from choosing three different points ( $P$ - $T$ ) on an isochore, and determining their densities from the MSD data using the procedure outlined in Section 3.2.1. Table 11 presents the three ( $P$ - $T$ ) pairs and their density values for isochores 7, 8 and 9. By way of illustration, Eqs. 21 to 23 were used for isochore 7. Similar fashion systems for isochores 8 and 9 provide values for  $n$ ,  $\alpha$  and  $\beta$ . The values appear in Table 12.

**Table 11.** LPI values to calculate distortion parameters for stainless steel

Isochore	T (K)	P (MPa)	$\rho_c$ (kmol/m <sup>3</sup> )	$\rho_t$ (kmol/m <sup>3</sup> )
7	300.00	11.962	5.909	4.518
	350.00	15.446	5.897	5.885
	400.00	18.790	5.864	7.143
8	300.00	6.421	2.915	2.343
	350.00	7.871	2.910	2.904
	400.00	9.291	2.902	3.461
9	300.00	5.262	2.338	1.901
	350.00	6.383	2.332	2.328
	400.00	7.481	2.326	2.752

$$n = (5.909 * 6.01 \cdot 10^{-5}) \exp\left[\left(\alpha(300 - 350) + \beta(11.962 - 15.446)\right)\right] + (4.518 * 2.05 \cdot 10^{-5}) \exp\left[\left(\alpha(350.45 - 350) + \beta(11.962 - 15.446)\right)\right] \quad (21)$$

$$n = (5.897 * 6.01 \cdot 10^{-5}) \exp\left[\left(\alpha(350 - 350) + \beta(15.446 - 15.446)\right)\right] + (5.885 * 2.05 \cdot 10^{-5}) \exp\left[\left(\alpha(350.45 - 350) + \beta(15.446 - 15.446)\right)\right] \quad (22)$$

$$n = (5.909 * 6.01 \cdot 10^{-5}) \exp\left[\left(\alpha(300 - 350) + \beta(11.962 - 15.446)\right)\right] + (4.518 * 2.05 \cdot 10^{-5}) \exp\left[\left(\alpha(350.45 - 350) + \beta(11.962 - 15.446)\right)\right] \quad (23)$$

**Table 12.** Parameters for stainless steel

Isochore	$n$ (mol)	$a$ (K <sup>-1</sup> )	$\beta$ (MPa <sup>-1</sup> )
7	0.355	4.88E-05	2.55E-05
8	0.175	4.86E-05	2.53E-05
9	0.141	4.86E-05	2.53E-05

The values for  $\alpha$  and  $\beta$  reported in Table 12 validate those reported by Stouffer, therefore Eqs. 20 and 17 along with the parameters for stainless steel reported in Table 9 are used to calculate the isochoric densities from the LPI. Figure 11 shows the % deviation of the isochoric densities in the LPI compared to GERG 2008 using Eq. 8. The numerical values are in Appendix B.

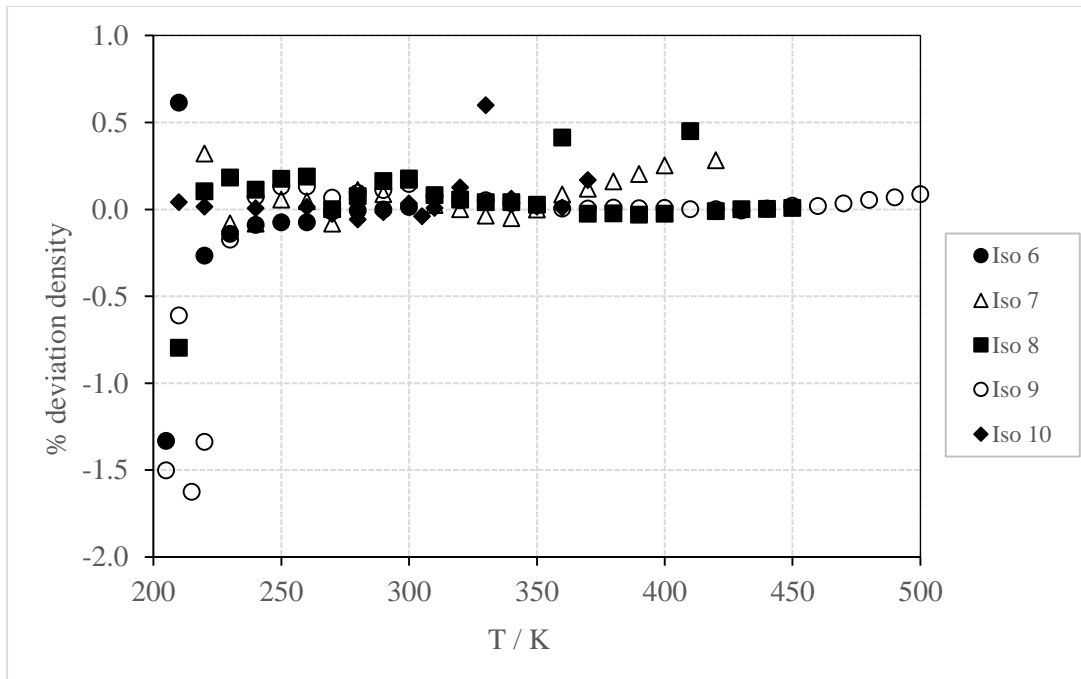


**Figure 11.** Per cent deviation of isochoric densities in the LPI

### 3.2.2.2 Isochoric Density for High Pressure Isochores

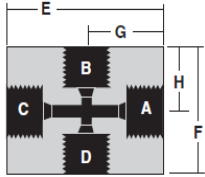
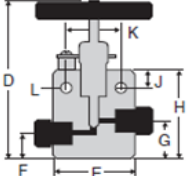
The quantification of the noxious volume and new values of  $\alpha$  and  $\beta$  for the high-pressure isochoric apparatus are new contributions from this research. To determine the noxious volume, it is necessary to estimate the volume of the transmission line that connects the isochoric cell to the pressure transducer. This line is stainless steel and has a working pressure of 60,000 psi, 1/8" OD and 0.020" ID. The lengths of the each segment of the transmission line were measured to determine the volumes reported in Table 13. The high pressure cross and valve manufactured by HiP Co and their respective volumes come from the technical information in Table 14. The pressure transducer, Model 430K-101 manufactured by Paroscientific Inc., has a range of operation up to 30,000 psi and an

internal volume of 0.142 cm<sup>3</sup>. Table 15 summarizes the operationing conditions and volumes for the HPI. The initial values for determining the parameters  $\alpha$  and  $\beta$  for the Cu-Be cell are those calculated by Lau and reported in Table 9. Figure 12 illustrates the three systems involved in the transport of mass in the HPI.

**Table 13** Lengths for noxious volume estimation in the HPI

From –To	Length (in)	Length (cm)	Volume (cm <sup>3</sup> )
Transducer – HIP Cross	3	7.62	0.0154
HIP Cross – HIP Valve	1	2.54	0.0051
HIP Cross –Aluminum Plate	7.75	19.69	0.0399
Aluminum Plate – Isochoric Cell	5	12.7	0.0257
<b>Total</b>	<b>16.75</b>	<b>42.55</b>	<b>0.0862</b>

**Table 14** Technical specifications for high pressure cross and valve in the HIP

<b>High Pressure Cross</b>	
Model 60-24HF2	
Working pressure: 60,000 psi	
Connection: Tube 1/8" OD	
Length (E): 1.5" = 3.81 cm	
<b>Volume: 0.0077 cm<sup>3</sup></b>	
<b>High Pressure Valve</b>	
Model 30-11HF2	
Working pressure: 30,000 psi	
Connection: Tube 1/8" OD	
Length (E): 1.5" = 3.81 cm	
<b>Volume: 0.0077 cm<sup>3</sup></b>	

**Table 15** Volumes for HPI

<b>High Pressure Isochoric Apparatus</b>	
Cell	Material: Beryllium Cooper 175 Volume: $1.05 \cdot 10^{-5} \text{ m}^3$ Temperature of operation: 200 - 500 K
Transmission Line	Material: Stainless Steel Volume: $1.02 \cdot 10^{-7} \text{ m}^3$ Temperature of operation: 333.15 K
Pressure Transducer (430K - 101)	Material: Stainless Steel Volume: $1.42 \cdot 10^{-7} \text{ m}^3$ Temperature of operation: 309.15 K

From Table 15, the volume of the transmission line is approximately equal to the volume of the pressure transducer. In addition, the temperature of operation is different for the two systems. Consequently, both contributions must be taken into account when calculating the noxious volume and isochoric densities from the HPI.

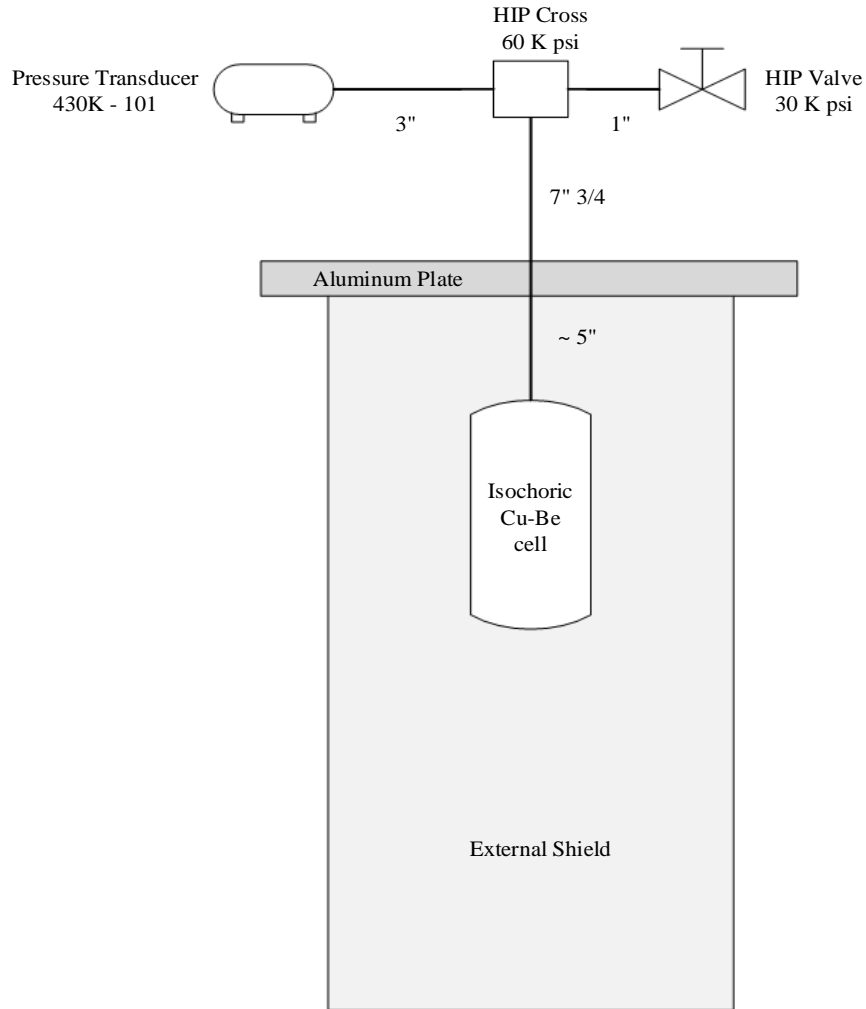


**Figure 12** Layout of high pressure isochoric cell

The noxious volume for the HIP corresponds to 2.3% of the volume of the cell. Due to the broad range in temperature and pressure in the HIP and with the aim to determine the isochoric densities as accurate as possible, it is imperative to consider the whole noxious volume and to determine new distortion parameters for this particular experiment. The procedure for calculating the parameters  $\alpha$  and  $\beta$  is the same as the one

explained in section 3.2.2.1 for the LPI isochores. Table 16 presents the pairs ( $P$ - $T$ ) and density values for isochores 2, 3 and 4. The densities of the transmission line and pressure transducer come from GERG 2008 and the densities of the cell come from MSD data. Table 17 has the values found for  $n$ ,  $\alpha$  and  $\beta$ . Compared to those presented in Table 9, parameter  $\alpha$  differs by two orders of magnitude from the value reported by Lau, however the value of the parameter  $\beta$  is fairly close. The new parameters seem to be more nearly in agreement with those reported by Cristancho. The average in the values of  $\alpha$  and  $\beta$  for isochores 2, 3 and 4 will be used.

**Table 16.** HPI values to calculate distortion parameters for Cu-Be

Isochore	T (K)	P (MPa)	$\rho_c$ (kmol/m <sup>3</sup> )	$\rho_t$ (kmol/m <sup>3</sup> )	$\rho_l$ (kmol/m <sup>3</sup> )
2	300.00	138.909	22.830	22.529	21.792
	325.00	156.694	22.742	23.200	22.498
	350.00	174.109	22.664	23.786	23.115
3	300.00	107.927	21.448	21.114	20.294
	325.00	123.137	21.348	21.855	21.080
	350.00	138.193	21.267	22.500	21.761
4	350.00	101.041	19.333	20.740	19.896
	400.00	124.565	19.202	21.920	21.148

**Table 17.** Parameters for Cu-Be

Isochore	$n$ (mol)	$\alpha$ (K <sup>-1</sup> )	$\beta$ (MPa <sup>-1</sup> )
2	0.355	1.240E-04	3.370E-05
3	0.175	1.520E-04	3.380E-05
4	0.141	1.220E-04	3.370E-05
<b>Average</b>		<b>1.327E-04</b>	<b>3.373E-05</b>

Determining the isochoric densities from the HPI requires Eqs. 16, 17 and the parameters for stainless steel and Cu-Be. Three different cases analyzed using the parameters  $\alpha$  and  $\beta$  for Be-Cu reported by Cristancho, Lau and the new parameters that appear in Table 17. Figure 13 shows the % deviation of the isochoric densities from the HPI with respect to GERG 2008 using Eq. 8. The new parameters for Be-Cu and the effect of the noxious volume allow calculation of the gas densities from isochoric ( $P$ - $T$ ) data with an uncertainty of  $\pm 0.5\%$  from 150 to 450 K at pressures up to 200 MPa. The numerical values for the isochoric densities from the HPI using the new parameters  $\alpha$  and  $\beta$  appear in Appendix B.

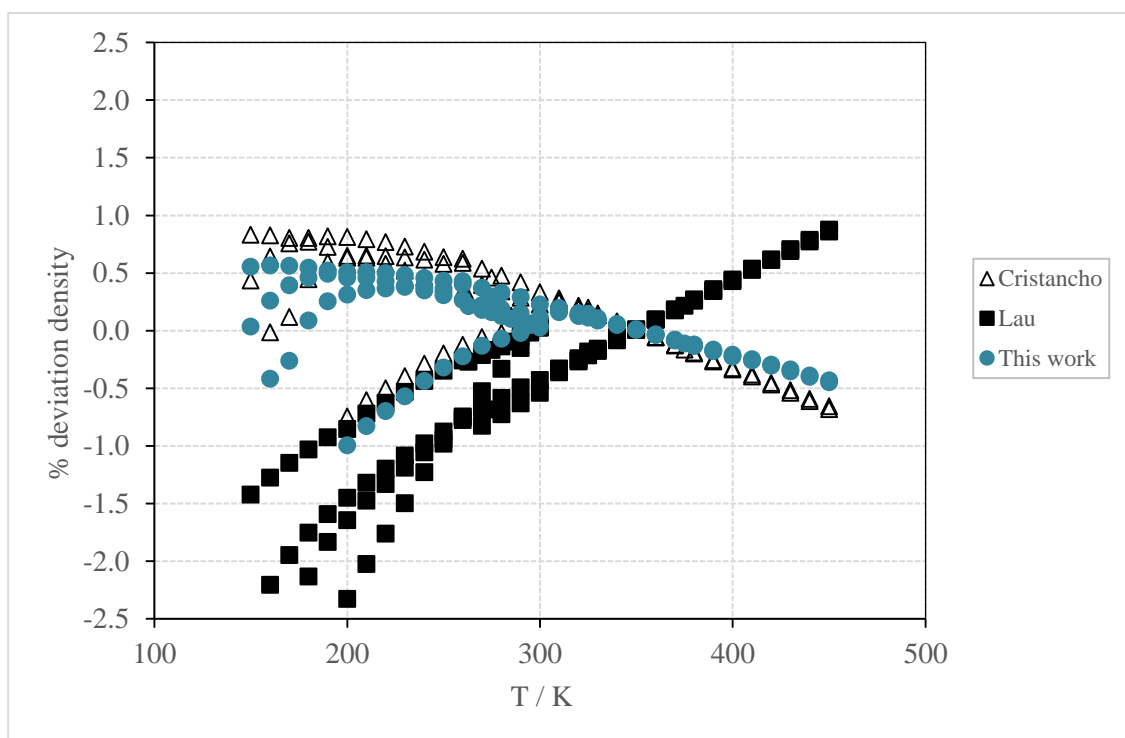


**Figure 13.** Percentage of deviation of isochoric densities from HPI



### 3.2.3 True Isochores Determination

The last step in the isochoric corrections consists of transforming the experimental pressure into values that conform to true isochores at constant densities ( $\rho^*$ ). To achieve this, it is necessary to quantify the difference between the reference density ( $\rho^*$ ) and the isochoric density ( $\rho_c$ ) along the isochoric path, then multiply this difference by the change in pressure with respect to the change in density at constant temperature. This final value corresponds to the correction for the experimental pressure to account for the noxious volume effect and the not truly isochore nature of the experimental data. The corrected pressures from the isochoric experiments, denoted as ( $P'$ ) are:

$$P' = P + \left( \frac{\partial P}{\partial \rho^*} \right)_T (\rho^* - \rho_c) \quad (24)$$

Because the changes in the fluid densities are small (up to 3.5%), Eq. 24 provides sufficiently accurate pressure adjustments when using values of derivatives from an accurate EoS such as GERG 2008. With the true isochoric set of data ( $P'$ - $\rho^*$ - $T$ ), it is possible to determine the first and second derivatives of pressure with respect to temperature for the 10 isochores from the LPI and the HPI. Appendix B report the values of the derivatives used in Eq. 24 as well as the new values of ( $P'$ ). Figure 14 presents the lines that corresponds to true isochores. It is noteworthy that the change in the slopes for the isochores from the HPI is more significant than the isochores from the LPI for which the true isochore line lies almost on top of the experimental values.

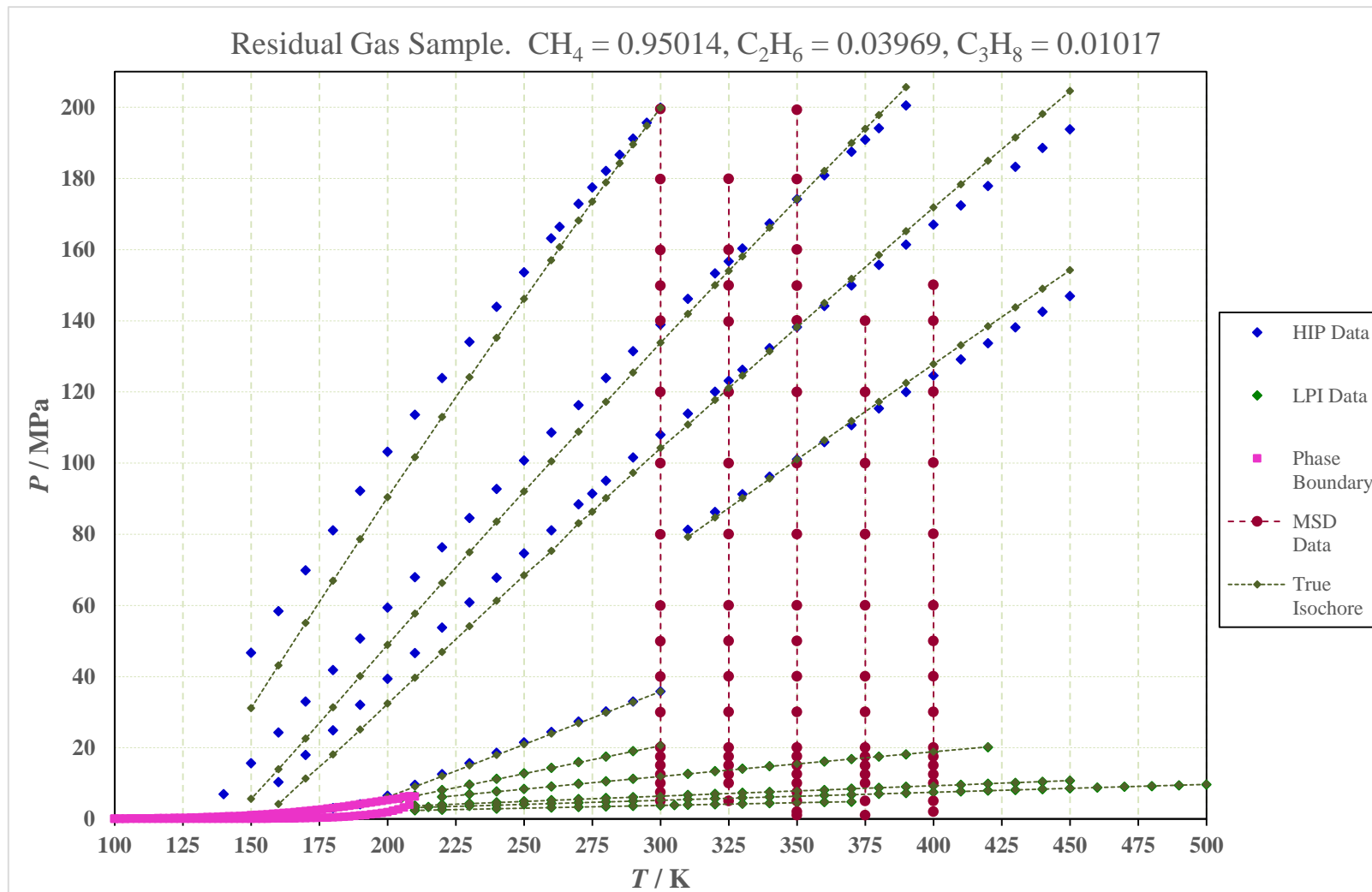


**Figure 14.** True isochores diagram

### 3.3 Stage 3. Derivative Determination

After determining the true isochoric pressure ( $P'$ ), the first and second derivatives of temperature with respect to pressure at constant density come from applying the strategy outlined in Figure 15.

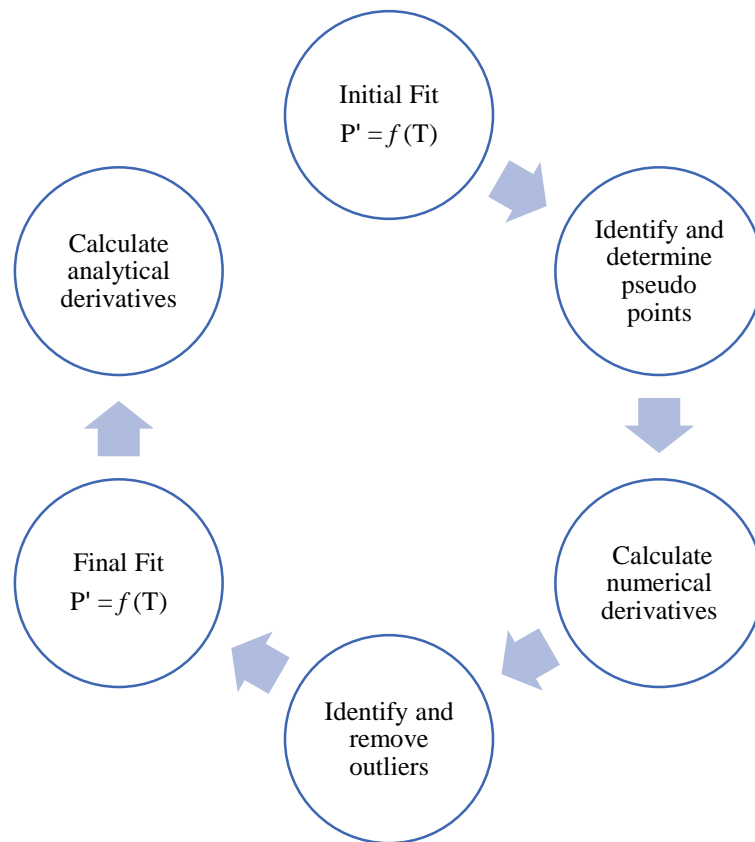


**Figure 15.** Strategy to calculate numerical and analytical derivatives

The initial fit of pressure as function of temperature is a 5<sup>th</sup> degree polynomial for isochores 1 to 3 and a 3<sup>rd</sup> polynomial for isochores 4 to 10.

$$P'_{fit} = \sum_{i=0} a_{(i+1)} T^i \quad (25)$$

Although the isochoric experiment provided measurements of  $P$ - $T$  in 10 K increments, some points were not measured. Thus, the next step is to establish the missing temperatures for every isochore, the missing  $P$ - $T$  are called “pseudo points”. This project required three pseudo points whose values of temperature and predicted pressure using Eq. 25 are reported in Table 18.

**Table 18.** Pseudo points in the isochoric experiment

Isochore	T (K)	P' (MPa)
7	410	19.542
10	250	3.014
10	230	2.702

The next step is to determine the numerical derivatives for evenly spaced temperatures. The central differences<sup>35</sup> method provides the numerical approximation of the first and second derivatives

$$\left. \frac{df}{dx} \right|_{f=f_0} = \frac{f_+ - f_-}{2\Delta x} \quad (26)$$

$$\left. \frac{d^2 f}{dx^2} \right|_{f=f_0} = \frac{f_+ - 2f_0 + f_-}{(\Delta x)^2} \quad (27)$$

Because the isochoric experiment contain fluctuations in temperature, pressure, transport of gas in the noxious volume and human error, some data points are “outliers” that are statistically inconsistent with the rest of the data<sup>36</sup>. Identification of the outliers for this work uses subjective criteria for choosing the points that deviate from the random or systematic tendency in the plots of the residuals in pressure (Figures 16, 18 and 20) after fitting the data using Eq. 25 and the plots of the numerical derivatives (Figures 22 to 41) using Eqs. 26 and 27. By definition the residual of a property X is the difference between the experimental value and the value predicted by the fit:

$$\text{Residual X} = X^{\text{exp}} - X_{\text{fit}} \quad (28)$$

Because the central differences method for determining the numerical derivatives always involve three points, it is possible to identify the outliers in each isochore (Table 19) that affect the calculations associated with high uncertainty in the data.

**Table 19.** Outliers in the isochoric experiment

Isochore	T (K)	P' (MPa)	Isochore	T (K)	P' (MPa)	Isochore	T (K)	P' (MPa)
1	260	157.011	3	290	97.209	6	220	8.08
1	250	146.157	3	280	90.161	7	270	9.819
1	200	90.42	3	270	83.088	8	410	9.564
2	325	153.941	3	260	75.309	8	360	8.131
2	300	133.775	3	170	11.355	9	220	3.432
2	270	108.796	4	420	138.429	9	215	3.319
3	400	171.827	5	270	26.888	10	330	4.214
3	300	104.212	6	260	14.318	10	320	4.084

It is valid to remove the outliers to improve the overall performance in the fit of pressure as a function of temperature to determine the analytical derivatives. The rounded evaluation of polynomial, exponential and rational equations used the following criteria:

1. The model must be straightforward in representing the isochoric behavior but also determine precisely the first and second derivatives.
2. The scatter band in the plot of the residuals of pressure.
3. The coefficient values and their standard deviations.
4. The root mean square (rms) value.

$$rms = \sqrt{\frac{1}{n} \sum_{i=1}^n |P' - P_{fit}|^2} \quad (29)$$

The rational equation expressed as Eq. 30 appears to be the most appropriate equation for modeling the ( $P'$ - $T$ ) data throughout the isochoric experiment.

$$P = \frac{a_1 + a_2T + a_3T^2}{b_1 + b_2T + b_3T^2} \quad (30)$$

The values of the coefficients, standard error, rms and number of points used per isochore for modeling the data appear in Appendix C. The residuals in pressure calculated using Eqs. 28 and 30 appear in Figures 17, 19 and 21. Besides the numerical and analytical derivatives, the results of this stage indicate that the reproducibility in the values of

pressure is  $\pm 0.1$  MPa and  $\pm 0.01$  MPa for the measurements from the high and low pressure isochoric apparatus respectively.

Finally, the analytical first and second derivatives of Eq. 30 appears in Eqs. 31 and 32 respectively:

$$\left(\frac{\partial P'}{\partial T}\right)_\rho = \frac{(-a_1 - a_2T - a_3T^2)(b_2 + 2b_3T) + (b_1 + b_2T + b_3T^2)(a_2 + 2a_3T)}{(b_1 + b_2T + b_3T^2)^2} \quad (31)$$

$$\left(\frac{\partial^2 P'}{\partial T^2}\right)_\rho = \frac{\left\{ \begin{array}{l} (b_1 + b_2T + b_3T^2)^2 [2b_3(-a_1 - a_2T - a_3T^2) + 2a_3(b_1 + b_2T + b_3T^2)] - \\ 2(b_2 + 2b_3T)(b_1 + b_2T + b_3T^2) \left[ \begin{array}{l} (b_2 + 2b_3T)(-a_1 - a_2T - a_3T^2) \\ + (b_1 + b_2T + b_3T^2)(a_2 + 2a_3T) \end{array} \right] \end{array} \right\}}{(b_1 + b_2T + b_3T^2)^4} \quad (32)$$

Because of extension of the data, the results of this section appear as plots and the numerical values for the first and second derivatives appear in Appendix D. Figures 22 to 41 show the tendency of the first and second derivatives as functions of temperature for the ten isochores. Furthermore, three sets of points appear per graph: the numerical derivatives, the analytical derivatives and the values predicted by GERG 2008 EoS.

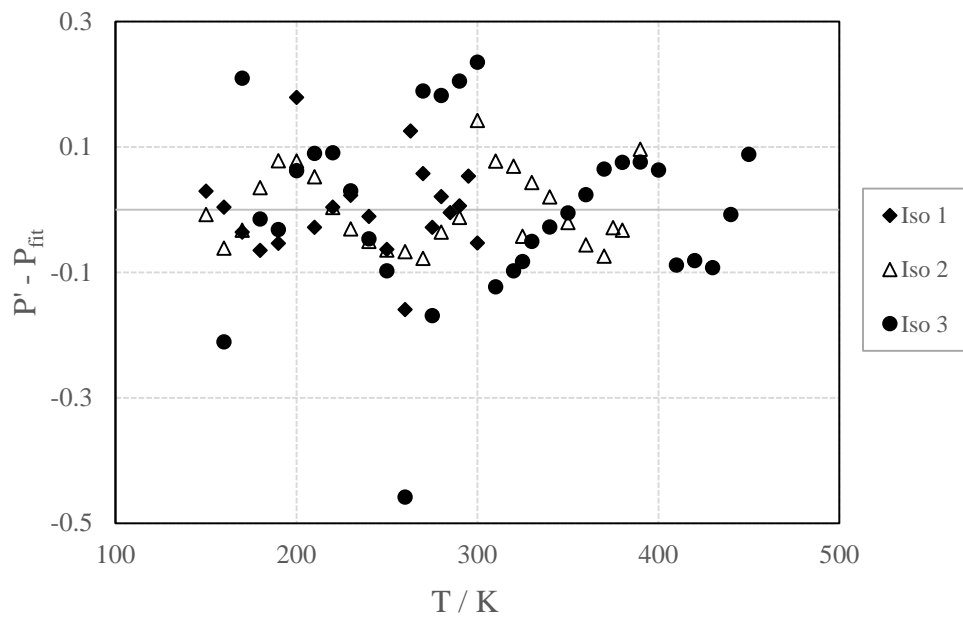


**Figure 16** Residuals in pressure for isochores 1 to 3 using Eq. 25

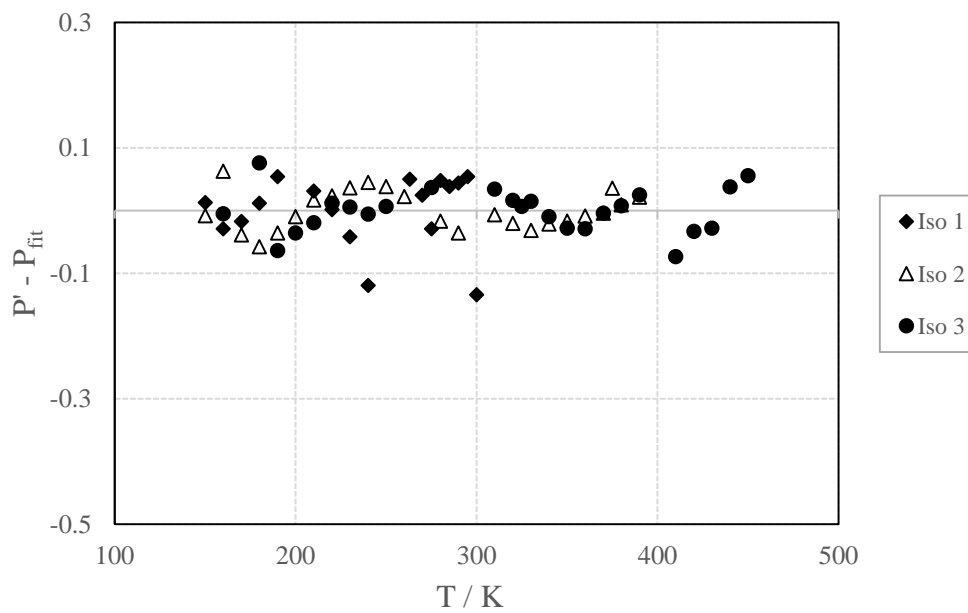


**Figure 17** Residuals in pressure for isochores 1 to 3 using Eq. 30



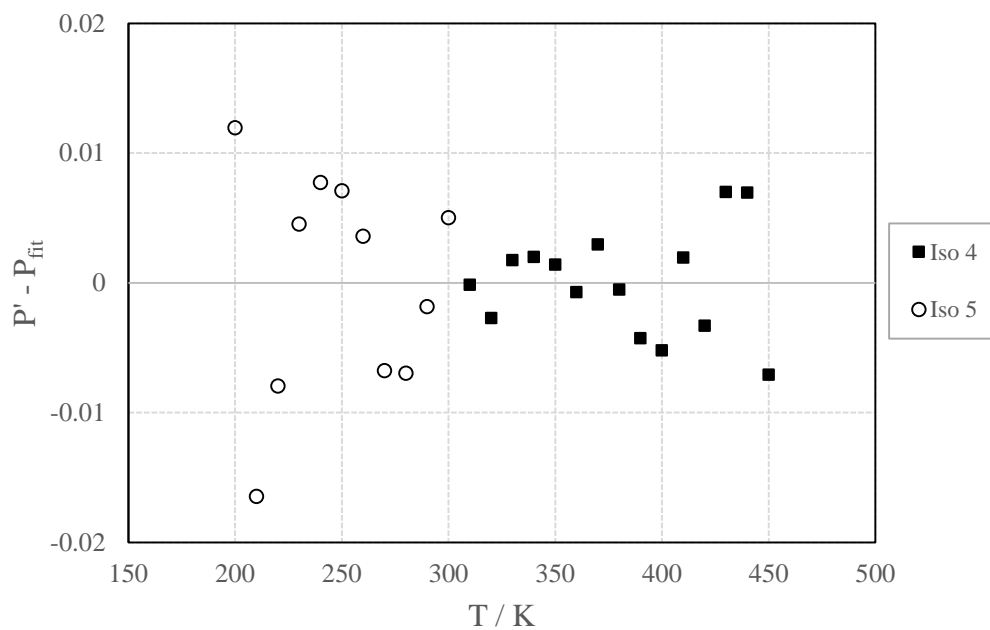


**Figure 18** Residuals in pressure for isochores 4 and 5 using Eq. 25

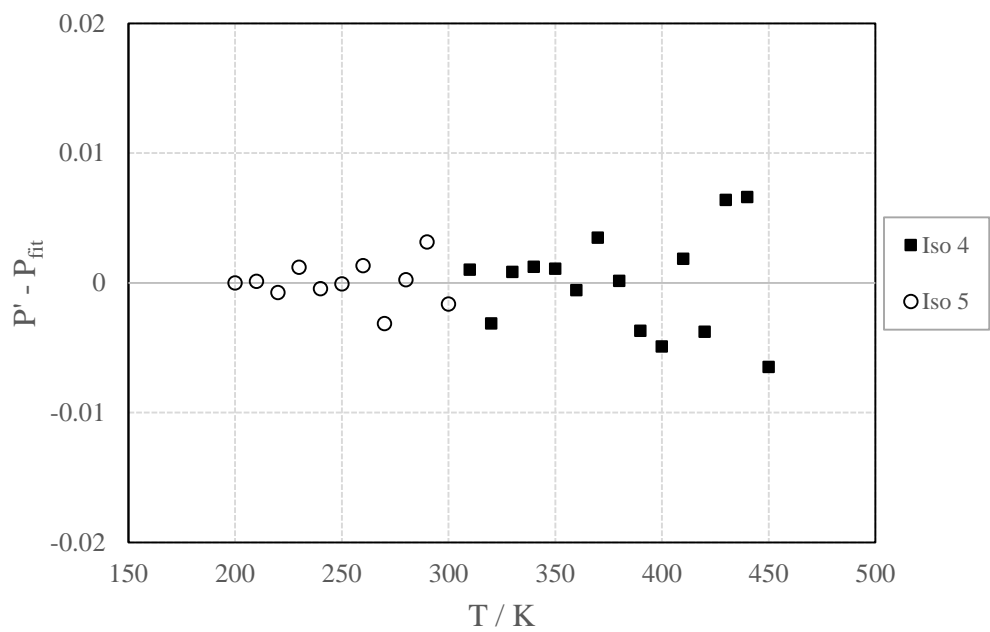


**Figure 19** Residuals in pressure for isochores 4 and 5 using Eq. 30

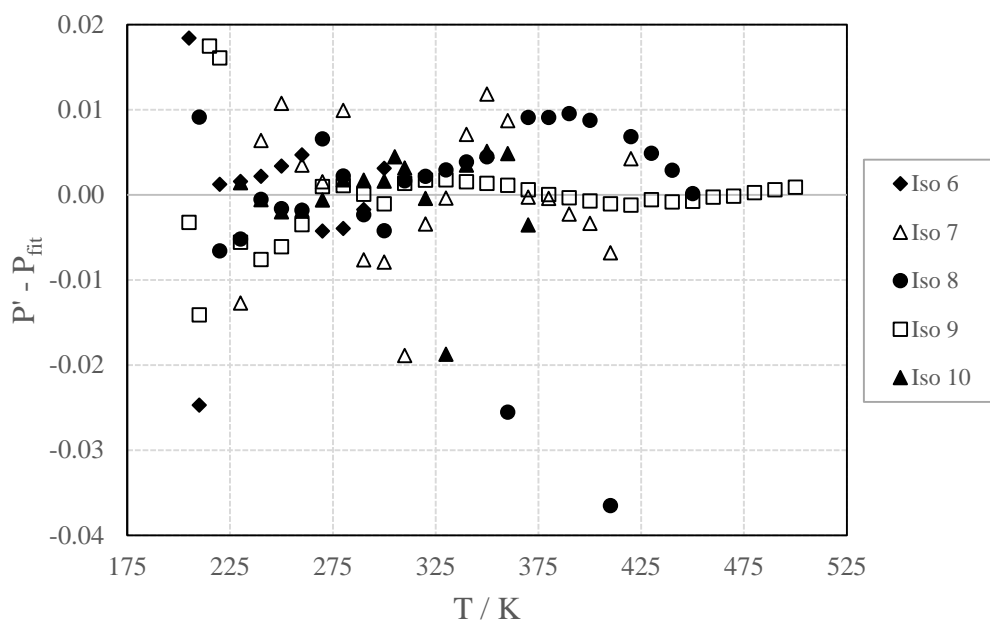


**Figure 20** Residuals in pressure for isochores 6 to 10 using Eq. 25

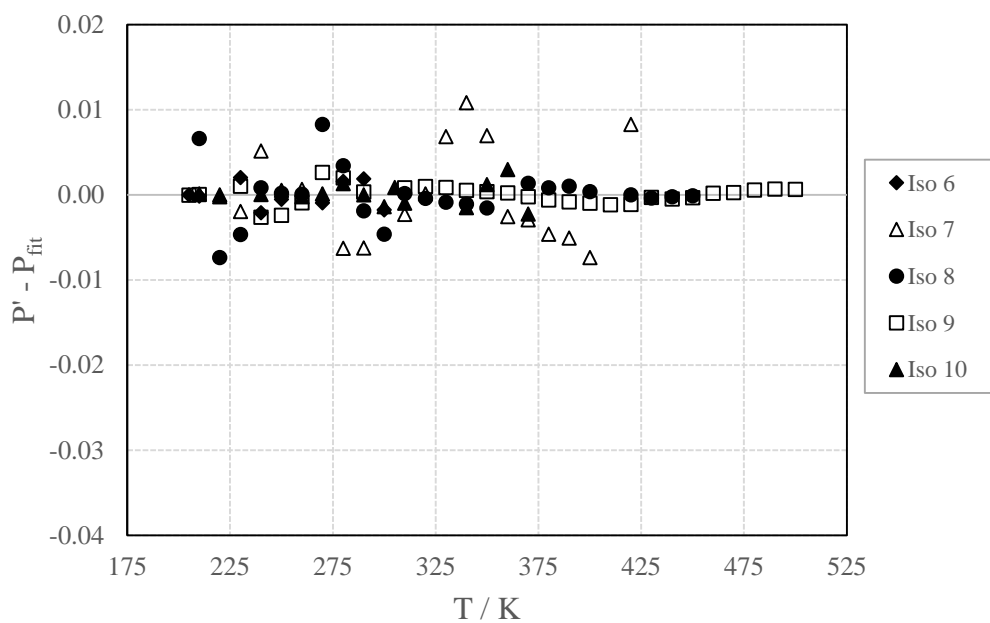


**Figure 21** Residuals in pressure for isochores 6 to 10 using Eq. 30

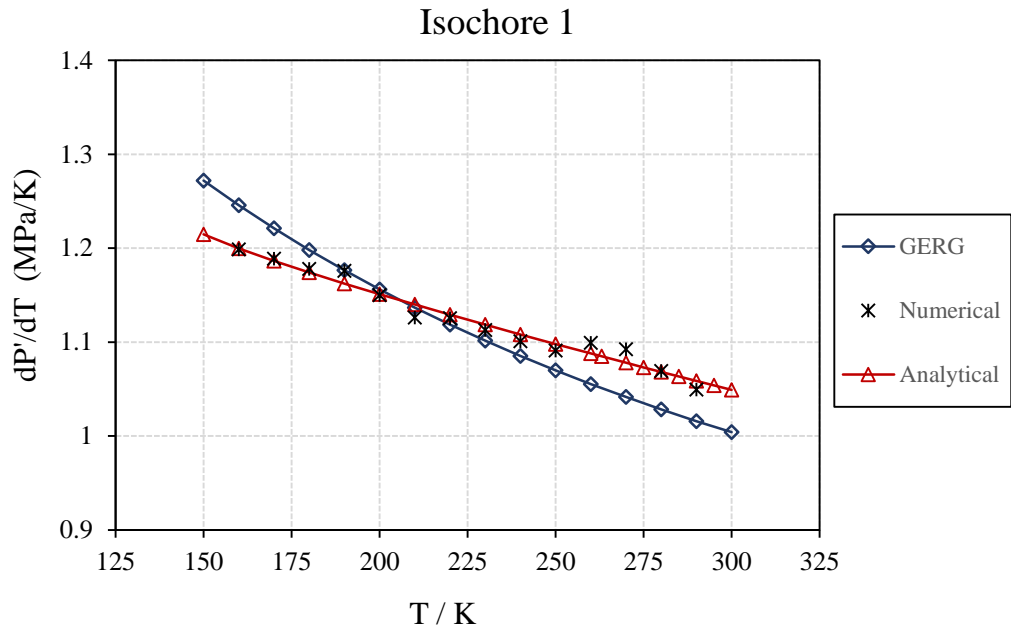


**Figure 22** First derivative for isochore 1

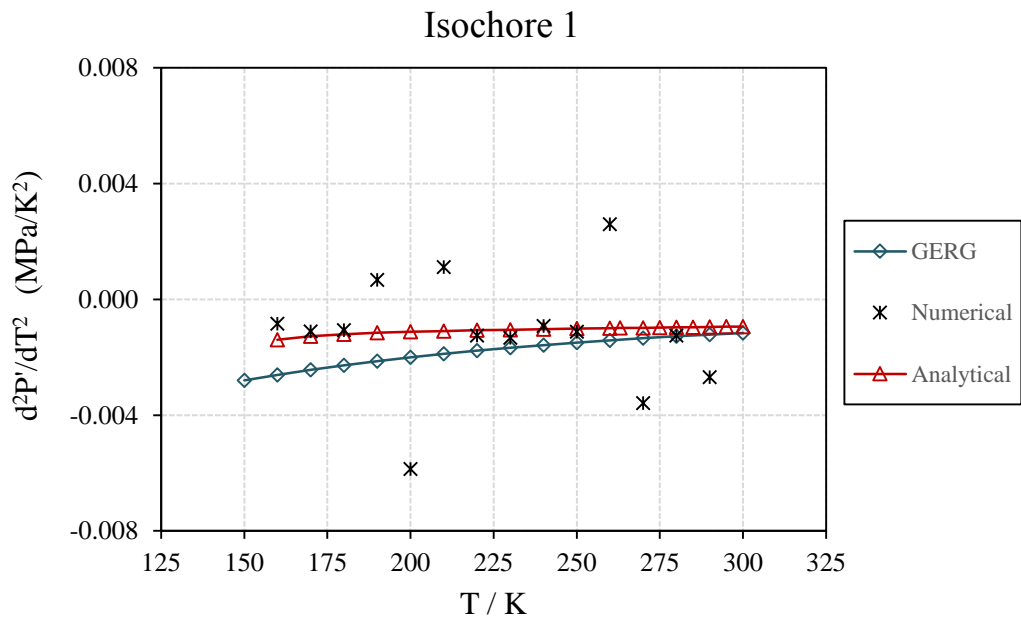


**Figure 23** Second derivative for isochore 1

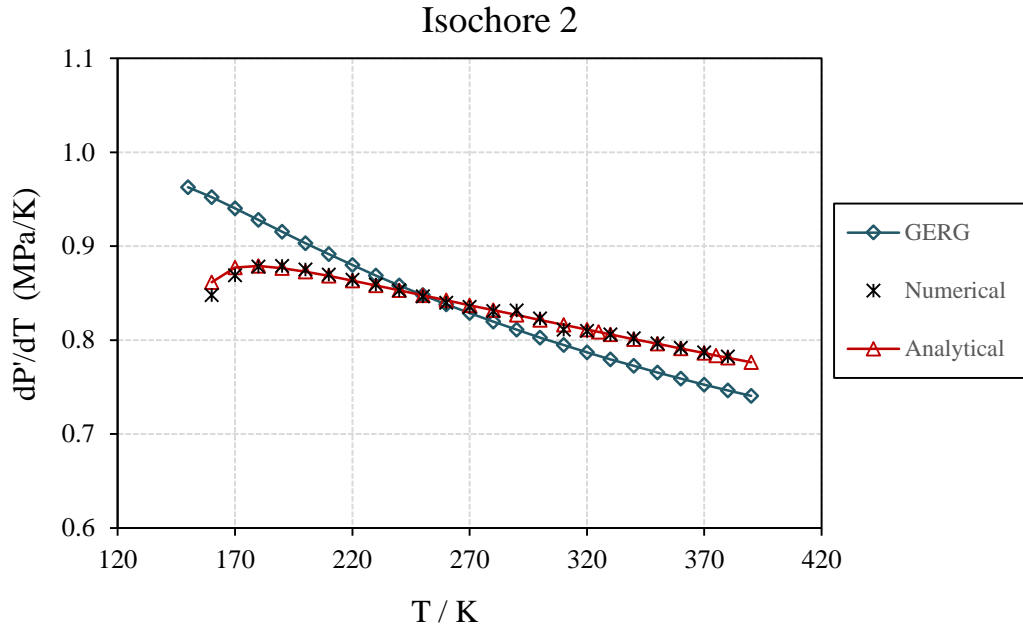


**Figure 24** First derivative for isochore 2

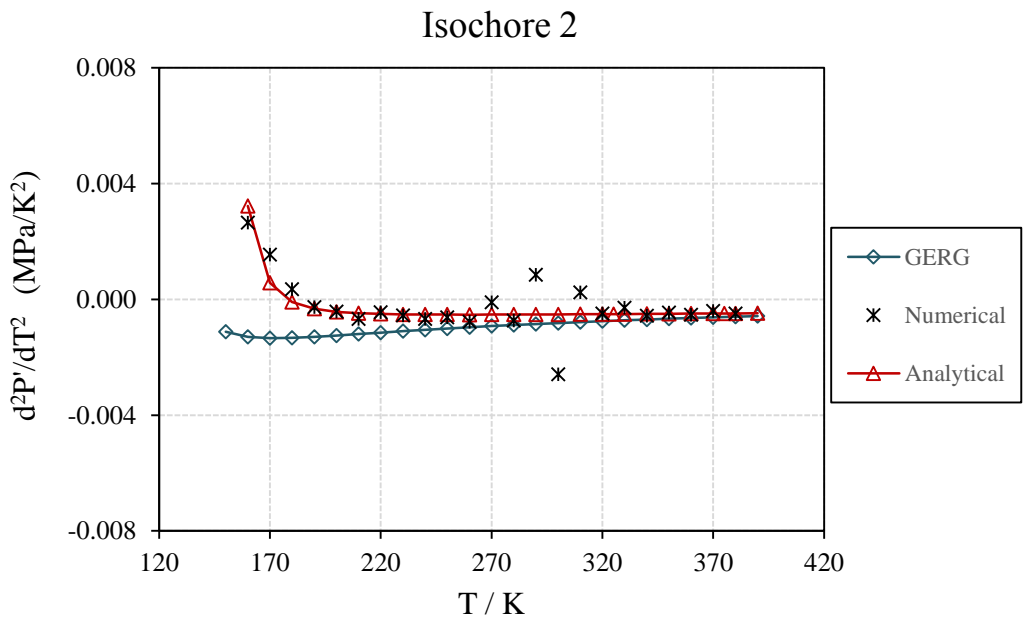


**Figure 25** Second derivative for isochore 2

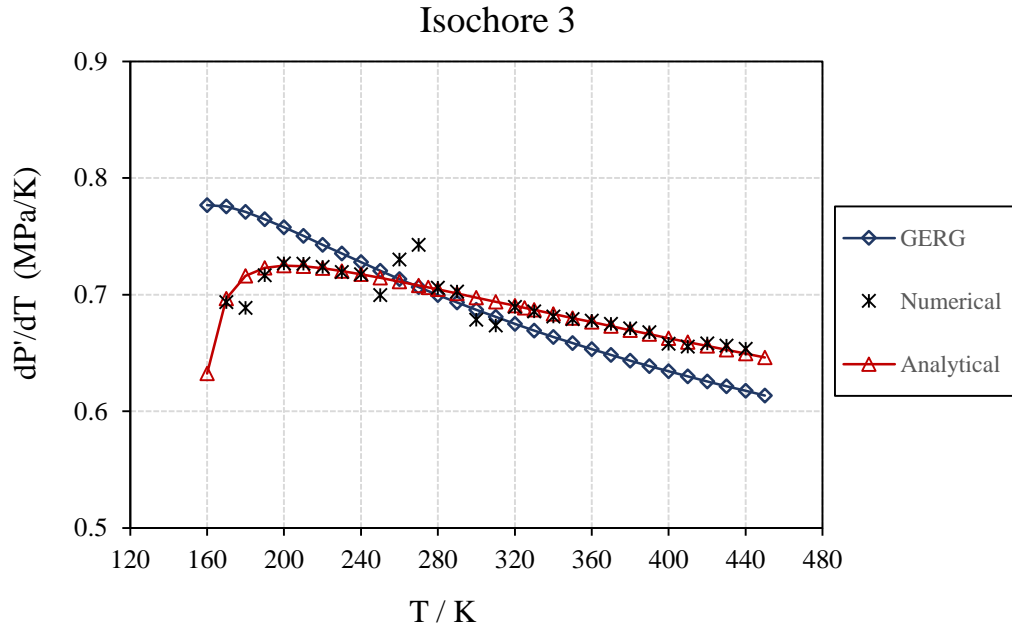


**Figure 26** First derivative for isochore 3

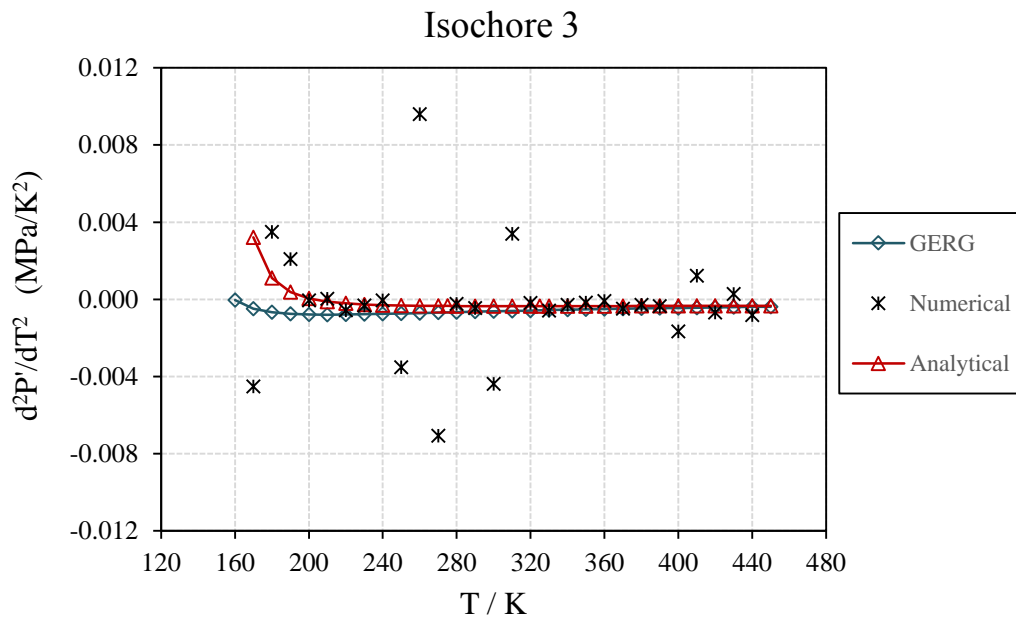


**Figure 27** Second derivative for isochore 3

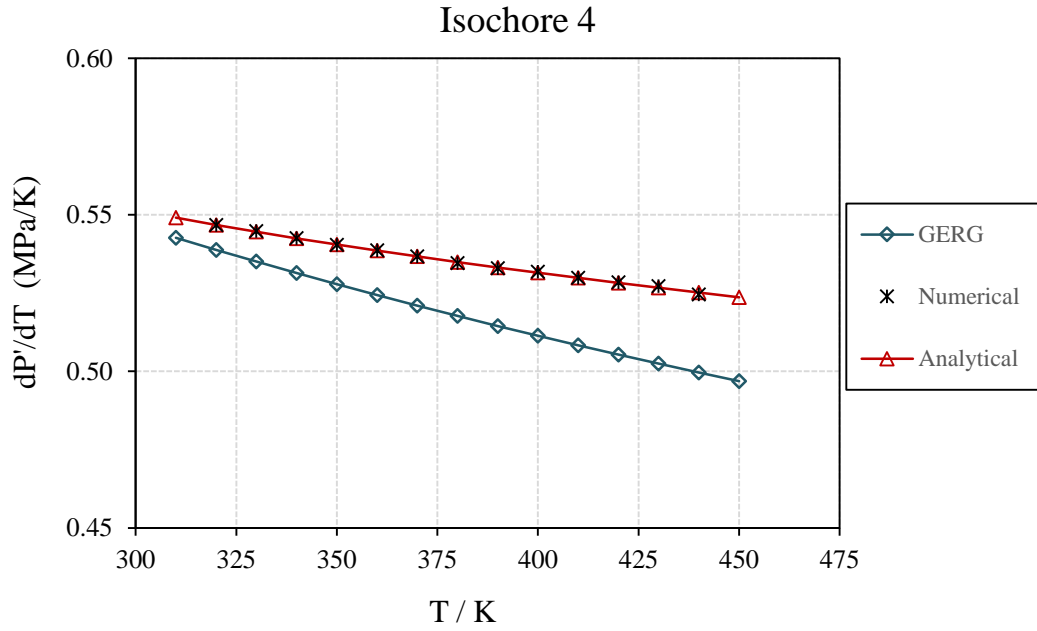


**Figure 28** First derivative for isochore 4

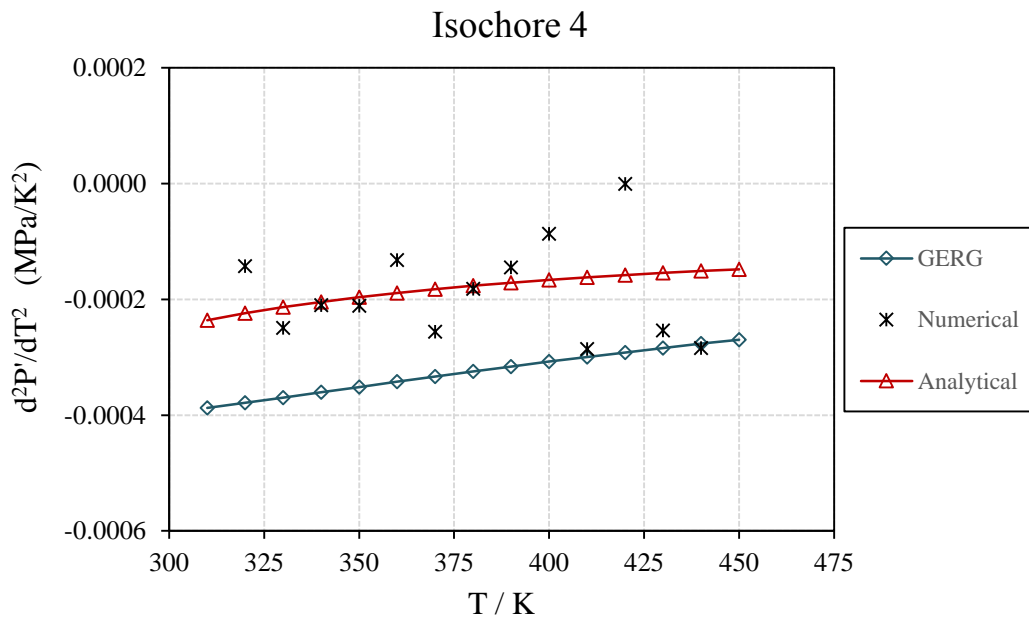


**Figure 29** Second derivative for isochore 4

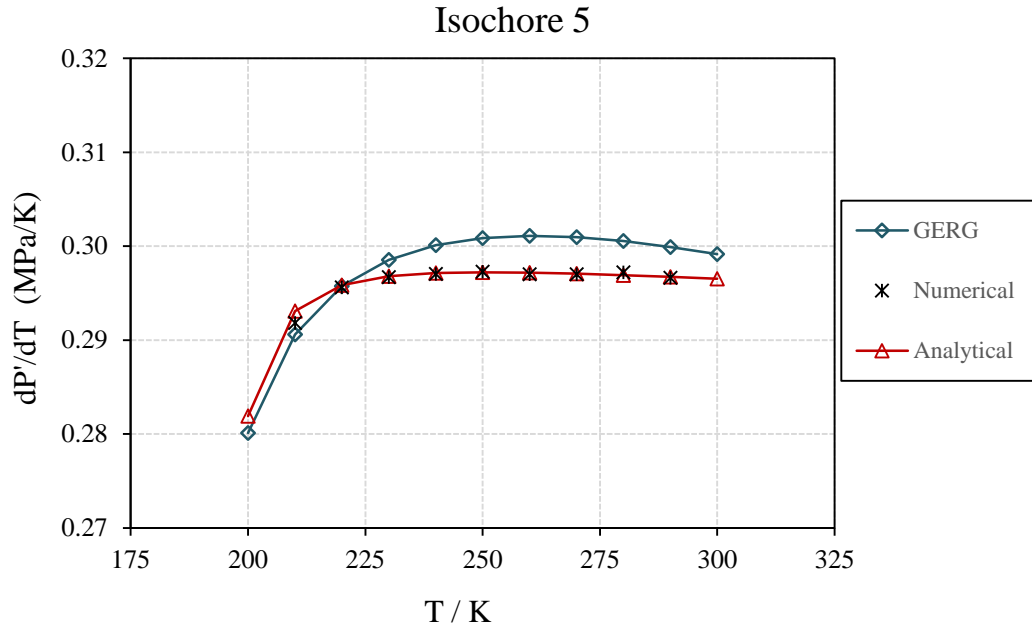


**Figure 30** First derivative for isochore 5

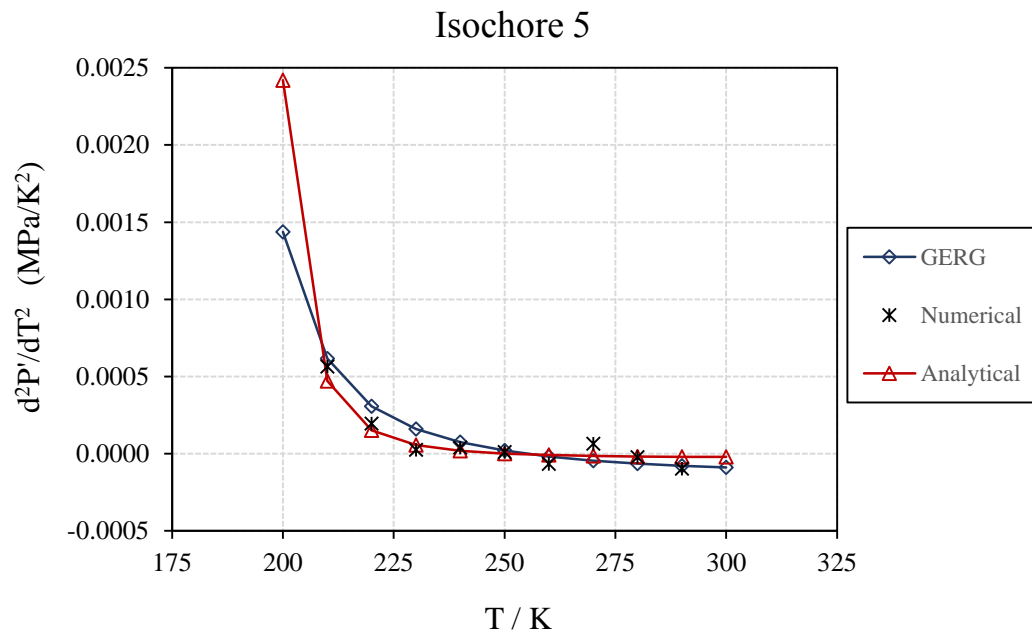


**Figure 31** Second derivative for isochore 5

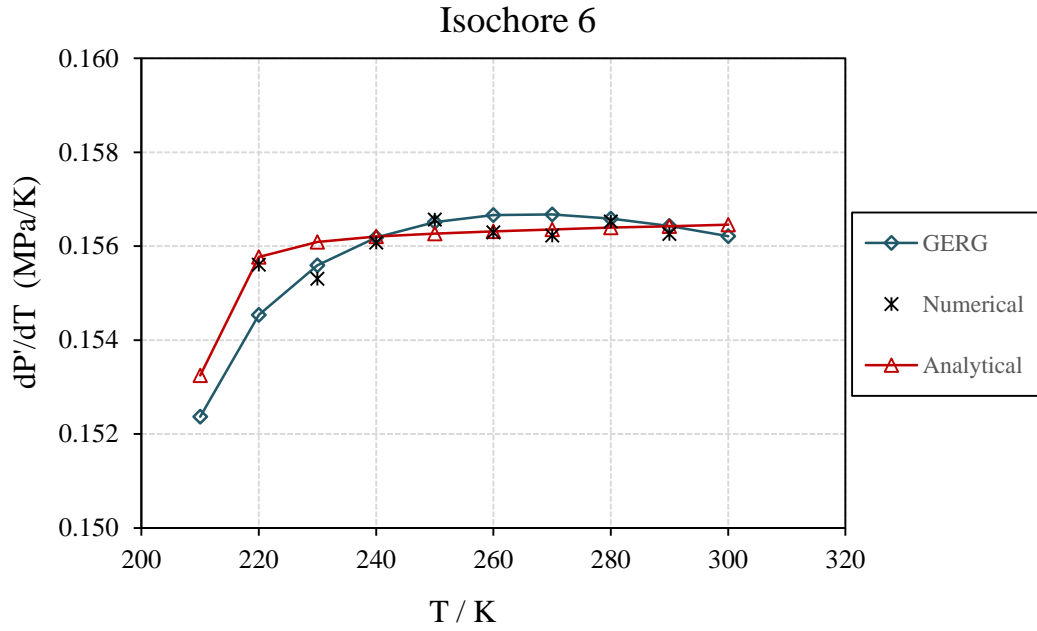


**Figure 32** First derivative for isochore 6

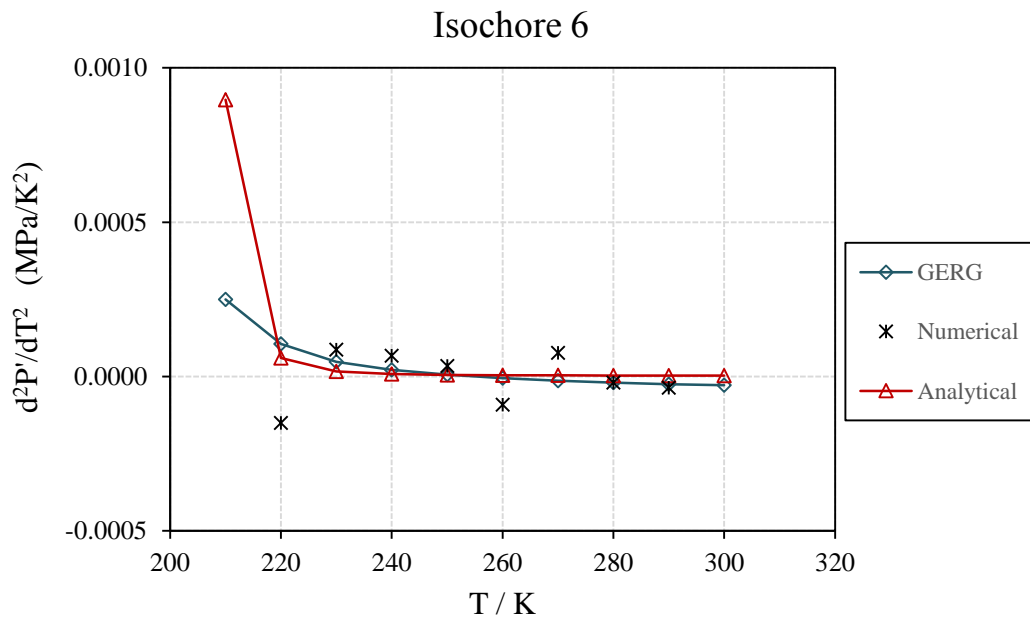


**Figure 33** Second derivative for isochore 6



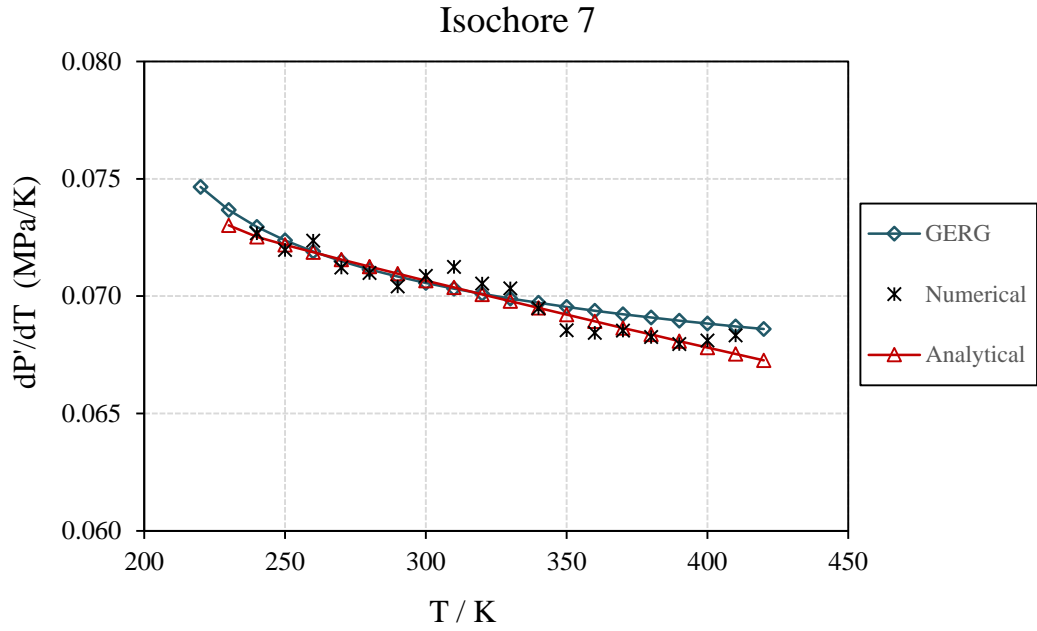


**Figure 34** First derivative for isochore 7

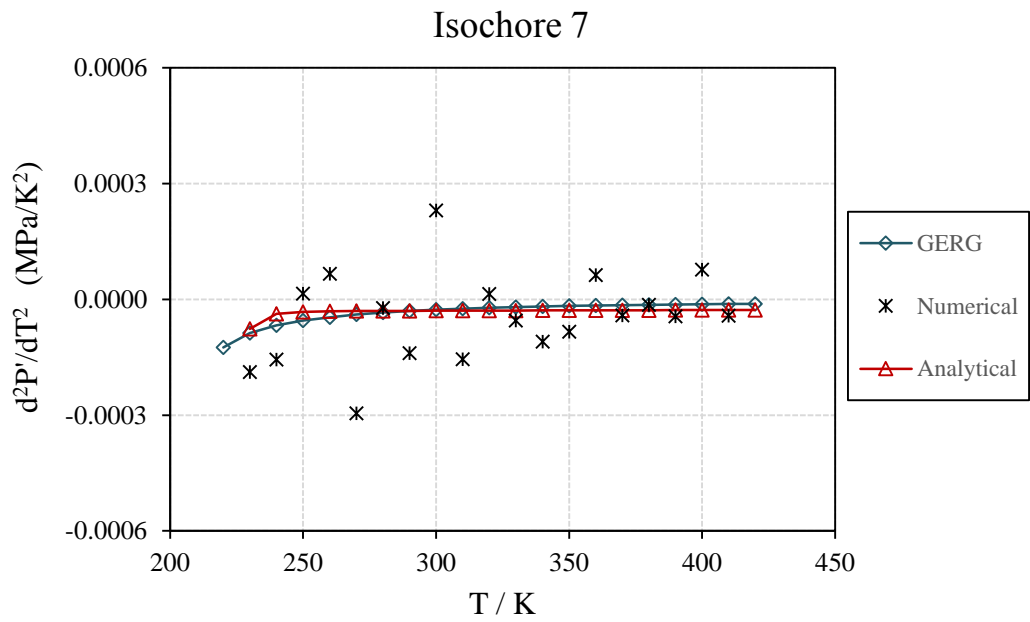


**Figure 35** Second derivative for isochore 7

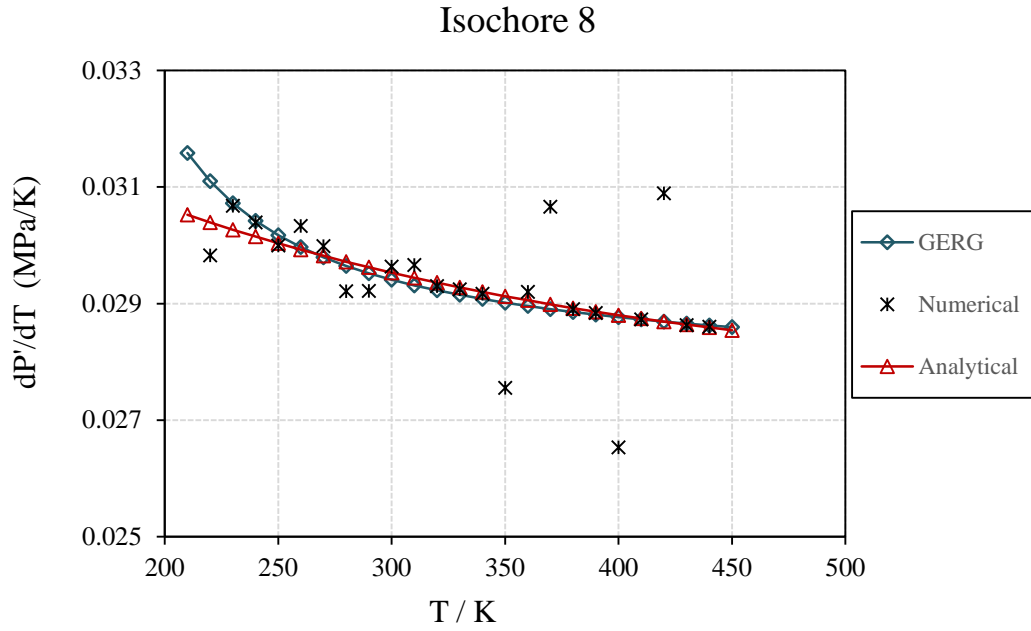


**Figure 36** First derivative for isochore 8

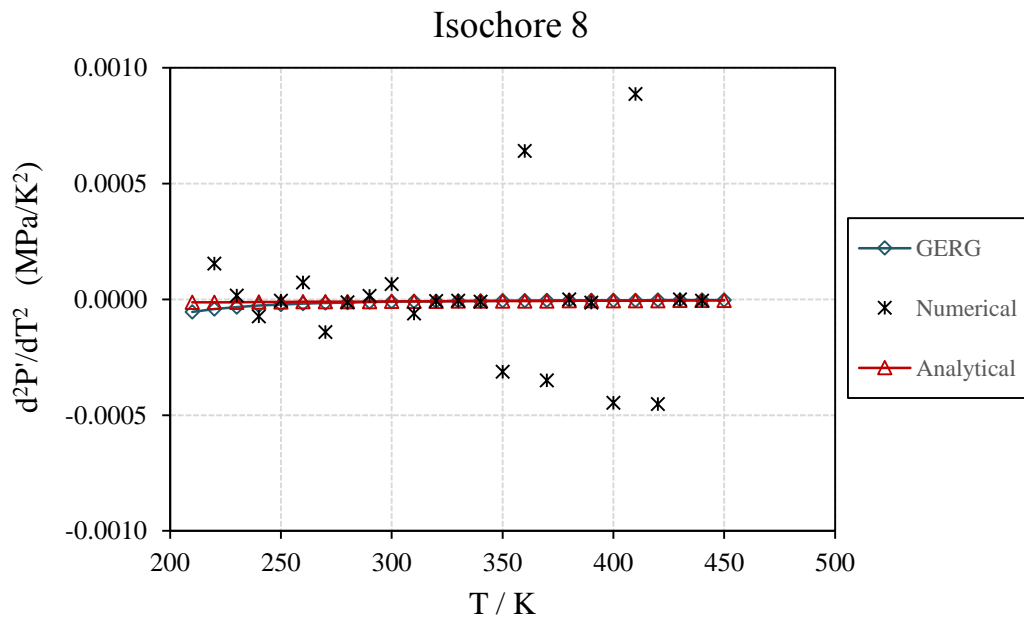


**Figure 37** Second derivative for isochore 8

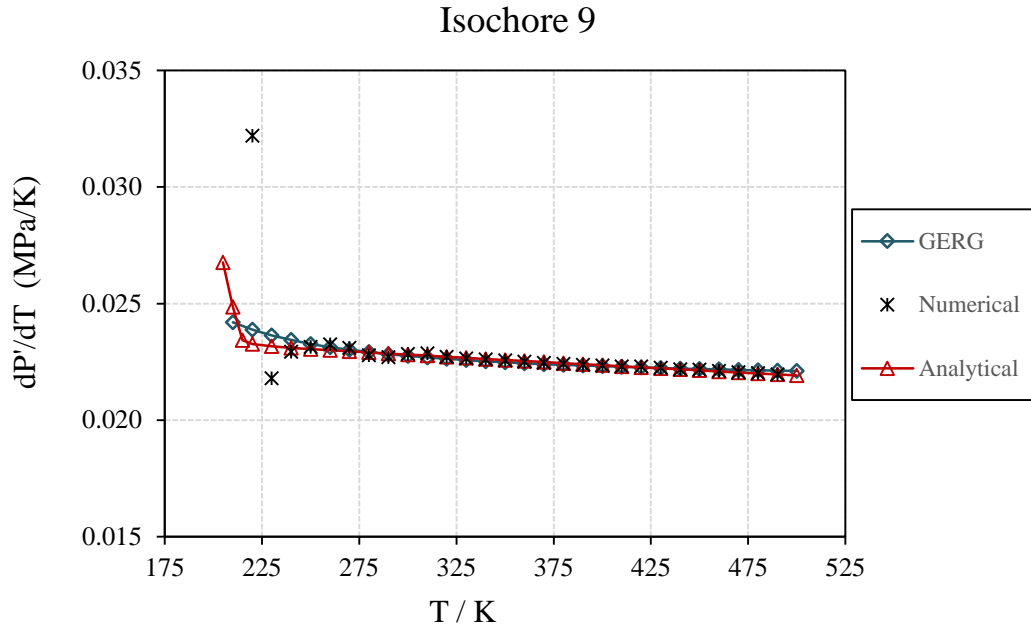


**Figure 38** First derivative for isochore 9

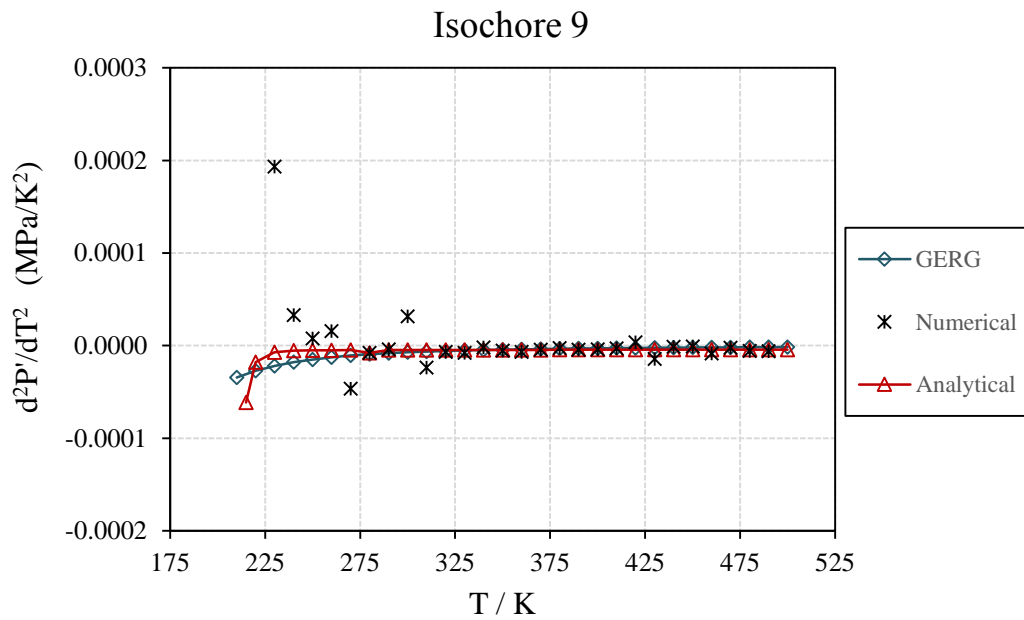


**Figure 39** Second derivative for isochore 9

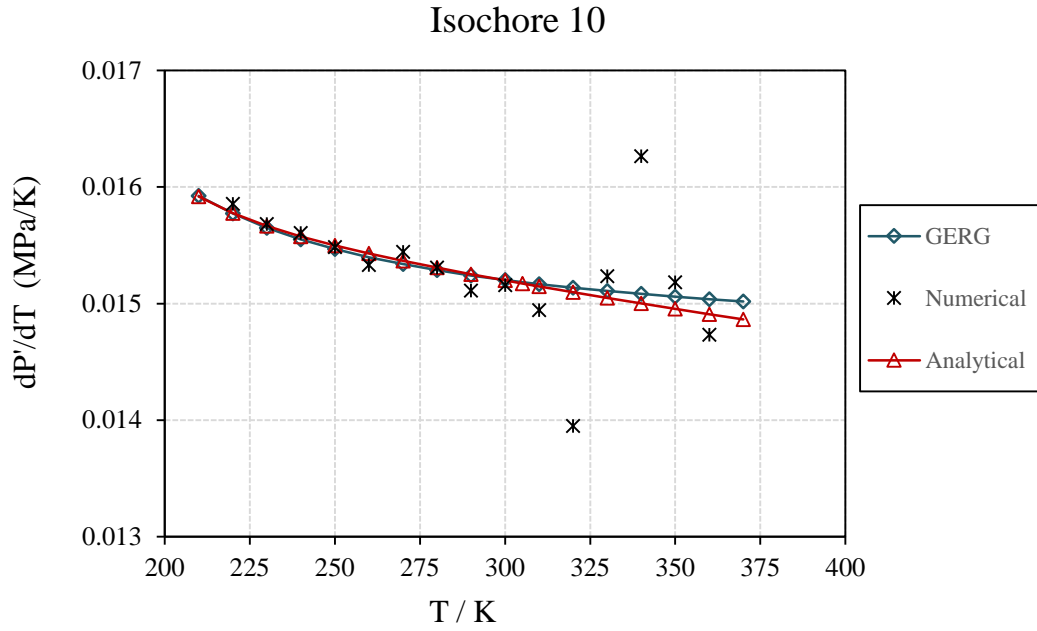


**Figure 40** First derivative for isochore 10

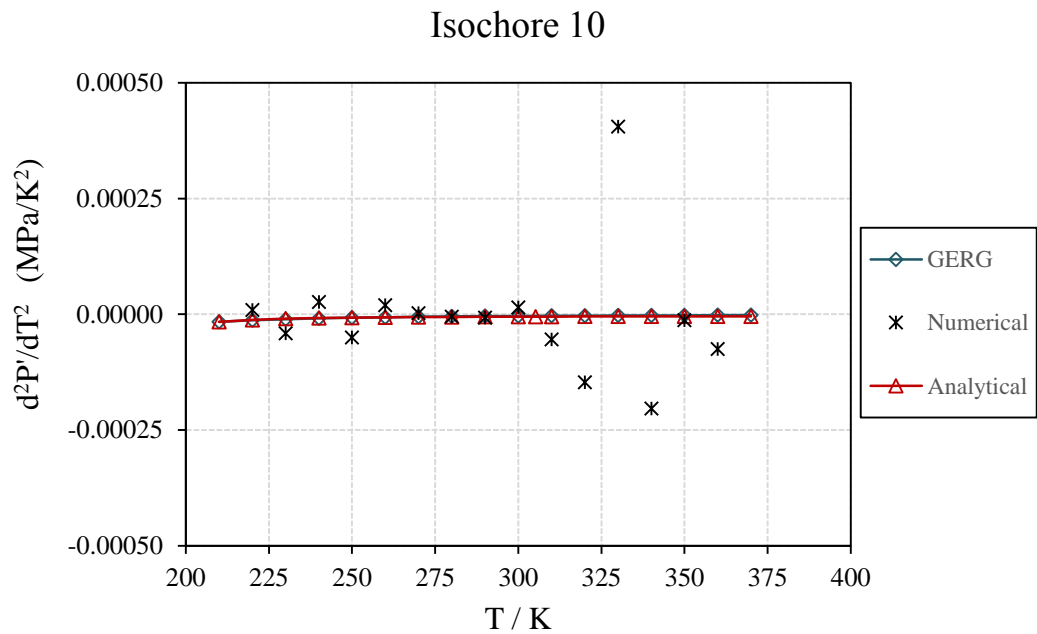


**Figure 41** Second derivative for isochore 10

### 3.4 Stage 4. Residual and Absolute Properties

A residual density function is the difference between the value of a property for a real fluid and the value of the same property for an ideal gas at the same temperature and density:

$$X^r(T, \rho) = X(T, \rho) - X^{ig}(T, \rho) \quad (33)$$

By transformation of thermodynamic properties (Appendix E), it is possible to have an expression for the residual heat capacity at constant volume as function of the second derivative of pressure with respect to temperature at constant density and the inverse of the square of the density:

$$C_v^r = -T \int_0^\rho \left( \frac{\partial^2 P'}{\partial T^2} \right)_\rho \frac{d\rho}{\rho^2} \quad (34)$$

The integration indicated in Eq. 34 proceeds along isothermal paths, so it is necessary to reorganize the isochoric data into isothermal sets to perform the integration. Because the experimental matrix for this residual gas mixture has 10 isochores measured at evenly spaced temperature, it would seem that every isothermal set would contain 10 pairs of points of the second derivative and the square of the molar density. Unfortunately, the isochores do not overlap the whole range of temperature as seen in Figure 14. Table 20 presents the number of pairs and the corresponding isochores for the 24 set of isotherms analyzed in this section.

**Table 20.** Subset of temperatures for integral of residual heat capacity

	Subset 1	Subset 2	Subset 3		
Temperature Range (K)	220 - 300	310 - 370	380 - 390	400 - 420	430 - 450
Pairs of points ( $d^2P/dT^2$ ) - ( $\rho^{*2}$ )	9	7	6	5	4
Isochores	1,2,3,5,6,7,8,9 and 10	2,3,4,7,8,9 and 10	2,3,4,7,8 and 9	3,4,7,8 and 9	3,4,8 and 9

Table 20 has three subsets of temperature depending upon the inclusion of the high density isochores, i.e isochores 1 to 3. The pair of points correspond to the square of the reference molar density ( $\rho^{*2}$ ) and the analytical second derivatives ( $d^2P/dT^2$ ) obtained from stage 3. The residual heat capacity calculated in this stage uses only analytical integration of Eq. 34. The use of numerical second derivatives is useless here because of significant scatter and no clear tendency along isotherms. Stage 5 contains an analysis of the uncertainty in the residual heat capacity.

Figures 42 to 44 represent the integrand of Eq. 34 as a function of the reference molar density for the three subsets of temperatures in Table 13. The integrands appear to dictate a quadratic model represented by Eq. 35.

$$\left( \frac{\partial^2 P'}{\partial T^2} \right)_{\rho} = c_1 \rho^2 + c_2 \rho + c_3 \quad (35)$$

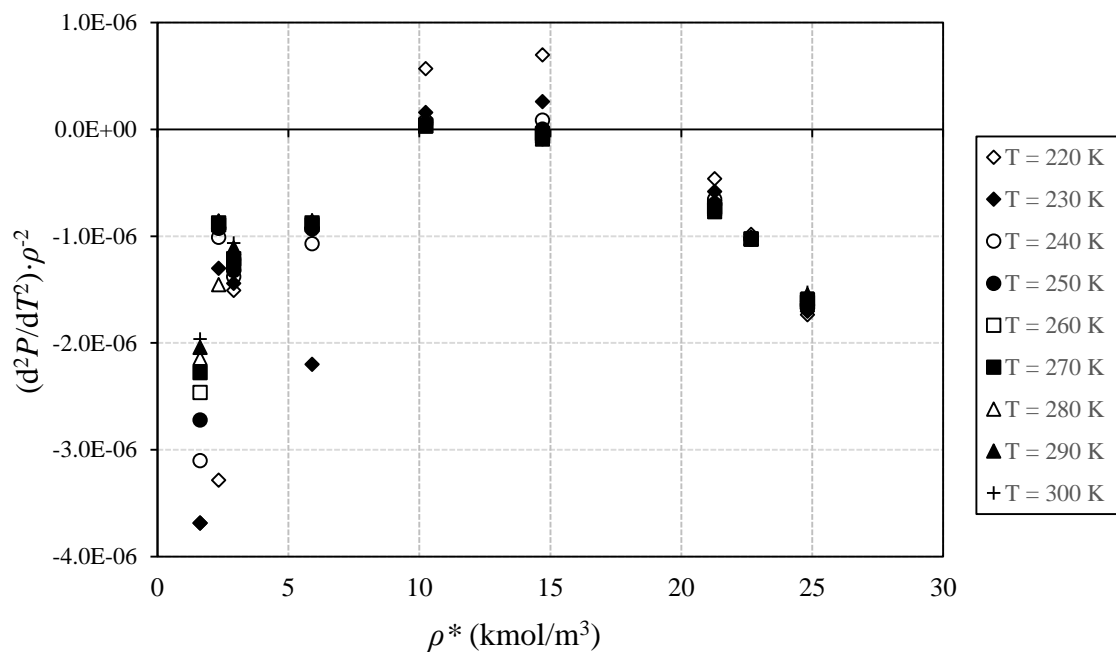


**Figure 42.** Integrand function of  $(C_v')$  equation for subset 1

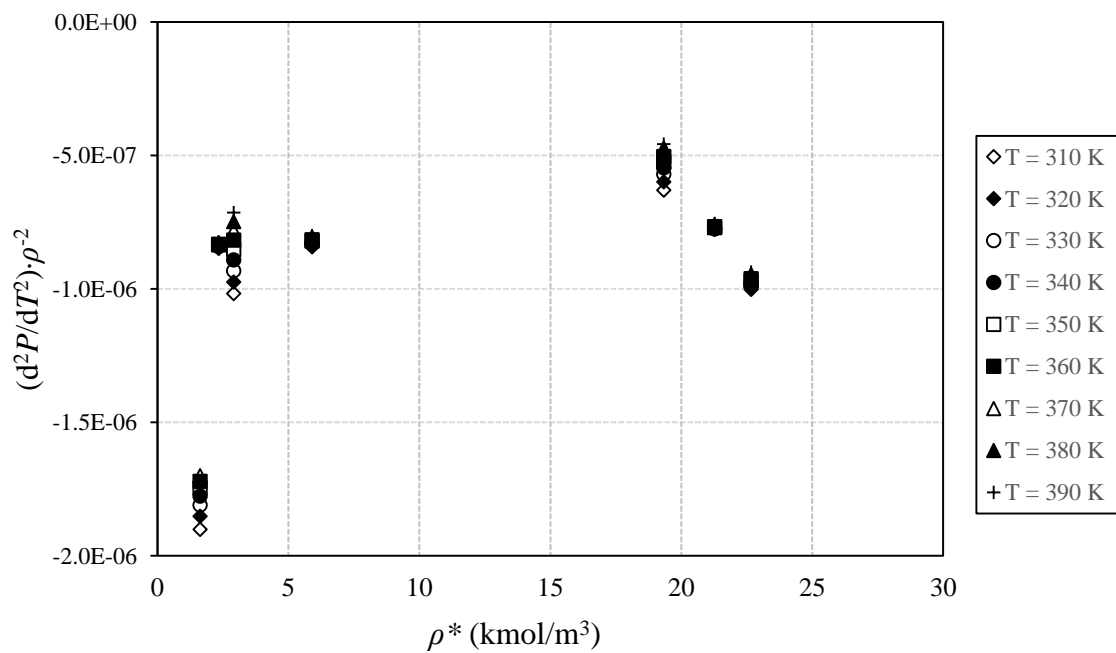


**Figure 43.** Integrand function of  $(C_v')$  equation for subset 2

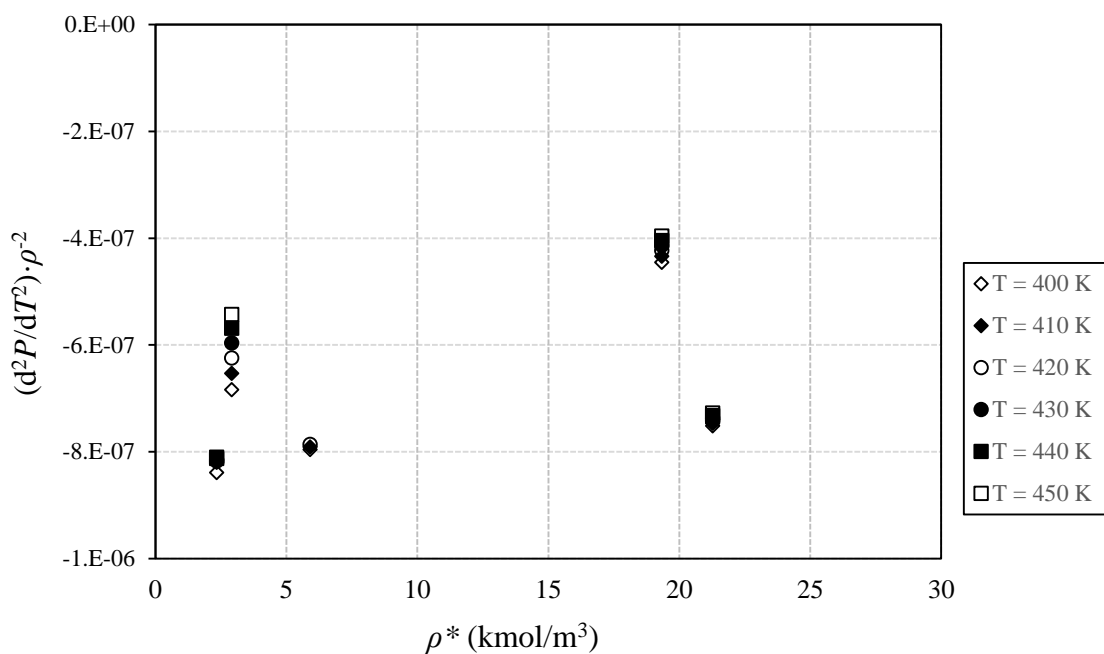


**Figure 44.** Integrand function of  $(C_v^r)$  equation for subset 3

The values of the coefficients, standard error, rms, and interval of confidence of the integrand function represented by Eq. 35 for each isotherm appear in Appendix F. The residual heat capacity that results after analytical integration of Eqs. 35 is:

$$C_v^r = -T \left( \frac{c_1}{3} \rho^3 + \frac{c_2}{2} \rho^2 + c_3 \rho \right) \quad (36)$$

The residual values of the heat capacity calculate with Eq. 36 are compared to the predictions from GERG 2008 EoS and appear in Figures 45 to 47 for subsets 1 to 3 respectively.



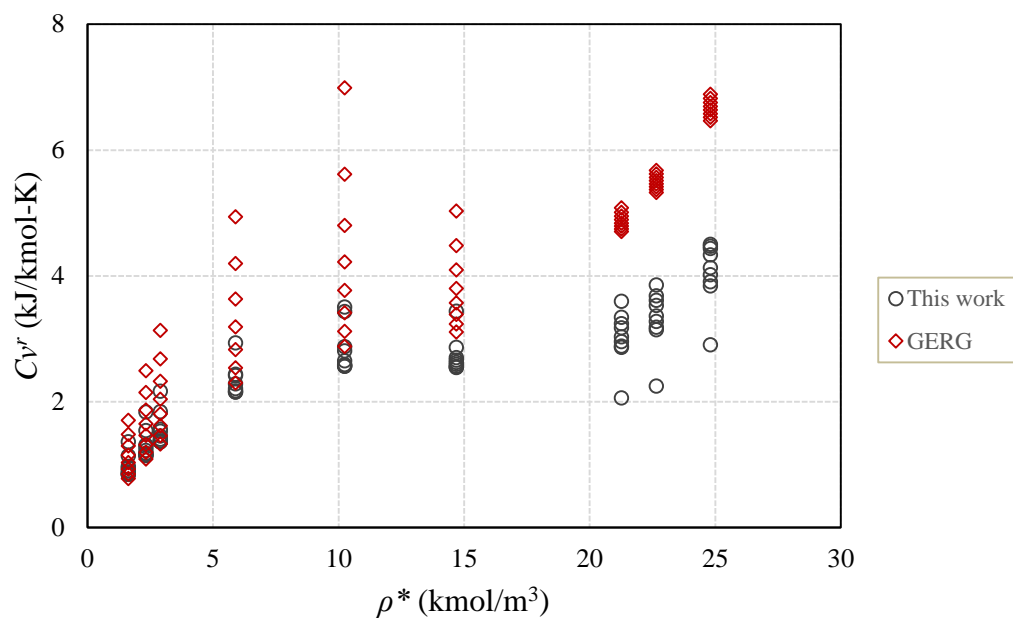


**Figure 45.** ( $C_v^r$ ) for subset 1. (220 – 300 K)

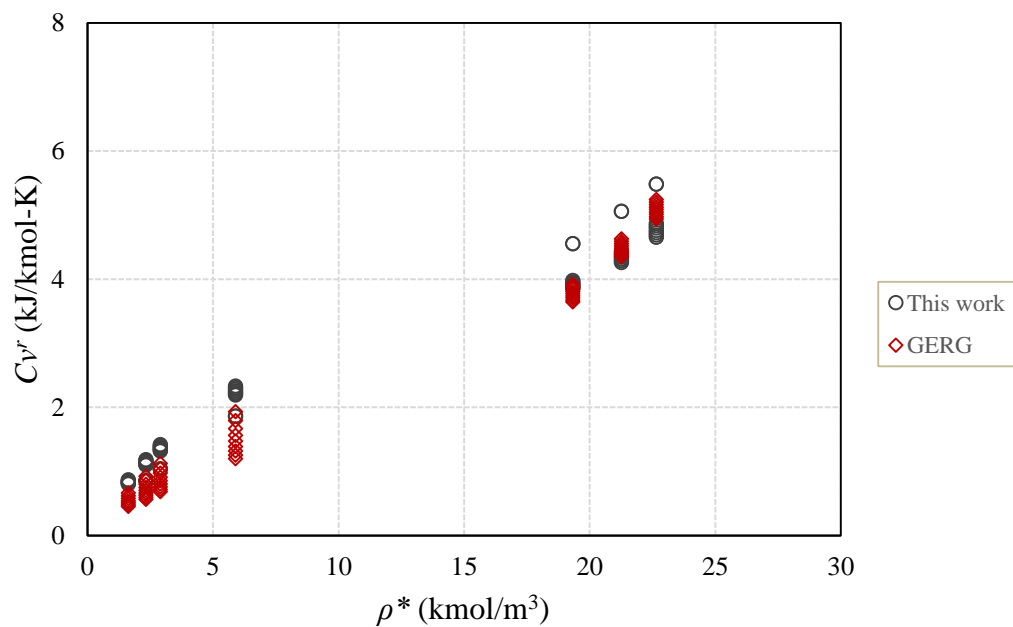


**Figure 46.** ( $C_v^r$ ) for subset 2. (310 – 390 K)

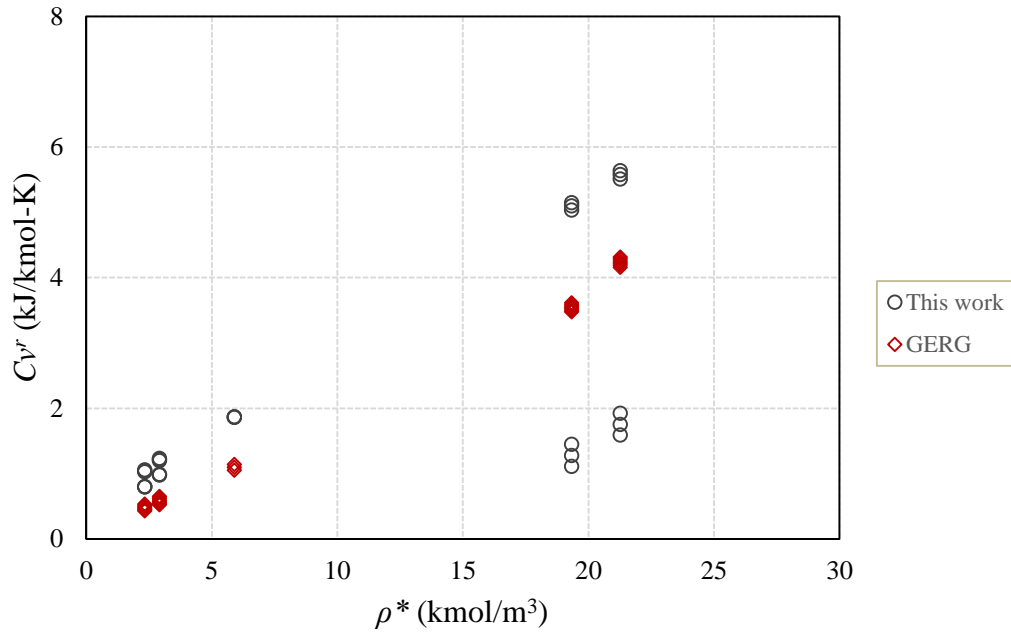


**Figure 47.** ( $C_v^r$ ) for subset 3. (400 – 450 K)

The last step in stage 4 consists of determining the absolute value for the heat capacity at constant volume ( $C_v$ ) using residual properties:

$$C_v(T, \rho) = C_v^r(T, \rho) + C_v^{ig}(T, \rho) \quad (37)$$

The ideal gas heat capacity at constant volume ( $C_v^{ig}$ ) is a function only of temperature, for a mixture of n components with mole fraction ( $y_i$ ) is the weighted sum of the individual heat capacities:

$$C_v^{ig} = \sum_{i=1}^n y_i C_{v,i}^{ig} \quad (38)$$

The Thermodynamics Research Center (TRC) has published heat capacities at constant pressure in the ideal gas state ( $C_p^{ig}$ ) for methane, ethane and propane and other components, which appear several databases and EoS such as DIPPR Project 801 and GERG 2008 EoS. The relationship between ideal gas, heat capacities and gas constant is:

$$C_v^{ig} = C_p^{ig} - R \quad (39)$$

Complete expressions and parameters for ethane, propane and methane from the DIPPR Project 801 appear in Appendix G. The heat capacities at constant volume predicted by DIPPR Project 801 and GERG 2008 EoS appear in Table 21, the difference in the values of ( $C_v^{ig}$ ) from both sources is about 0.05%. The values of ( $C_v^{ig}$ ) from GERG 2008 EoS along with the Eq. 36 provide the absolute values of ( $C_v$ ) shown in Figures 48 to 50. The numerical values of the residual and absolute heat capacities determined in this stage are reported in Appendix H and their uncertainty will be analyzed in stage 5.

**Table 21.** Ideal gas heat capacities at constant volume

T (K)	$C_v^{ig}$ (kJ / kmol-K)	
	GERG 2008	DIPPR
220	26.085	26.186
230	26.281	26.356
240	26.507	26.559
250	26.764	26.797
260	27.054	27.070
270	27.375	27.378
280	27.727	27.720
290	28.109	28.095
300	28.520	28.502
310	28.958	28.938
320	29.422	29.402
330	29.909	29.891
340	30.418	30.404
350	30.947	30.937
360	31.493	31.489
370	32.055	32.058
380	32.631	32.640
390	33.219	33.235
400	33.818	33.841
410	34.425	34.455
420	35.041	35.077
430	35.663	35.704
440	36.290	36.335
450	36.921	36.971

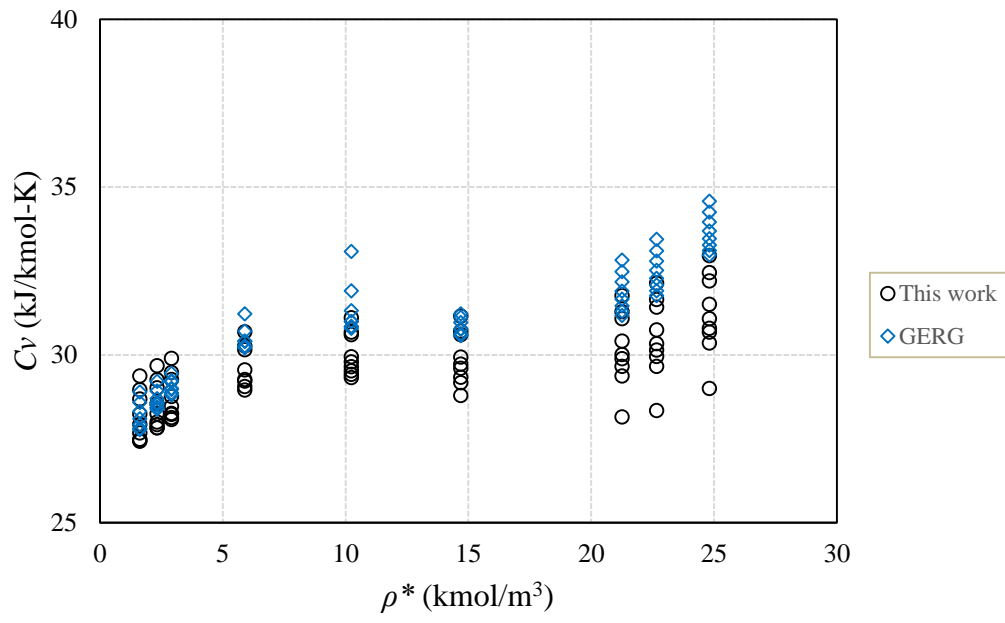


**Figure 48.** ( $C_v$ ) for subset 1. Temperatures 220 – 300 K

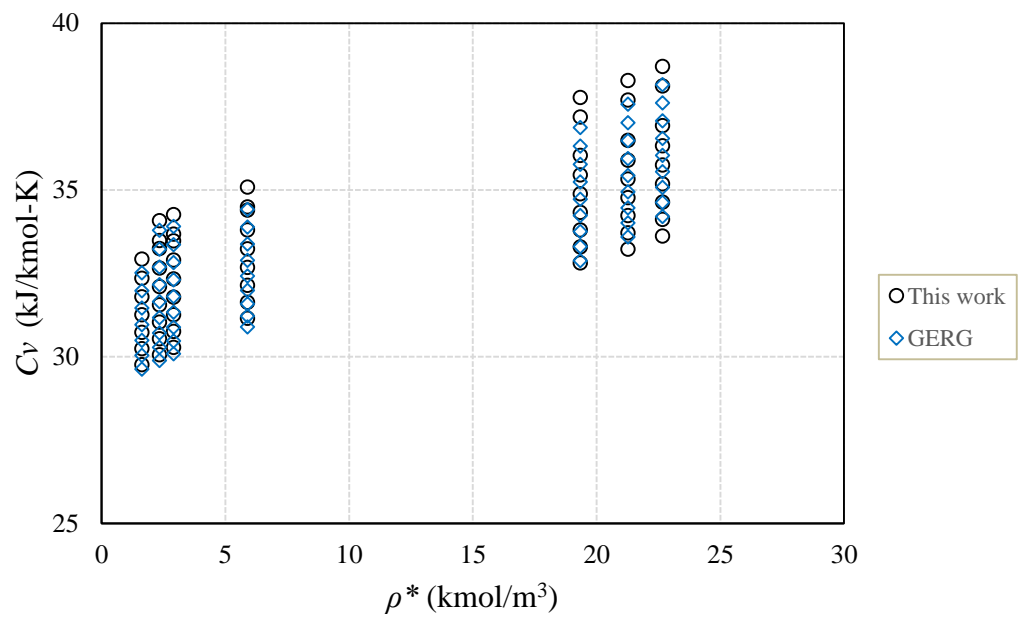


**Figure 49.** ( $C_v$ ) for subset 2. Temperatures 310 – 390 K

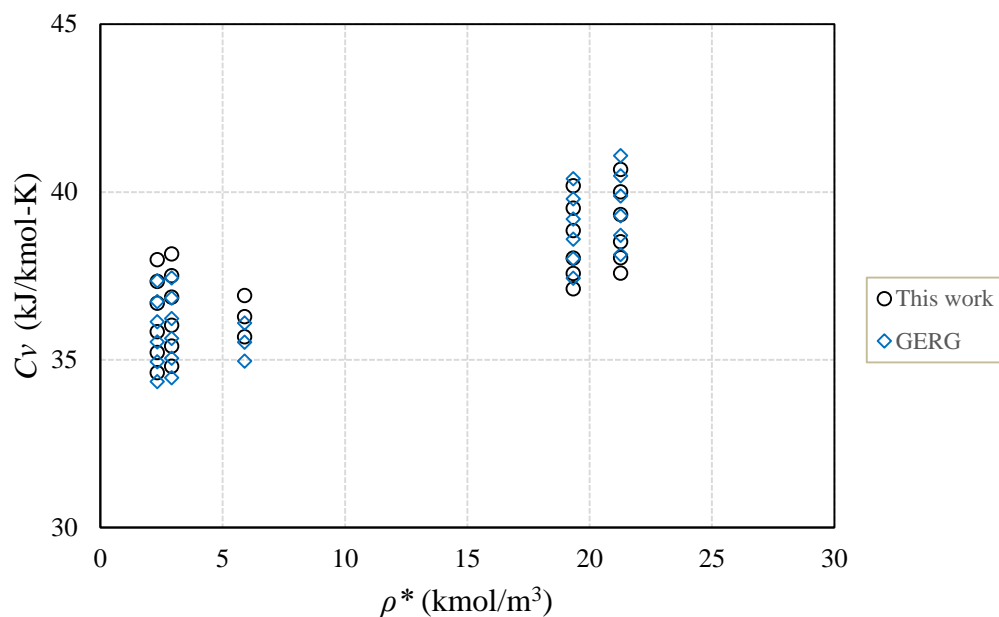


**Figure 50.** ( $C_v$ ) for subset 3. Temperatures 400 – 450 K

### 3.5 Stage 5. Uncertainty Analysis

The last step in this methodology consists of estimating of the uncertainty in the values of the residual and total heat capacity at constant volume. A rigorous analysis of the numerical second derivatives would provide an estimate of the uncertainty in the residual ( $C_v$ ) from experimental ( $P$ - $\rho$ - $T$ ) data. Even though the analysis of the data provided values for first and second derivatives in stage 3, it was not possible to calculate the ( $C_v'$ ) from those values because their scatter (shown for every isochore in Figures 22 to 41) increases significantly when the data are available on isothermal paths. Consequently, the numerical integration of such random data (Appendix I) is very inaccurate for the purpose of this project and was not implemented in stage 4.

However, if it is necessary to estimate the uncertainty from the data, then at least one isotherm with smooth behavior in the integrand function of Eq. 33 using the numerical derivative must be available. The numerical derivatives at 280 K in Figure 51 resembles the tendency from the analytical derivatives in Figure 52.

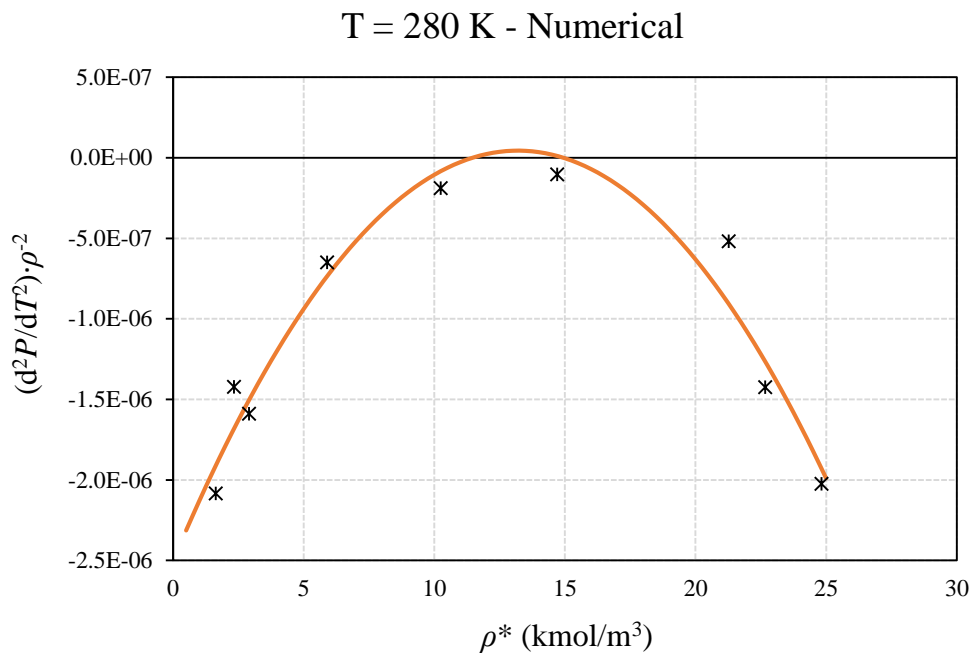


**Figure 51.** Integrand function of Eq. 34 using numerical derivatives

**Table 22.** Regression results using numerical derivatives. T = 280 K

	Coefficient	Standard Error	Lower 95%	Upper 95%
$c_1$	-1.46E-08	4.72E-10	-1.86E-08	-1.06E-08
$c_2$	3.86E-07	1.02E-08	2.80E-07	4.91E-07
$c_3$	-2.50E-06	1.50E-07	-2.98E-06	-2.03E-06

The approach to determine the uncertainty in  $(C_v)$  starts with the fit of the integrand function in Figure 51 and 52 using the same quadratic expression as in Eq. 35. The results of the regression appear in Table 22 and 23 and Figure 53 shows the fits of the integrand function using both numerical and analytical derivatives.

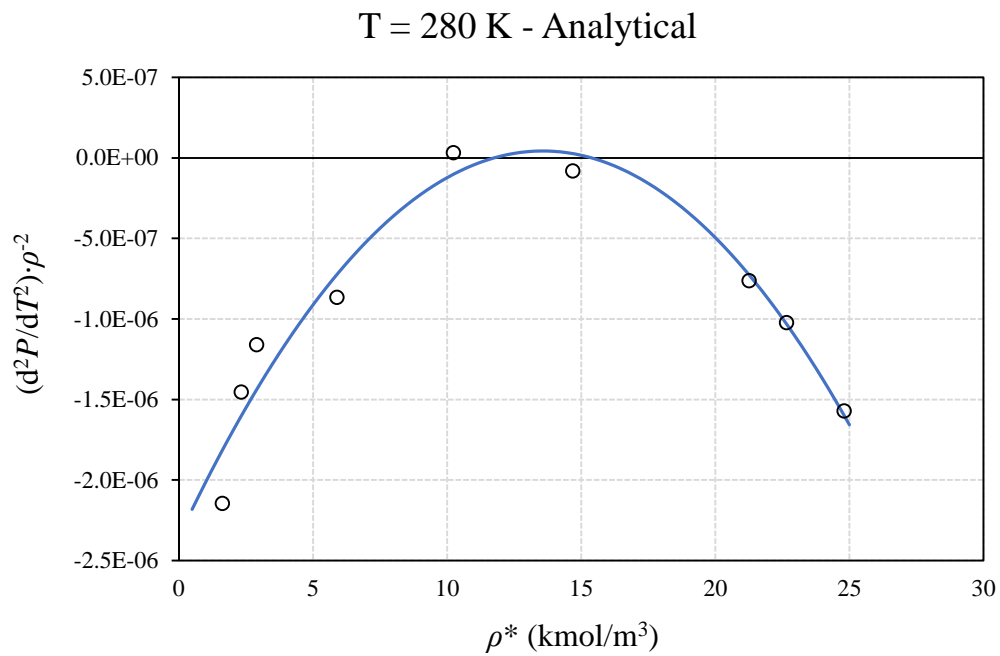


**Figure 52.** Integrand function of Eq. 34 using analytical derivatives

**Table 23.** Regression results using analytical derivatives. T = 280 K

	Coefficient	Standard Error	Lower 95%	Upper 95%
$c_1$	-1.30E-08	4.25E-10	-1.66E-08	-9.41E-09
$c_2$	3.53E-07	9.14E-09	2.58E-07	4.48E-07
$c_3$	-2.36E-06	1.35E-07	-2.78E-06	-1.93E-06



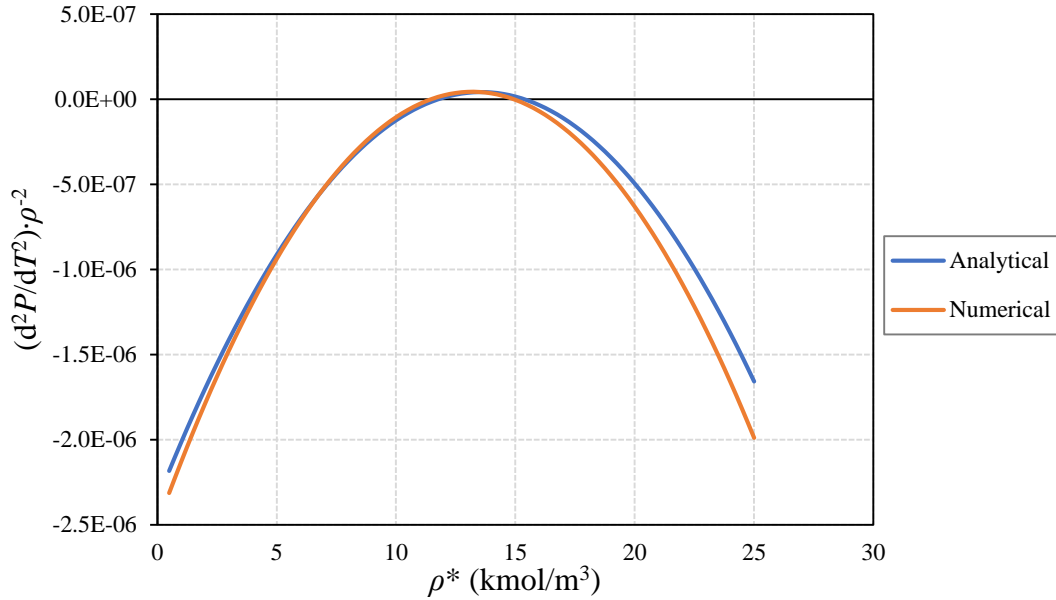


**Figure 53.** Integrand function predicted. T = 280 K

The area under the curves of Figure 47 represents the  $C_v^r$  for both sets of data calculated using Eq. 35 and reported in Tables 24 and 25 for the numerical and analytical fit respectively. The difference between the values of  $C_v^r$  is an indication of uncertainty of the analytical method used in Stage 4.

The absolute heat capacity ( $C_v$ ) results from using Eq. 36 and the ( $C_v^{ig}$ ) at 280 K from GERG 2008 EoS are reported in Table 2. The global uncertainty in the value of the absolute heat capacity ( $U_{C_v}$ ) as percentage deviation is:

$$U_{C_v} = \% \text{ deviation} = \frac{C_{v_{analytical}} - C_{v_{numerical}}}{C_{v_{numerical}}} * 100 \quad (40)$$

**Table 24.** Residual heat capacity at T = 280 K from numerical derivatives

T = 280 K					
Isochore	P' (MPa)	$\rho^*$ (kmol/m <sup>3</sup> )	d <sup>2</sup> P/dT <sup>2</sup>	(d <sup>2</sup> P/dT <sup>2</sup> )· $\rho^{-2}$	$C_v^r$ (kJ/kmol-K)
1	178.880	24.817	-1.25E-03	-2.02E-06	4.969
2	117.143	22.664	-7.31E-04	-1.42E-06	4.014
3	90.161	21.267	-2.35E-04	-5.19E-07	3.591
5	29.861	14.699	-2.23E-05	-1.03E-07	2.962
6	17.442	10.242	-1.99E-05	-1.90E-07	2.977
7	10.517	5.897	-2.26E-05	-6.49E-07	2.534
8	5.817	2.910	-1.35E-05	-1.59E-06	1.616
9	4.793	2.332	-7.74E-06	-1.42E-06	1.358
10	3.475	1.630	-5.54E-06	-2.08E-06	1.005

**Table 25.** Residual heat capacity at T = 280 K from analytical derivatives

T = 280 K					
Isochore	P' (MPa)	$\rho^*$ (kmol/m <sup>3</sup> )	d <sup>2</sup> P/dT <sup>2</sup>	(d <sup>2</sup> P/dT <sup>2</sup> )· $\rho^{-2}$	$C_v^r$ (kJ/kmol-K)
1	178.880	24.817	-9.67E-04	-1.57E-06	4.474
2	117.143	22.664	-5.25E-04	-1.02E-06	3.685
3	90.161	21.267	-3.45E-04	-7.62E-07	3.342
5	29.861	14.699	-1.75E-05	-8.10E-08	2.867
6	17.442	10.242	3.48E-06	3.31E-08	2.873
7	10.517	5.897	-3.01E-05	-8.65E-07	2.420
8	5.817	2.910	-9.82E-06	-1.16E-06	1.531
9	4.793	2.332	-7.91E-06	-1.45E-06	1.285
10	3.475	1.630	-5.70E-06	-2.14E-06	0.949

Table 26 contains the absolute heat capacity ( $C_v$ ) with a maximum uncertainty (percentage deviation) of 1.5%. This estimation is an indication of the error in the

analytical method used to determine the residual values without including the uncertainty of the ideal gas heat capacity.

**Table 26.** Absolute heat capacity and global uncertainty at T = 280K

T = 280 K						
Isochore	P' (MPa)	$\rho^*$ (kmol/m <sup>3</sup> )	$C_{vig}$ (kJ/kmol-K)	$C_v$ (kJ/kmol-K)		% deviation
				Analytical	Numerical	
1	178.880	24.817	27.727	32.696	32.201	1.514
2	117.143	22.664	27.727	31.740	31.411	1.037
3	90.161	21.267	27.727	31.318	31.068	0.796
5	29.861	14.699	27.727	30.689	30.594	0.307
6	17.442	10.242	27.727	30.704	30.600	0.337
7	10.517	5.897	27.727	30.261	30.147	0.378
8	5.817	2.910	27.727	29.342	29.258	0.288
9	4.793	2.332	27.727	29.085	29.012	0.250
10	3.475	1.630	27.727	28.732	28.676	0.193

Finally, the values of the ( $C_v'$ ) calculated in Stage 4 correspond up to 15% of the total ( $C_v$ ) as shown in Figure 54.

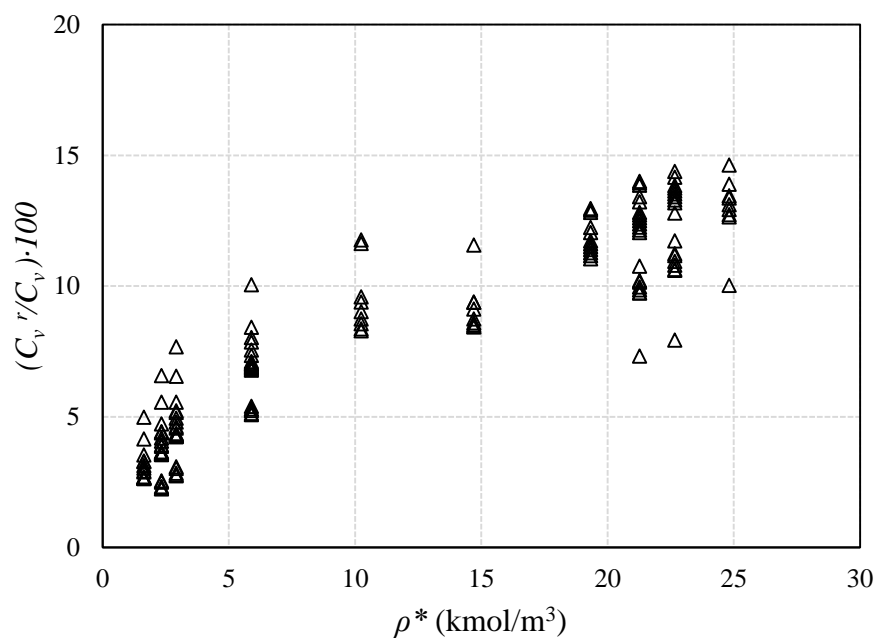


**Figure 54.** Percentage of residual heat capacity

## 4. CONCLUSIONS

This thesis reports highly accurate experimental ( $P$ - $\rho$ - $T$ ) data for a ternary mixture of methane, ethane, and propane measured with the Magnetic Suspension Densimeter (MSD) and isochoric apparatus at Texas A&M University. The set of data contains 10 isochores and 5 isotherms covering a range of temperature from 140 to 500 K at pressures up to 200 MPa. The relative uncertainty in pressure is 0.02 MPa for measurements up to 20 MPa, and 0.2 MPa in measurements for 20 to 200 MPa. The uncertainty in temperature is 10 mK. From the specifications of the MSD, the relative uncertainty for density measurements is  $\leq 0.05\%$ .

A rigorous technique allows combining the experimental data from the MSD with the isochoric data to determine the isochoric density was proposed. This new technique, based upon selection of a constant reference density ( $\rho^*$ ) for each isochore, corrects for the effect of the noxious volume in each isochoric apparatus.

The analysis of the noxious volume for the high pressure isochoric apparatus (HPI) is one of the main contributions of this research work. The volume of the pressure transducer and the connection line comprise 2.3 % of the volume of the cell. New distortion parameters for the beryllium copper alloy result from the mass balance and algebraic manipulations of the volume expressions. The final values for the thermal expansion and isothermal compressibility coefficients are  $1.327 \cdot 10^{-4} \text{ K}^{-1}$  and  $3.373 \cdot 10^{-5} \text{ MPa}$  respectively, which, along with the new methodology, allow determination of the isochoric densities from the HPI within a band  $\pm 0.5\%$  when compared to values predicted

by the GERG 2008 EoS. Furthermore, the distortion parameters found in the literature review for stainless steel were validated and allowed calculation of isochoric densities from the low pressure isochoric apparatus (LPI) within a band of  $\pm 0.2\%$  for temperatures removed from the phase loop of the ternary mixture.

The isochoric densities are not truly isochoric from the measurements. Adjusting the data ( $P$ - $\rho$ - $T$ ) such that they correspond to truly isochores is necessary when determining the first and second derivatives of the pressure with respect to temperature at constant density for both analytical and numerical techniques. A rational equation of second order in both numerator and denominator fits the truly isochoric data with residuals in pressure of  $\pm 0.1$  MPa (data from HPI) and  $\pm 0.01$  MPa (data from LPI). Moreover, this equation could calculate derivative values having the same tendency as those predicted by the GERG 2008 EoS.

The method of the central differences used for determining the numerical derivatives enabled identifying those data that deviates from the tendency a result of the experimental errors. The values of the second derivatives are about two orders of magnitude smaller than the first derivatives and have a band of scatter of  $\pm 0.0003$  MPa/K<sup>2</sup>. Because of the small values, the sensitivity to fluctuations of temperature and pressure of the experimental data is noticeable. Consequently, it is important to improve the methodology of data acquisition to ensure not only evenly space data to reduce the error for the numerical method, but also to select accurate ( $P$ - $T$ ) points for purposes of heat capacity determination.

It was possible to apply thermodynamic relationships to calculate an expression for the residual heat capacity at constant volume that requires an isothermal integration of the second derivative of the pressure with respect to temperature at constant density. Twenty four isotherms covering a range from 220 to 450 K resulted from adjusting the experimental data to true isochores. The values in the integrand function clearly reveal a quadratic tendency when are plotted as function of the molar density. The quadratic model agrees with the tendency in predictions from the GERG 2008 EoS and applies to all the isotherms, even those with insufficient data. The values of the residual heat capacity result from analytical integration of the quadratic function. Finally, the absolute heat capacities result from using residual gas properties and ideal gas values predicted from the GERG 2008 EoS.

Although the main purpose of the ( $P$ - $\rho$ - $T$ ) measurements is to provide accurate data for the primary properties, it is possible to expand the initial scope and to calculate values for the residual and absolute heat capacity at constant volume. The uncertainty estimation requires a rigorous analysis of the numerical second derivatives because they provide a connection to the uncertainty of the raw data. In this project, it is not possible to calculate the residual values of the heat capacity from the numerical derivatives because of their significant scatter on isothermal paths. Only numerical derivatives for one isotherm ( $T = 280$  K) were used to determine the residual heat capacity and compare them with the values predicted from the analytical approach. The difference between both values is an indication of the uncertainty of the ( $P$ - $\rho$ - $T$ ) data when calculating the absolute

heat capacity. The maximum uncertainty in the absolute heat capacity is 1.5% with residual values up to 15% of the absolute heat capacity at constant volume.

The value of the uncertainty in the absolute heat capacities agree with those in the literature review for binary mixtures in the vapor phase (around 2%). Apparently, the whole set of ( $P$ - $\rho$ - $T$ ) data along with the numerical derivatives and heat capacities constitute valuable input for developing equations of state such as GERG 2008, for example, to optimize the mixing rules and parameters used in the prediction of natural gas properties.

Finally, for future gas ( $P$ - $\rho$ - $T$ ) measurements, the experimental design should provide evenly spaced data in temperatures and densities to facilitate calculating numerical derivatives and integration methods. Furthermore, a truly isochoric behavior is achievable using a single apparatus, such as the Magnetic Suspension Densimeter (MSD), by installing a means (e.g. hand pump) to make fine pressure adjustments and essentially dial in the density.



## REFERENCES

1. International Energy Agency (IEA). "Natural Gas". Available at: <http://www.iea.org/aboutus/faqs/naturalgas/>. Accessed: February 2015.
2. U.S Energy Information Administration (EIA). "Energy Explained". Available at: <http://www.eia.gov/energyexplained/index.cfm>. Accessed: February 2015.
3. International Energy Agency (IEA). "Medium-Term Gas Market Report 2013". Available at: [http://www.iea.org/publications/freepublications/publication/MTGMR2013\\_free.pdf](http://www.iea.org/publications/freepublications/publication/MTGMR2013_free.pdf). Published: June 2013.
4. Patchworks Working Energy. "Conventional vs. Unconventional Resources". Available at: [http://www.oilandgasinfo.ca/wp-content/uploads/Nov\\_2013\\_conv\\_vs\\_unconv.pdf](http://www.oilandgasinfo.ca/wp-content/uploads/Nov_2013_conv_vs_unconv.pdf). Published: November 2013.
5. U.S Energy Information Administration (EIA). "Technically Reciverable Shale Gas Resources: An Assessment of 137 Shale Formations in 41 Countries". Available at: <http://www.eia.gov/analysis/studies/worldshalegas/>. Published: June 2013.
6. Cristancho, D.; Experimental Characterization and Molecular Study of Natural Gas Mixtures. PhD. Dissertation, Texas A&M University, College Station, TX, USA, 2010.
7. Gomez-Osorio, M.A.; Ortiz-Vega, D.O.; Mantilla, I.D.; Acosta, H.Y.; Holste, J.C.; Hall, K.R.; Iglesias-Silva, G.A.; A Formulation for the Flow Rate of a Fluid Passing through an Orifice Plate from the First Law of Thermodynamics. *Flow Meas. Instrum* 2013, 33, 197-201.
8. Cristancho, D.E.; Mantilla, I.D.; Coy, L.A.; Tibaduiza, A.; Ortiz-Vega, D.O; Hall, K.R.; Accurate P - rho - T Data and Phase Boundary Determination for a Synthetic Residual Natural Gas Mixture. *J. Chem. Eng. Data* 2011, 56 (4), 826-832.
9. Atilhan, M.; Aparicio, S.; Ejaz, S.; Cristancho, D.; Hall, K.R.; P - rho - T Behavior of a Lean Synthetic Natural Gas Mixture Using Magnetic Suspension Densimeters and an Isochoric Apparatus: Part I. *J. Chem. Eng. Data* 2011, 92 (8), 212-221.

10. Atilhan, M.; Aparicio, S.; Ejaz, S.; Cristancho, D.; Mantilla, I.; Hall, K.R.; P - rho - T Behavior of Three Lean Synthetic Natural Gas Mixtures Using a Magnetic Suspension Densimeter and Isochoric Apparatus from (250 to 450) K with Pressures up to 150 MPa: Part II. *J. Chem. Eng. Data* 2011, 56 (10), 3766-3774.
11. Starling, K.E., Savidge, J.L.; Compressibility Factors of Natural Gas and Other Related Hydrocarbon Gases. *American Gas Association, Operating Section*. Arlington, VA, USA, 1992.
12. Kunz, O.; Wagner, W.; The GERG-2008 Wide-Range Equation of State for Natural Gases and Other Mixtures: An Expansion of GERG-2004. *J. Chem. Eng. Data* 2012, 57 (11), 3032-3091.
13. Tibaduiza, A.D.P.; Cristancho, D.E.; Ortiz-Vega, D.; Mantilla, I.D.; Gomez-Osorio, M.A.; Browne, R.A.; Holste, J.C.; Hall, K.R.; Calculation of Energies and Entropies from Isochoric and Isothermal Experimental Data. *J. Chem. Eng. Data* 2014, 59 (4), 999-1005.
14. PetroSkills John M. Campbell. "Variation of Ideal Gas Heat Capacity Ratio with Temperature and Relative Density". Available at: <http://www.jmcampbell.com/tip-of-the-month/2013/05/variation-of-ideal-gas-heat-capacity-ratio-with-temperature-and-relative-density/>. Published: May 2013.
15. PetroSkills John M. Campbell. "Variation of Natural Gas Heat Capacity with Temperature, Pressure, and Relative Density". Available at: <http://www.jmcampbell.com/tip-of-the-month/2009/07/variation-of-natural-gas-heat-capacity-with-temperature-pressure-and-relative-density/>. Published: July 2009.
16. Magee, J.W.; Deal, R.J.; Blanco, J.C.; High-Temperature Adiabatic Calorimeter for Constant-Volume Heat Capacity Measurements of Compressed Gases and Liquids. *J. Res. Natl. Inst. Stand. Technol* 1998, 103 (1), 63-75.
17. Duarte-Garza, H.A.; Magee, J.W.; Isochoric P - rho - T and Heat Capacity  $C_V$  Measurements on  $[xC_3H_8 + (1 - x) i-C_4H_{10}]$ ,  $x \approx 0.7, 0.3$  from 200 to 400 K at Pressures to 35 MPa. *J. Chem. Eng. Data* 1999, 44 (5), 1048-1054.
18. Perkins, R.A.; Magee, J.W.; Molar Heat Capacity at Constant Volume for Isobutane at Temperatures from (114 to 345) K and at Pressures to 35 MPa. *J. Chem. Eng. Data* 2009, 54 (9), 2646-2655.
19. Perkins, R.A.; Ochoa, J.C.S.; Magee, J.W.; Thermodynamic Properties of Propane II. Molar Heat Capacity at Constant Volume from ( 85 to 345 ) K with Pressures to 35 MPa. *J. Chem. Eng. Data* 2009, 54 (12), 3192-3201.

20. Magee, J.W.; Molar Heat Capacity  $C_v$  for Saturated and Compressed Liquid and Vapor Nitrogen from 65 to 300 K at Pressures to 35 MPa. *J. Res. Natl. Inst. Stand. Technol* 1991, 96 (6), 725-740.
21. Magee, J.W.; Molar Heat Capacity at Constant Volume for  $[x\text{CO}_2 + (1 - x)\text{C}_2\text{H}_6]$  from 220 to 340 K at Pressures to 35 MPa. *J. Chem. Eng. Data* 1995, 40 (2), 438-442.
22. Ernest, G.; Brauning, G.; Lai, J.F.; Calorimetric Determination of the Deviation between the International Practical Temperature Scale 1968 and the Thermodynamic Temperature Scale. *Can. J. Chem* 1988, 66 (4), 999-1004.
23. Mathonat, C.; Majer, V.; Mather, A.E.; Grolier, J.P.E.; Use of Flow Calorimetry for Determining Enthalpies of Absorption and the Solubility of  $\text{CO}_2$  in Aqueous Monoethanolamine Solutions. *Ind. Eng. Chem. Res* 1998, 37 (10), 4136-4141.
24. Dolan, J.P.; Eakin, B.E.; Bukacek, R.F.; Measurement of Enthalpy Differences with a Flow Calorimeter. *I&EC Fundam* 1968, 7 (4), 645-651.
25. Rubotherm. "Magnetic Suspension Balances". Available at: <http://www.rubotherm.com/magnetic-suspension-balances>. Accessed: March 2015.
26. Cristancho, D.E.; Mantilla, I.D.; Ejaz S.; Hall, K.R.; Atilhan, M.; Iglesias-Silva, G.A.; Accurate P - rho - T Data for Ethane from (298 to 450) K up to 200 MPa. *J. Chem. Eng. Data* 2010, 55 (8), 2746-2749.
27. Mantilla, I.D.; Cristancho, D.E.; Ejaz, S.; Hall, K.R.; Atilhan, M.; Iglesias-Silva, G.A.; P - rho - T Data for Carbon Dioxide from (310 to 450) K up to 160 MPa. *J. Chem. Eng. Data* 2010, 55 (11), 4611-4613.
28. Cristancho, D.E.; Mantilla, I.D.; Ejaz, S.; Hall, K.R.; Atilhan, M.; Iglesia-Silva, G.A.; Accurate P-rho-T Data for Methane from (300 to 450) K up to 180 MPa. *J. Chem. Eng. Data* 2010, 55 (2), 826-829.
29. Mantilla, I.D.; Cristancho, D.E.; Ejaz, S.; Hall, K.R.; Atilhan, M.; Iglesias-Silva, G.A.; New P - rho - T Data for Nitrogen at Temperatures from (265 to 400) K at Pressures up to 150 MPa. *J. Chem. Thermodyn* 2010, 55 (10) 4277-4230.
30. Zhou, J.; Automatic Isochoric Apparatus for PVT and Phase Equilibrium Studies of Natural Gas Mixtures. PhD. Dissertation, Texas A&M University, College Station, TX, USA, 2005.

31. Lau, W.W.R. A.; Continuously Weighed Pycnometer Providing Densities for Carbon Dioxide + Ethane Mixtures between 240 and 350 K at Pressures up to 35 MPa. PhD. Dissertation, Texas A&M University, College Station, TX, USA, 1986.
32. DCG Partnership I. "Certified Reference Materials". Available at: <https://www.dcgpartnership.com/certified-reference-materials.html>. Accessed: 2/2/2015.
33. Smith, J.M.; Van Ness, H.C.; Abbott, M.M.; Introduction to Chemical Engineering Thermodynamics. Seventh Edition. *McGraw-Hill's Chemical Engineering Series*. 2005.
34. Stouffer, C.E.; Kellerman, S.J.; Hall, K.R.; Holste, J.C.; Gammon, B.E.; Marsh, K.N.; Densities of Carbon Dioxide + Ethane Mixtures from 240 K to 450 K at Pressures up to 25 MPa. *J. Chem. Eng. Data* 2001, 46 (5), 1309-1318.
35. Kreyszing, E.; Advanced Engineering Mathematics. Ninth Edition. *John Wiley & Sons, Inc.* 2006.
36. Penn State University. Cimbala, J.M.; "Outlier Points". Available at: <https://www.coursehero.com/file/63697/Outlierpoints/>. Published: September 2007.

## APPENDIX A. EXPERIMENTAL ISOTHERMAL AND ISOCHORIC DATA

**Table 27.** MSD measurements and compared to values predicted by GERG 2008

P (MPa)	$\rho_{MSD}$ (kg/m <sup>3</sup> )	$\rho_{EoS}$ (kg/m <sup>3</sup> )	$100 \cdot (\rho_{MSD} - \rho_{EoS}) / \rho_{MSD}$
T = 300 K			
4.999	37.306	37.287	0.051
7.503	58.646	58.62	0.045
10.002	81.394	81.357	0.046
12.505	104.869	104.819	0.048
14.999	127.822	127.793	0.022
17.508	149.468	149.437	0.02
19.995	168.813	168.788	0.015
29.984	225.81	225.738	0.032
39.987	261.352	261.289	0.024
49.935	286.23	286.088	0.05
59.928	305.314	305.16	0.051
79.952	333.809	333.646	0.049
99.947	354.975	354.803	0.049
119.913	371.914	371.736	0.048
139.983	386.188	386.007	0.047
149.8	392.43	392.245	0.047
159.85	398.411	398.221	0.048
179.73	409.211	409.025	0.045
199.494	418.862	418.676	0.044
T = 325 K			
5	33.485	33.474	0.033
10	70.876	70.845	0.043
12.5	90.289	90.261	0.031
15.006	109.585	109.539	0.042
17.507	128.112	128.058	0.042
19.996	145.414	145.355	0.04
30.059	201.282	201.21	0.036
40.015	238.616	238.539	0.032
49.963	265.488	265.346	0.054
59.992	286.267	286.116	0.053
79.963	317.017	316.863	0.049

**Table 27. Continued**

P (MPa)	$\rho_{MSD}$ (kg/m <sup>3</sup> )	$\rho_{EoS}$ (kg/m <sup>3</sup> )	$100 \cdot (\rho_{MSD} - \rho_{EoS}) / \rho_{MSD}$
T = 325 K			
99.953	339.762	339.608	0.045
119.937	357.863	357.713	0.042
139.769	372.872	372.709	0.044
149.914	379.699	379.537	0.043
159.898	385.959	385.808	0.039
179.838	397.373	397.223	0.038
T = 350 K			
1.006	5.891	5.899	-0.132
2.023	11.983	11.986	-0.024
4.998	30.470	30.465	0.016
7.495	46.652	46.639	0.027
10.021	63.431	63.418	0.021
12.526	80.209	80.209	0.000
15.025	96.805	96.806	-0.001
17.544	113.084	113.073	0.009
20.021	128.379	128.364	0.012
30.062	180.758	180.775	-0.01
40.025	218.503	218.531	-0.013
49.958	246.513	246.486	0.011
59.953	268.419	268.39	0.011
80.013	301.223	301.200	0.008
99.973	325.311	325.284	0.008
119.974	344.476	344.439	0.011
140.057	360.457	360.419	0.011
149.839	367.377	367.333	0.012
159.954	374.043	374.001	0.011
179.786	385.932	385.891	0.011
199.260	396.370	396.333	0.009
T = 375 K			
1.026	5.591	5.600	-0.16
5.017	28.131	28.141	-0.034
10.019	57.578	57.575	0.005
12.508	72.366	72.364	0.003
14.970	86.847	86.843	0.005

**Table 27. Continued**

P (MPa)	$\rho_{MSD}$ (kg/m <sup>3</sup> )	$\rho_{EoS}$ (kg/m <sup>3</sup> )	$100 \cdot (\rho_{MSD} - \rho_{EoS}) / \rho_{MSD}$
T = 375 K			
17.509	101.434	101.431	0.003
20.011	115.297	115.300	-0.002
30.035	163.982	163.972	0.006
40.061	201.33	201.321	0.004
59.976	252.342	252.334	0.003
80.023	286.582	286.572	0.004
99.910	311.732	311.730	0.001
119.931	331.832	331.823	0.003
140.002	348.536	348.526	0.003
T = 400 K			
2.054	10.539	10.543	-0.038
5.009	26.058	26.058	-0.001
10.024	52.951	52.932	0.036
12.499	66.231	66.209	0.033
15.018	79.591	79.563	0.036
17.495	92.444	92.415	0.031
20.025	105.175	105.148	0.025
30.033	150.277	150.267	0.007
40.031	186.306	186.326	-0.011
49.997	214.747	214.774	-0.012
59.979	237.723	237.756	-0.014
80.040	272.978	273.030	-0.019
100.082	299.242	299.289	-0.016
120.026	320.036	320.045	-0.003
139.961	337.257	337.263	-0.002
150.019	344.956	344.960	-0.001

**Table 28.** High pressure isochoric apparatus measurements. EoS: GERG 2008

T (K)	P (MPa)	$\rho$ (kg/m <sup>3</sup> )	$\rho_{\text{EoS}}$ (kg/m <sup>3</sup> )	$100 \cdot (\rho - \rho_{\text{EoS}}) / \rho$
Isochore 1				
300.00	199.871	419.037	418.851	0.044
295.00	195.624	419.424	419.219	0.049
290.00	191.147	419.817	419.500	0.076
285.00	186.633	420.213	419.785	0.102
280.00	182.090	420.612	420.080	0.126
275.00	177.422	421.015	420.336	0.161
270.00	172.833	421.418	420.656	0.181
263.06	166.346	421.984	421.084	0.213
259.99	163.152	422.245	421.124	0.265
250.00	153.629	423.076	421.771	0.308
240.00	143.91	423.923	422.439	0.350
230.00	134.009	424.789	423.143	0.387
220.00	123.882	425.676	423.863	0.426
210.00	113.535	426.588	424.619	0.462
200.00	103.186	427.523	425.555	0.460
190.00	92.171	428.512	426.281	0.521
180.00	81.107	429.544	427.194	0.547
170.00	69.828	430.641	428.217	0.563
160.00	58.336	431.833	429.385	0.567
150.00	46.673	433.170	430.769	0.554
Isochore 2				
390.00	200.509	379.994	380.661	-0.176
380.00	194.055	380.655	381.150	-0.13
375.00	190.822	380.986	381.411	-0.111
370.00	187.502	381.321	381.638	-0.083
360.00	180.858	381.993	382.134	-0.037
350.00	174.109	382.671	382.63	0.011
340.00	167.260	383.356	383.133	0.058
330.00	160.301	384.049	383.639	0.107
325.00	156.694	384.400	383.84	0.146
320.00	153.255	384.749	384.164	0.152
310.00	146.102	385.458	384.702	0.196
300.00	138.909	386.174	385.298	0.227
290.00	131.404	386.906	385.778	0.292



**Table 28.** Continued

T (K)	P (MPa)	$\rho$ (kg/m <sup>3</sup> )	$\rho_{\text{EoS}}$ (kg/m <sup>3</sup> )	$100 \cdot (\rho - \rho_{\text{EoS}}) / \rho$
Isochore 2				
280.00	123.913	387.647	386.363	0.331
270.00	116.283	388.401	386.956	0.372
260.00	108.572	389.170	387.606	0.402
250.00	100.712	389.956	388.272	0.432
240.00	92.716	390.765	388.972	0.459
230.00	84.574	391.599	389.708	0.483
220.00	76.296	392.465	390.502	0.500
210.00	67.890	393.371	391.377	0.507
200.00	59.332	394.332	392.333	0.507
190.00	50.644	395.368	393.418	0.493
180.00	41.844	396.516	394.686	0.461
170.00	32.998	397.835	396.265	0.395
160.00	24.230	399.427	398.383	0.261
150.00	15.612	401.402	401.259	0.036
Isochore 3				
450.00	193.800	352.941	354.461	-0.431
440.00	188.558	353.533	354.909	-0.389
430.00	183.199	354.131	355.327	-0.338
420.00	177.828	354.731	355.780	-0.296
410.00	172.351	355.337	356.212	-0.246
400.00	166.951	355.945	356.744	-0.224
390.00	161.350	356.560	357.195	-0.178
380.00	155.672	357.181	357.647	-0.131
370.00	149.924	357.808	358.108	-0.084
360.00	144.085	358.441	358.563	-0.034
350.00	138.193	359.081	359.043	0.011
340.00	132.236	359.727	359.543	0.051
330.00	126.204	360.382	360.058	0.090
325.00	123.137	360.713	360.304	0.113
320.00	120.066	361.046	360.567	0.133
310.00	113.859	361.719	361.104	0.170
300.00	107.927	362.392	361.970	0.116
290.00	101.518	363.089	362.533	0.153
280.00	95.010	363.801	363.112	0.189

**Table 28.** Continued

T (K)	P (MPa)	$\rho$ (kg/m <sup>3</sup> )	$\rho_{\text{EoS}}$ (kg/m <sup>3</sup> )	$100 \cdot (\rho - \rho_{\text{EoS}}) / \rho$
Isochore 3				
275.00	91.387	364.176	363.095	0.297
270.00	88.411	364.530	363.721	0.222
260.00	81.090	365.303	363.732	0.430
250.00	74.622	366.063	364.730	0.364
240.00	67.751	366.865	365.471	0.380
230.00	60.808	367.702	366.309	0.379
220.00	53.767	368.587	367.235	0.367
210.00	46.602	369.540	368.238	0.352
200.00	39.369	370.585	369.421	0.314
190.00	32.061	371.770	370.822	0.255
180.00	24.878	373.144	372.819	0.087
170.00	17.926	374.758	375.738	-0.262
160.00	10.359	376.726	378.293	-0.416
Isochore 4				
450.00	146.879	320.809	322.241	-0.447
440.00	142.519	321.348	322.638	-0.401
430.00	138.102	321.893	323.029	-0.353
420.00	133.630	322.442	323.418	-0.303
410.00	129.127	322.995	323.826	-0.257
400.00	124.565	323.554	324.230	-0.209
390.00	119.962	324.118	324.648	-0.163
380.00	115.312	324.688	325.076	-0.120
370.00	110.611	325.264	325.515	-0.077
360.00	105.850	325.848	325.955	-0.033
350.00	101.041	326.439	326.413	0.008
340.00	96.175	327.039	326.881	0.049
330.00	91.252	327.649	327.362	0.088
320.00	86.267	328.270	327.856	0.126
310.00	81.228	328.903	328.373	0.161

**Table 28.** Continued

T (K)	P (MPa)	$\rho$ (kg/m <sup>3</sup> )	$\rho_{\text{EoS}}$ (kg/m <sup>3</sup> )	$100 \cdot (\rho - \rho_{\text{EoS}}) / \rho$
Isochore 5				
300.00	35.793	248.183	248.112	0.029
290.00	32.993	248.781	248.827	-0.018
280.00	30.162	249.412	249.581	-0.068
270.00	27.306	250.082	250.407	-0.130
260.00	24.432	250.798	251.358	-0.224
250.00	21.523	251.568	252.375	-0.321
240.00	18.583	252.396	253.493	-0.434
230.00	15.612	253.281	254.727	-0.571
220.00	12.599	254.209	255.982	-0.697
210.00	9.558	255.154	257.272	-0.830
200.00	6.517	256.083	258.634	-0.996

**Table 29.** Low pressure isochoric apparatus measurements. EoS: GERG 2008

T (K)	P (MPa)	$\rho$ (kg/m <sup>3</sup> )	$\rho_{\text{EoS}}$ (kg/m <sup>3</sup> )	$100 \cdot (\rho - \rho_{\text{EoS}}) / \rho$
Isochore 6				
300.00	20.567	172.942	172.917	0.015
290.00	19.023	173.065	173.066	-0.001
280.00	17.471	173.190	173.200	-0.006
270.00	15.914	173.315	173.335	-0.011
260.00	14.361	173.441	173.568	-0.073
250.00	12.795	173.569	173.698	-0.075
240.00	11.229	173.696	173.851	-0.089
230.00	9.666	173.824	174.067	-0.140
220.00	8.109	173.951	174.411	-0.264
210.00	6.534	174.079	173.006	0.616
205.00	5.806	174.141	176.458	-1.330

**Table 29.** Continued

T (K)	P (MPa)	$\rho$ (kg/m <sup>3</sup> )	$\rho_{\text{EoS}}$ (kg/m <sup>3</sup> )	$100 \cdot (\rho - \rho_{\text{EoS}}) / \rho$
Isochore 7				
420.00	20.120	99.115	98.833	0.284
400.00	18.790	99.241	98.989	0.255
390.00	18.128	99.305	99.103	0.203
380.00	17.461	99.369	99.208	0.162
370.00	16.791	99.434	99.315	0.119
360.00	16.116	99.498	99.413	0.086
350.00	15.446	99.563	99.565	-0.001
340.00	14.766	99.629	99.678	-0.050
330.00	14.074	99.694	99.731	-0.037
320.00	13.376	99.761	99.759	0.001
310.00	12.677	99.827	99.802	0.025
300.00	11.962	99.894	99.723	0.171
290.00	11.268	99.960	99.872	0.088
280.00	10.559	100.027	99.915	0.112
270.00	9.863	100.093	100.176	-0.082
260.00	9.136	100.160	100.112	0.048
250.00	8.413	100.228	100.170	0.057
240.00	7.691	100.295	100.376	-0.081
230.00	6.953	100.362	100.442	-0.079
220.00	6.193	100.430	100.106	0.323
Isochore 8				
450.00	10.683	48.825	48.820	0.010
440.00	10.406	48.855	48.852	0.005
430.00	10.128	48.885	48.884	0.002
420.00	9.850	48.915	48.920	-0.009
410.00	9.527	48.947	48.726	0.451
400.00	9.291	48.976	48.988	-0.024
390.00	9.010	49.007	49.021	-0.030
380.00	8.727	49.037	49.048	-0.022
370.00	8.444	49.068	49.080	-0.024
360.00	8.126	49.099	48.896	0.413
350.00	7.871	49.129	49.116	0.027
340.00	7.584	49.160	49.139	0.042
330.00	7.297	49.190	49.170	0.042

**Table 29.** Continued

T (K)	P (MPa)	$\rho$ (kg/m <sup>3</sup> )	$\rho_{\text{EoS}}$ (kg/m <sup>3</sup> )	$100 \cdot (\rho - \rho_{\text{EoS}}) / \rho$
Isochore 8				
320.00	7.008	49.221	49.194	0.055
310.00	6.717	49.252	49.211	0.083
300.00	6.421	49.283	49.196	0.177
290.00	6.130	49.314	49.233	0.163
280.00	5.841	49.344	49.307	0.076
270.00	5.549	49.375	49.375	0.001
260.00	5.243	49.406	49.313	0.189
250.00	4.944	49.437	49.350	0.177
240.00	4.644	49.469	49.412	0.114
230.00	4.336	49.500	49.408	0.185
220.00	4.029	49.531	49.479	0.104
210.00	3.737	49.562	49.956	-0.794
Isochore 9				
500.00	9.625	39.023	38.987	0.092
490.00	9.414	39.046	39.018	0.073
480.00	9.202	39.070	39.047	0.058
470.00	8.990	39.094	39.079	0.038
460.00	8.777	39.118	39.109	0.022
450.00	8.562	39.142	39.133	0.024
440.00	8.348	39.166	39.163	0.007
430.00	8.133	39.190	39.191	-0.004
420.00	7.916	39.214	39.213	0.003
410.00	7.699	39.238	39.237	0.003
400.00	7.481	39.262	39.259	0.009
390.00	7.263	39.286	39.284	0.007
380.00	7.044	39.310	39.306	0.011
370.00	6.825	39.334	39.332	0.005
360.00	6.605	39.359	39.357	0.005
350.00	6.383	39.383	39.373	0.026
340.00	6.161	39.407	39.393	0.036
330.00	5.938	39.431	39.411	0.052
320.00	5.715	39.456	39.435	0.053
310.00	5.490	39.480	39.450	0.077
300.00	5.262	39.505	39.447	0.146

**Table 29. Continued**

T (K)	P (MPa)	$\rho$ (kg/m <sup>3</sup> )	$\rho_{\text{EoS}}$ (kg/m <sup>3</sup> )	$100 \cdot (\rho - \rho_{\text{EoS}}) / \rho$
Isochore 9				
290.00	5.038	39.529	39.485	0.112
280.00	4.812	39.553	39.516	0.094
270.00	4.585	39.578	39.551	0.067
260.00	4.353	39.602	39.550	0.133
250.00	4.122	39.627	39.574	0.132
240.00	3.891	39.651	39.622	0.074
230.00	3.663	39.676	39.745	-0.173
220.00	3.455	39.700	40.231	-1.337
215.00	3.340	39.712	40.357	-1.624
210.00	3.193	39.725	39.967	-0.610
205.00	3.088	39.737	40.333	-1.500
Isochore 10				
370.00	4.822	27.493	27.447	0.168
360.00	4.682	27.509	27.506	0.011
350.00	4.534	27.526	27.521	0.017
340.00	4.384	27.543	27.526	0.061
330.01	4.214	27.560	27.394	0.600
320.00	4.084	27.576	27.541	0.126
310.00	3.939	27.593	27.591	0.008
305.15	3.868	27.601	27.612	-0.040
300.00	3.788	27.609	27.600	0.033
290.00	3.639	27.626	27.630	-0.015
280.00	3.489	27.643	27.659	-0.057
270.00	3.336	27.660	27.667	-0.027
260.00	3.182	27.677	27.673	0.014
240.00	2.874	27.710	27.708	0.007
220.00	2.561	27.744	27.740	0.016
210.01	2.402	27.761	27.750	0.042

## APPENDIX B. ISOCHORIC DENSITY AND TRULY ISOCHORIC DATA

**Table 30.** Isochoric density and ( $P'$ - $\rho^*$ - $T$ ) data

T (K)	P (MPa)	$\rho_c$ (kg/m <sup>3</sup> )	$100 \cdot (\rho_c - \rho_{EoS}) / \rho_c$	$(dP/d\rho^*)_T$ (MPa·m <sup>3</sup> /kg)	P'	(MPa)
Isochore 1. $\rho^* = 419.037$ kg/m <sup>3</sup>						
300.00	199.871	419.037	0.044	2.159	199.871	
295.00	195.624	419.424	0.049	2.130	194.801	
290.00	191.147	419.817	0.076	2.100	189.510	
285.00	186.633	420.213	0.102	2.070	184.199	
280.00	182.090	420.612	0.126	2.039	178.880	
275.00	177.422	421.015	0.161	2.008	173.449	
270.00	172.833	421.418	0.181	1.977	168.125	
263.06	166.346	421.984	0.213	1.934	160.647	
259.99	163.152	422.245	0.265	1.914	157.011	
250.00	153.629	423.076	0.309	1.850	146.157	
240.00	143.910	423.923	0.350	1.784	135.191	
230.00	134.009	424.789	0.388	1.717	124.133	
220.00	123.882	425.676	0.426	1.648	112.942	
210.00	113.535	426.588	0.462	1.577	101.626	
200.00	103.186	427.523	0.460	1.504	90.420	
190.00	92.171	428.512	0.521	1.429	78.628	
180.00	81.107	429.544	0.547	1.352	66.902	
170.00	69.828	430.641	0.563	1.272	55.070	
160.00	58.336	431.833	0.567	1.189	43.128	
150.00	46.673	433.170	0.554	1.102	31.100	
Isochore 2. $\rho^* = 382.671$ kg/m <sup>3</sup>						
390.00	200.509	379.994	-0.176	1.899	205.593	
380.00	194.055	380.655	-0.130	1.854	197.792	
375.00	190.822	380.986	-0.111	1.831	193.907	
370.00	187.502	381.321	-0.083	1.808	189.943	
360.00	180.858	381.993	-0.037	1.761	182.052	
350.00	174.109	382.671	0.011	1.713	174.109	
340.00	167.260	383.356	0.058	1.665	166.119	
330.00	160.301	384.049	0.107	1.617	158.073	
325.00	156.694	384.400	0.146	1.592	153.941	

**Table 30.** Continued.

T (K)	P (MPa)	$\rho_c$ (kg/m <sup>3</sup> )	$100 \cdot (\rho_c - \rho_{EoS}) / \rho_c$	$(dP/d\rho^*)_T$ (MPa·m <sup>3</sup> /kg)	P' (MPa)
Isochore 2. $\rho^* = 382.671 \text{ kg/m}^3$					
320.00	153.255	384.749	0.152	1.567	149.998
310.00	146.102	385.458	0.196	1.517	141.875
300.00	138.909	386.174	0.227	1.466	133.775
290.00	131.404	386.906	0.292	1.414	125.417
280.00	123.913	387.647	0.331	1.361	117.143
270.00	116.283	388.401	0.372	1.307	108.796
260.00	108.572	389.170	0.402	1.252	100.439
250.00	100.712	389.956	0.432	1.195	92.003
240.00	92.716	390.765	0.459	1.138	83.506
230.00	84.574	391.599	0.483	1.079	74.941
220.00	76.296	392.465	0.500	1.019	66.321
210.00	67.890	393.371	0.507	0.957	57.655
200.00	59.332	394.332	0.507	0.893	48.923
190.00	50.644	395.368	0.493	0.827	40.148
180.00	41.844	396.516	0.461	0.758	31.346
170.00	32.998	397.835	0.395	0.687	22.579
160.00	24.230	399.427	0.261	0.613	13.967
150.00	15.612	401.402	0.036	0.533	5.620
Isochore 3. $\rho^* = 359.081 \text{ kg/m}^3$					
450.00	193.800	352.941	-0.431	1.752	204.556
440.00	188.558	353.533	-0.389	1.713	198.062
430.00	183.199	354.131	-0.338	1.674	191.487
420.00	177.828	354.731	-0.296	1.635	184.939
410.00	172.351	355.337	-0.246	1.595	178.322
400.00	166.951	355.945	-0.224	1.555	171.827
390.00	161.350	356.560	-0.178	1.514	165.166
380.00	155.672	357.181	-0.131	1.473	158.470
370.00	149.924	357.808	-0.084	1.431	151.746
360.00	144.085	358.441	-0.034	1.389	144.973
350.00	138.193	359.081	0.011	1.346	138.193
340.00	132.236	359.727	0.051	1.302	131.394
330.00	126.204	360.382	0.090	1.258	124.567
325.00	123.137	360.713	0.113	1.236	121.120



**Table 30. Continued**

T (K)	P (MPa)	$\rho_c$ (kg/m <sup>3</sup> )	$100 \cdot (\rho_c - \rho_{EoS}) / \rho_c$	$(dP/d\rho^*)_T$ (MPa·m <sup>3</sup> /kg)	P' (MPa)
Isochore 3. $\rho^* = 359.081 \text{ kg/m}^3$					
320.00	120.066	361.046	0.133	1.214	117.681
310.00	113.859	361.719	0.170	1.168	110.777
300.00	107.927	362.392	0.116	1.122	104.212
290.00	101.518	363.089	0.153	1.075	97.209
280.00	95.010	363.801	0.189	1.027	90.161
275.00	91.387	364.176	0.297	1.003	86.277
270.00	88.421	364.529	0.222	0.979	83.088
260.00	81.090	365.303	0.430	0.929	75.309
250.00	74.622	366.063	0.364	0.878	68.488
240.00	67.751	366.865	0.380	0.827	61.316
230.00	60.808	367.702	0.379	0.774	54.138
220.00	53.767	368.587	0.367	0.719	46.929
210.00	46.602	369.540	0.352	0.664	39.662
200.00	39.369	370.585	0.314	0.606	32.398
190.00	32.061	371.770	0.255	0.546	25.128
180.00	24.878	373.144	0.087	0.484	18.067
170.00	17.926	374.758	-0.262	0.419	11.355
160.00	10.359	376.726	-0.416	0.350	4.192
Isochore 4. $\rho^* = 326.439 \text{ kg/m}^3$					
450.00	146.879	320.809	-0.447	1.301	154.205
440.00	142.519	321.348	-0.401	1.268	148.974
430.00	138.102	321.893	-0.353	1.234	143.714
420.00	133.630	322.442	-0.303	1.200	138.429
410.00	129.127	322.995	-0.257	1.166	133.144
400.00	124.565	323.554	-0.209	1.132	127.830
390.00	119.962	324.118	-0.163	1.097	122.508
380.00	115.312	324.688	-0.120	1.061	117.171
370.00	110.611	325.264	-0.077	1.025	111.816
360.00	105.850	325.848	-0.033	0.989	106.435
350.00	101.041	326.439	0.008	0.953	101.041
340.00	96.175	327.039	0.049	0.916	95.626
330.00	91.252	327.649	0.088	0.878	90.190
320.00	86.267	328.270	0.126	0.840	84.729
310.00	81.228	328.903	0.161	0.801	79.253

**Table 30.** Continued

T (K)	P (MPa)	$\rho_c$ (kg/m <sup>3</sup> )	$100 \cdot (\rho_c - \rho_{EoS}) / \rho_c$	$(dP/d\rho^*)_T$ (MPa·m <sup>3</sup> /kg)	P' (MPa)
Isochore 5. $\rho^* = 248.183 \text{ kg/m}^3$					
300.00	35.793	248.183	0.028	0.294	35.793
290.00	32.993	248.781	-0.019	0.270	32.832
280.00	30.162	249.412	-0.068	0.245	29.861
270.00	27.306	250.082	-0.131	0.220	26.888
260.00	24.432	250.798	-0.223	0.195	23.921
250.00	21.523	251.568	-0.320	0.170	20.947
240.00	18.583	252.396	-0.436	0.144	17.975
230.00	15.612	253.281	-0.570	0.119	15.007
220.00	12.599	254.209	-0.698	0.093	12.041
210.00	9.558	255.155	-0.828	0.066	9.094
200.00	6.517	256.083	-0.994	0.040	6.204
Isochore 6. $\rho^* = 172.942 \text{ kg/m}^3$					
300.00	20.567	172.942	0.015	0.141	20.567
290.00	19.023	173.065	-0.001	0.126	19.007
280.00	17.471	173.189	-0.006	0.112	17.444
270.00	15.914	173.315	-0.011	0.097	15.878
260.00	14.361	173.441	-0.074	0.083	14.32
250.00	12.795	173.568	-0.075	0.069	12.752
240.00	11.229	173.695	-0.09	0.054	11.188
230.00	9.666	173.822	-0.141	0.041	9.631
220.00	8.109	173.949	-0.265	0.027	8.081
210.00	6.534	174.077	0.615	0.014	6.517
205.00	5.806	174.138	-1.332	0.009	5.796
Isochore 7. $\rho^* = 99.563 \text{ kg/m}^3$					
420.00	20.120	99.113	0.282	0.217	20.218
400.00	18.790	99.241	0.254	0.199	18.854
390.00	18.128	99.305	0.203	0.190	18.177
380.00	17.461	99.369	0.161	0.181	17.496
370.00	16.791	99.433	0.119	0.171	16.813
360.00	16.116	99.498	0.086	0.162	16.127
350.00	15.446	99.563	-0.001	0.153	15.446
340.00	14.766	99.629	-0.050	0.144	14.757
330.00	14.074	99.695	-0.037	0.134	14.057

**Table 30.** Continued

T (K)	P (MPa)	$\rho_c$ (kg/m <sup>3</sup> )	$100 \cdot (\rho_c - \rho_{EoS}) / \rho_c$	$(dP/d\rho^*)_T$ (MPa·m <sup>3</sup> /kg)	P' (MPa)
Isochore 7. $\rho^* = 99.563 \text{ kg/m}^3$					
320.00	13.376	99.761	0.001	0.125	13.351
310.00	12.677	99.827	0.025	0.116	12.647
300.00	11.962	99.894	0.171	0.106	11.927
290.00	11.268	99.960	0.088	0.097	11.230
280.00	10.559	100.027	0.112	0.088	10.519
270.00	9.863	100.093	-0.082	0.078	9.821
260.00	9.136	100.160	0.048	0.069	9.094
250.00	8.413	100.227	0.057	0.059	8.374
240.00	7.691	100.294	-0.082	0.050	7.655
230.00	6.953	100.362	-0.080	0.041	6.920
220.00	6.193	100.429	0.322	0.031	6.166
Isochore 8. $\rho^* = 49.129 \text{ kg/m}^3$					
450.00	10.683	48.824	0.008	0.220	10.750
440.00	10.406	48.854	0.003	0.213	10.465
430.00	10.128	48.884	0.001	0.206	10.179
420.00	9.850	48.915	-0.010	0.199	9.893
410.00	9.527	48.946	0.450	0.193	9.562
400.00	9.291	48.976	-0.025	0.186	9.319
390.00	9.010	49.006	-0.030	0.179	9.032
380.00	8.727	49.037	-0.022	0.172	8.743
370.00	8.444	49.068	-0.025	0.165	8.454
360.00	8.126	49.099	0.413	0.158	8.131
350.00	7.871	49.129	0.027	0.152	7.871
340.00	7.584	49.160	0.042	0.145	7.580
330.00	7.297	49.190	0.042	0.138	7.288
320.00	7.008	49.221	0.056	0.131	6.996
310.00	6.717	49.252	0.083	0.124	6.702
300.00	6.421	49.283	0.177	0.117	6.403
290.00	6.130	49.314	0.164	0.110	6.110
280.00	5.841	49.344	0.076	0.103	5.819
270.00	5.549	49.375	0.001	0.095	5.526
260.00	5.243	49.406	0.189	0.088	5.219
250.00	4.944	49.437	0.177	0.081	4.919

**Table 30.** Continued

T (K)	P (MPa)	$\rho_c$ (kg/m <sup>3</sup> )	$100 \cdot (\rho_c - \rho_{EoS}) / \rho_c$	$(dP/d\rho^*)_T$ (MPa·m <sup>3</sup> /kg)	P'
Isochore 8. $\rho^* = 49.129$ kg/m <sup>3</sup>					
240.00	4.644	49.468	0.114	0.074	4.619
230.00	4.336	49.499	0.184	0.066	4.311
220.00	4.029	49.531	0.104	0.059	4.005
210.00	3.737	49.561	-0.795	0.051	3.715
Isochore 9. $\rho^* = 39.383$ kg/m <sup>3</sup>					
500.00	9.625	39.021	0.088	0.250	9.715
490.00	9.414	39.045	0.069	0.244	9.497
480.00	9.202	39.069	0.055	0.237	9.277
470.00	8.990	39.093	0.035	0.231	9.057
460.00	8.777	39.117	0.020	0.225	8.837
450.00	8.562	39.141	0.022	0.218	8.615
440.00	8.348	39.165	0.005	0.212	8.394
430.00	8.133	39.189	-0.006	0.206	8.172
420.00	7.916	39.213	0.001	0.199	7.949
410.00	7.699	39.238	0.002	0.193	7.727
400.00	7.481	39.262	0.008	0.186	7.504
390.00	7.263	39.286	0.006	0.180	7.281
380.00	7.044	39.310	0.010	0.173	7.057
370.00	6.825	39.334	0.005	0.167	6.833
360.00	6.605	39.359	0.004	0.161	6.608
350.00	6.383	39.383	0.026	0.154	6.383
340.00	6.161	39.407	0.036	0.148	6.158
330.00	5.938	39.432	0.052	0.141	5.932
320.00	5.715	39.456	0.053	0.134	5.705
310.00	5.490	39.480	0.077	0.128	5.477
300.00	5.262	39.505	0.146	0.121	5.248
290.00	5.038	39.529	0.112	0.115	5.021
280.00	4.812	39.553	0.094	0.108	4.794
270.00	4.585	39.578	0.067	0.101	4.565
260.00	4.353	39.602	0.132	0.094	4.332
250.00	4.122	39.627	0.132	0.088	4.100
240.00	3.891	39.651	0.074	0.081	3.869
230.00	3.663	39.676	-0.174	0.074	3.642

**Table 30.** Continued

T (K)	P (MPa)	$\rho_c$ (kg/m <sup>3</sup> )	$100 \cdot (\rho_c - \rho_{EoS}) / \rho_c$	$(dP/d\rho^*)_T$ (MPa·m <sup>3</sup> /kg)	P' (MPa)
Isochore 9. $\rho^* = 39.383$ kg/m <sup>3</sup>					
220.00	3.455	39.700	-1.338	0.067	3.433
215.00	3.340	39.712	-1.624	0.063	3.320
210.00	3.193	39.725	-0.611	0.059	3.173
205.00	3.088	39.737	-1.501	0.056	3.069
Isochore 10. $\rho^* = 27.526$ kg/m <sup>3</sup>					
370.00	4.822	27.493	0.168	0.170	4.828
360.00	4.682	27.509	0.010	0.164	4.684
350.00	4.534	27.526	0.017	0.158	4.534
340.00	4.384	27.543	0.061	0.152	4.381
330.01	4.214	27.560	0.600	0.146	4.209
320.00	4.084	27.576	0.126	0.140	4.077
310.00	3.939	27.593	0.008	0.134	3.930
305.15	3.868	27.601	-0.040	0.131	3.858
300.00	3.788	27.609	0.033	0.128	3.778
290.00	3.639	27.626	-0.015	0.122	3.627
280.00	3.489	27.643	-0.057	0.116	3.476
270.00	3.336	27.660	-0.027	0.109	3.321
260.00	3.182	27.677	0.014	0.103	3.167
240.00	2.874	27.710	0.006	0.091	2.857
220.00	2.561	27.744	0.015	0.078	2.544
210.01	2.402	27.761	0.041	0.071	2.386

### APPENDIX C. REGRESSION RESULTS OF FIT P VS T

**Table 31.** Coefficients, standard error, rms and number of points per isochore (n) for regression analysis using Eq. 30

<b>Isochore</b>	<b>Parameter</b>	<b>a1</b>	<b>a2</b>	<b>a3</b>	<b>b1</b>	<b>b2</b>	<b>b3</b>	<b>rms</b>	<b>n</b>
1	Coefficient	10.009	-1.75E-01	7.57E-04	-6.15E-02	5.45E-04	2.96E-07	4.71E-03	17
	Standard error	1.73E-03	9.09E-06	4.27E-08	7.35E-06	1.60E-07	1.28E-11		
2	Coefficient	9.052	-1.27E-01	4.46E-04	-6.49E-02	4.43E-04	1.65E-07	1.23E-03	24
	Standard error	5.98E-05	3.63E-07	2.12E-09	2.70E-06	3.49E-08	1.55E-12		
3	Coefficient	11.148	-1.50E-01	5.03E-04	-8.92E-02	6.11E-04	1.85E-07	1.53E-03	25
	Standard error	6.50E-04	3.34E-06	1.42E-08	4.82E-06	8.98E-08	3.16E-12		
4	Coefficient	2.332	-5.53E+00	3.21E-02	-1.02E+00	5.72E-02	6.50E-06	2.32E-05	15
	Standard error	4.83E-02	1.30E-04	3.40E-07	8.69E-07	1.09E-06	5.51E-12		
5	Coefficient	15.119	-1.65E-01	4.52E-04	-2.78E-01	1.48E-03	6.62E-08	5.31E-06	11
	Standard error	7.33E-05	3.42E-07	1.56E-09	3.41E-05	2.75E-07	1.53E-13		
6	Coefficient	10.718	-1.16E-01	3.13E-04	-4.08E-01	2.01E-03	-1.85E-08	6.27E-06	9
	Standard error	1.87E-05	9.11E-08	4.43E-10	1.54E-04	1.07E-06	2.58E-14		
7	Coefficient	20.197	-2.40E-01	6.75E-04	-1.89E+00	8.23E-03	1.92E-06	4.27E-05	18
	Standard error	1.12E-04	5.10E-07	2.31E-09	5.26E-04	3.75E-06	7.57E-11		
8	Coefficient	-17.486	1.71E-01	2.06E-04	5.61E+00	8.65E-03	-5.34E-07	1.38E-05	23
	Standard error	1.12E-02	3.46E-05	9.77E-08	6.53E-04	5.50E-07	6.78E-13		
9	Coefficient	19.567	-3.55E-01	1.26E-03	-1.08E+01	5.11E-02	5.44E-06	1.52E-06	29
	Standard error	1.87E-04	9.03E-07	4.32E-09	5.82E-04	5.71E-06	2.74E-11		
10	Coefficient	13.357	-3.23E-01	1.57E-03	-1.41E+01	9.37E-02	1.45E-05	2.88E-06	14
	Standard error	9.84E-03	3.81E-05	1.38E-07	2.60E-03	3.76E-05	2.84E-10		

## APPENDIX D. FIRST AND SECOND DERIVATIVES

**Table 32.** First and second derivatives for set 1

Isochore	P' (MPa)	$\rho^*$ (kmol/m <sup>3</sup> )	Analytical Derivatives		Numerical Derivatives	
			(dP/dT)	(d <sup>2</sup> P/dT <sup>2</sup> )	(dP/dT)	(d <sup>2</sup> P/dT <sup>2</sup> )
			(MPa/K)	(MPa/K <sup>2</sup> )	(MPa/K)	(MPa/K <sup>2</sup> )
T = 220 K						
1	112.942	24.817	1.1291	-1.07E-03	1.1253	-1.25E-03
2	66.321	22.664	0.8634	-5.05E-04	0.8643	-4.44E-04
3	46.929	21.267	0.7227	-2.09E-04	0.7238	-5.76E-04
5	12.041	14.699	0.2958	1.51E-04	0.2956	1.95E-04
6	8.08	10.242	0.1558	5.97E-05	0.1556	-1.50E-04
8	4.004	2.91	0.0304	-1.28E-05	0.0298	1.54E-04
9	3.432	2.332	0.0233	-1.79E-05	0.0322	3.79E-03
10	2.543	1.63	0.0158	-9.80E-06	0.0159	9.10E-06
T = 230 K						
1	124.133	24.817	1.1186	-1.05E-03	1.1128	-1.34E-03
2	74.941	22.664	0.8582	-5.19E-04	0.8593	-5.59E-04
3	54.138	21.267	0.7203	-2.63E-04	0.7194	-3.17E-04
5	15.007	14.699	0.2968	5.60E-05	0.2967	2.44E-05
6	9.629	10.242	0.1561	1.67E-05	0.1553	8.69E-05
7	6.918	5.897	0.073	-7.65E-05	-0.0002	-1.88E-04
8	4.31	2.91	0.0303	-1.22E-05	0.0307	1.61E-05
9	3.641	2.332	0.0232	-7.08E-06	0.0218	1.93E-04
10	2.702	1.63	0.0157	-9.80E-06	0.0157	-4.13E-05
T = 240 K						
1	135.191	24.817	1.1082	-1.03E-03	1.101	-9.18E-04
2	83.506	22.664	0.853	-5.25E-04	0.8531	-6.77E-04
3	61.316	21.267	0.7175	-2.95E-04	0.7175	-5.20E-05
5	17.975	14.699	0.2971	1.85E-05	0.297	4.04E-05
6	11.186	10.242	0.1562	8.21E-06	0.1561	6.71E-05
7	7.653	5.897	0.0725	-3.72E-05	0.0727	-1.56E-04
8	4.618	2.91	0.0301	-1.17E-05	0.0304	-7.31E-05
9	3.868	2.332	0.0231	-5.49E-06	0.0229	3.29E-05
10	2.856	1.63	0.0156	-8.25E-06	0.0156	2.62E-05

**Table 32. Continued**

Isochore	P' (MPa)	$\rho^*$ (kmol/m <sup>3</sup> )	Analytical Derivatives		Numerical Derivatives	
			(dP/dT) (MPa/K)	(d <sup>2</sup> P/dT <sup>2</sup> ) (MPa/K <sup>2</sup> )	(dP/dT) (MPa/K)	(d <sup>2</sup> P/dT <sup>2</sup> ) (MPa/K <sup>2</sup> )
T = 250 K						
1	146.16	24.82	1.10	-1.01E-03	1.0911	-1.12E-03
2	92.00	22.66	0.85	-5.28E-04	0.8466	-6.20E-04
3	68.49	21.27	0.71	-3.16E-04	0.6996	-3.52E-03
5	20.95	14.70	0.30	7.44E-07	0.2973	1.15E-05
6	12.75	10.24	0.16	5.47E-06	0.1566	3.44E-05
7	8.37	5.90	0.07	-3.24E-05	0.072	1.44E-05
8	4.92	2.91	0.03	-1.12E-05	0.03	-5.88E-06
9	4.10	2.33	0.02	-5.04E-06	0.0231	7.73E-06
10	3.01	1.63	0.02	-7.24E-06	0.0155	-5.05E-05
T = 260 K						
1	157.011	24.817	1.0879	-9.97E-04	1.0991	-1.12E-03
2	100.439	22.664	0.8319	-5.28E-04	0.8396	-6.20E-04
3	75.309	21.267	0.7112	-3.30E-04	0.73	9.60E-03
5	23.921	14.699	0.2972	-8.67E-06	0.297	-6.70E-05
6	14.318	10.242	0.1563	4.33E-06	0.1563	-9.16E-05
7	9.092	5.897	0.0719	-3.11E-05	0.0724	6.61E-05
8	5.218	2.91	0.0299	-1.07E-05	0.0303	7.23E-05
9	4.331	2.332	0.023	-4.86E-06	0.0233	1.57E-05
10	3.166	1.63	0.0154	-6.55E-06	0.0153	1.99E-05
T = 270 K						
1	168.125	24.817	1.078	-9.82E-04	1.0925	-3.58E-03
2	108.796	22.664	0.8372	-5.27E-04	0.8352	-1.03E-04
3	83.088	21.267	0.7078	-3.39E-04	0.7426	-7.08E-03
5	26.888	14.699	0.2971	-1.41E-05	0.297	6.46E-05
6	15.876	10.242	0.1564	3.78E-06	0.1562	7.71E-05
7	9.819	5.897	0.0716	-3.05E-05	0.0712	-2.95E-04
8	5.525	2.91	0.0298	-1.03E-05	0.03	-1.41E-04
9	4.564	2.332	0.023	-4.77E-06	0.0231	-4.65E-05
10	3.32	1.63	0.0154	-6.06E-06	0.0154	2.58E-06



**Table 32. Continued**

Isochore	P' (MPa)	$\rho^*$ (kmol/m <sup>3</sup> )	Analytical Derivatives		Numerical Derivatives	
			(dP/dT) (MPa/K)	(d <sup>2</sup> P/dT <sup>2</sup> ) (MPa/K <sup>2</sup> )	(dP/dT) (MPa/K)	(d <sup>2</sup> P/dT <sup>2</sup> ) (MPa/K <sup>2</sup> )
T = 280 K						
1	178.88	24.817	1.0683	-9.67E-04	1.0692	-1.25E-03
2	117.143	22.664	0.8319	-5.25E-04	0.831	-7.31E-04
3	90.161	21.267	0.7044	-3.45E-04	0.706	-2.35E-04
5	29.861	14.699	0.2969	-1.75E-05	0.2972	-2.23E-05
6	17.442	10.242	0.1564	3.48E-06	0.1565	-1.99E-05
7	10.517	5.897	0.0713	-3.01E-05	0.0704	-2.26E-05
8	5.817	2.91	0.0297	-9.82E-06	0.0292	-1.35E-05
9	4.793	2.332	0.0229	-7.91E-06	0.0228	-7.74E-06
10	3.475	1.63	0.0153	-5.70E-06	0.0153	-5.54E-06
T = 290 K						
1	189.51	24.817	1.0587	-9.53E-04	1.0496	-2.69E-03
2	125.417	22.664	0.8267	-5.22E-04	0.8316	8.49E-04
3	97.209	21.267	0.701	-3.48E-04	0.7026	-4.57E-04
5	32.832	14.699	0.2967	-1.97E-05	0.2966	-9.67E-05
6	19.007	10.242	0.1564	3.30E-06	0.1563	-3.63E-05
7	11.228	5.897	0.071	-2.98E-05	0.0704	-1.40E-04
8	6.109	2.91	0.0296	-9.40E-06	0.0292	1.51E-05
9	5.02	2.332	0.0229	-4.67E-06	0.0227	-4.02E-06
10	3.626	1.63	0.0153	-5.43E-06	0.0151	-7.35E-06
T = 300 K						
1	199.871	24.817	1.0492	-9.40E-04	N/A	N/A
2	133.775	22.664	0.8215	-5.19E-04	0.8229	-2.59E-03
3	104.212	21.267	0.6975	-3.50E-04	0.6784	-4.38E-03
5	35.793	14.699	0.2965	-2.12E-05	N/A	N/A
6	20.567	10.242	0.1565	3.19E-06	N/A	N/A
7	11.925	5.897	0.0707	-2.95E-05	0.0709	2.30E-04
8	6.402	2.91	0.0295	-9.00E-06	0.0296	6.65E-05
9	5.247	2.332	0.0228	-4.64E-06	0.0228	3.15E-05
10	3.777	1.63	0.0152	-5.22E-06	0.0152	1.45E-05

**Table 33.** First and second derivatives for set 2

Isochore	$P'$ (MPa)	$\rho^*$ (kmol/m <sup>3</sup> )	Analytical Derivatives		Numerical Derivatives	
			(dP/dT) (MPa/K)	(d <sup>2</sup> P/dT <sup>2</sup> ) (MPa/K <sup>2</sup> )	(dP/dT) (MPa/K)	(d <sup>2</sup> P/dT <sup>2</sup> ) (MPa/K <sup>2</sup> )
T = 310 K						
2	141.875	22.664	0.8163	-5.15E-04	0.811	2.36E-04
3	110.777	21.267	0.694	-3.51E-04	0.673	3.39E-03
4	79.253	19.333	0.5491	-2.36E-04	N/A	N/A
7	12.645	5.897	0.0704	-2.93E-05	0.071	-1.55E-04
8	6.701	2.91	0.0294	-8.62E-06	0.03	-6.11E-05
9	5.477	2.332	0.0227	-4.62E-06	0.023	-2.36E-05
10	3.929	1.63	0.0151	-5.05E-06	0.015	-5.40E-05
T = 320 K						
2	149.998	22.664	0.8112	-5.11E-04	0.8099	-4.84E-04
3	117.681	21.267	0.6905	-3.51E-04	0.6895	-1.87E-04
4	84.729	19.333	0.5468	-2.24E-04	0.5468	-1.43E-04
7	13.35	5.897	0.0701	-2.91E-05	0.0705	1.42E-05
8	6.995	2.91	0.0294	-8.25E-06	0.0293	-7.92E-06
9	5.704	2.332	0.0227	-4.60E-06	0.0227	-6.73E-06
10	4.076	1.63	0.0151	-4.92E-06	0.014	-1.47E-04
T = 330 K						
2	158.073	22.664	0.8061	-5.07E-04	0.806	-2.91E-04
3	124.567	21.267	0.6869	-3.51E-04	0.6856	-5.77E-04
4	90.19	19.333	0.5446	-2.14E-04	0.5449	-2.49E-04
7	14.056	5.897	0.0698	-2.89E-05	0.0703	-5.51E-05
8	7.288	2.91	0.0293	-7.90E-06	0.0292	-5.54E-06
9	5.931	2.332	0.0227	-4.58E-06	0.0226	-7.68E-06
10	4.208	1.63	0.015	-4.81E-06	0.0152	4.05E-04
T = 340 K						
2	166.119	22.664	0.801	-5.03E-04	0.8018	-5.64E-04
3	131.394	21.267	0.6834	-3.50E-04	0.6813	-2.93E-04
4	95.626	19.333	0.5425	-2.04E-04	0.5426	-2.10E-04
7	14.756	5.897	0.0695	-2.87E-05	0.0695	-1.10E-04
8	7.58	2.91	0.0292	-7.56E-06	0.0292	-9.99E-06
9	6.157	2.332	0.0226	-4.56E-06	0.0226	-1.98E-06
10	4.381	1.63	0.015	-4.72E-06	0.0163	-2.03E-04

**Table 33.** Continued

Isochore	$P'$ (MPa)	$\rho^*$ (kmol/m <sup>3</sup> )	Analytical Derivatives		Numerical Derivatives	
			(dP/dT) (MPa/K)	(d <sup>2</sup> P/dT <sup>2</sup> ) (MPa/K <sup>2</sup> )	(dP/dT) (MPa/K)	(d <sup>2</sup> P/dT <sup>2</sup> ) (MPa/K <sup>2</sup> )
T = 350 K						
2	174.109	22.664	0.796	-4.99E-04	0.7967	-5.64E-04
3	138.193	21.267	0.6799	-3.49E-04	0.679	-1.76E-04
4	101.041	19.333	0.5405	-1.96E-04	0.5405	-2.11E-04
7	15.446	5.897	0.0692	-2.86E-05	0.0686	-8.39E-05
8	7.871	2.91	0.0291	-7.23E-06	0.0276	-3.12E-04
9	6.383	2.332	0.0226	-4.55E-06	0.0226	-5.37E-06
10	4.534	1.63	0.015	-4.64E-06	0.0152	-1.28E-05
T = 360 K						
2	182.052	22.664	0.791	-4.95E-04	0.7917	-5.32E-04
3	144.973	21.267	0.6765	-3.47E-04	0.6777	-8.13E-05
4	106.435	19.333	0.5386	-1.89E-04	0.5387	-1.32E-04
7	16.127	5.897	0.0689	-2.84E-05	0.0684	6.28E-05
8	8.131	2.91	0.0291	-6.92E-06	0.0292	6.41E-04
9	6.609	2.332	0.0225	-4.53E-06	0.0225	-6.76E-06
10	4.685	1.63	0.0149	-4.58E-06	0.0147	-7.52E-05
T = 370 K						
2	189.943	22.664	0.7837	-4.90E-04	0.787	-4.05E-04
3	151.746	21.267	0.673	-3.46E-04	0.6748	-4.85E-04
4	111.816	19.333	0.5367	-1.82E-04	0.5368	-2.56E-04
7	16.815	5.897	0.0686	-2.82E-05	0.0685	-4.17E-05
8	8.455	2.91	0.029	-6.62E-06	0.0307	-3.50E-04
9	6.833	2.332	0.0225	-4.52E-06	0.0224	-4.26E-06
10	4.828	1.63	0.0149	-4.52E-06	N/A	N/A
T = 380 K						
2	197.792	22.664	0.7812	-4.86E-04	0.7825	-4.95E-04
3	158.47	21.267	0.6696	-3.44E-04	0.671	-2.83E-04
4	117.171	19.333	0.535	-1.77E-04	0.5346	-1.82E-04
7	17.498	5.897	0.0684	-2.80E-05	0.0685	-1.44E-05
8	8.744	2.91	0.0289	-6.33E-06	0.0289	2.46E-07
9	7.058	2.332	0.0224	-4.50E-06	0.0224	-2.44E-06

**Table 33.** Continued

Isochore	$P'$ (MPa)	$\rho^*$ (kmol/m <sup>3</sup> )	Analytical Derivatives		Numerical Derivatives	
			(dP/dT) (MPa/K)	(d <sup>2</sup> P/dT <sup>2</sup> ) (MPa/K <sup>2</sup> )	(dP/dT) (MPa/K)	(d <sup>2</sup> P/dT <sup>2</sup> ) (MPa/K <sup>2</sup> )
T = 390 K						
2	205.593	22.664	0.776	-4.82E-04	N/A	N/A
3	165.166	21.267	0.666	-3.42E-04	0.668	-3.48E-04
4	122.508	19.333	0.533	-1.71E-04	0.533	-1.45E-04
7	18.18	5.897	0.068	-2.78E-05	0.068	-4.41E-05
8	9.033	2.91	0.029	-6.06E-06	0.029	-1.45E-05
9	7.282	2.332	0.022	-4.49E-06	0.022	-3.98E-06

**Table 34.** First and second derivatives for set 3

Isochore	$P'$ (MPa)	$\rho^*$ (kmol/m <sup>3</sup> )	Analytical Derivatives		Numerical Derivatives	
			(dP/dT) (MPa/K)	(d <sup>2</sup> P/dT <sup>2</sup> ) (MPa/K <sup>2</sup> )	(dP/dT) (MPa/K)	(d <sup>2</sup> P/dT <sup>2</sup> ) (MPa/K <sup>2</sup> )
T = 400 K						
3	171.827	21.267	0.6627	-3.40E-04	0.6578	-1.66E-03
4	127.83	19.333	0.5315	-1.66E-04	0.5318	-8.66E-05
7	18.857	5.897	0.0678	-2.77E-05	0.0681	7.69E-05
8	9.321	2.91	0.0288	-5.79E-06	0.0265	-4.47E-04
9	7.505	2.332	0.0224	-4.56E-06	0.0223	-3.98E-06
T = 410 K						
3	178.322	21.267	0.6593	-3.38E-04	0.6556	1.22E-03
4	133.144	19.333	0.5299	-1.62E-04	0.5299	-2.86E-04
7	19.542	5.897	0.0675	-2.75E-05	0.0683	-4.27E-05
8	9.564	2.91	0.0287	-5.53E-06	0.0287	8.86E-04
9	7.728	2.332	0.0223	-4.46E-06	0.0223	-3.01E-06
T = 420 K						
3	184.939	21.267	0.656	-3.36E-04	0.6582	-6.86E-04
4	138.429	19.333	0.5283	-1.58E-04	0.5285	-5.11E-07
7	20.223	5.897	0.0673	-2.73E-05	N/A	N/A
8	9.895	2.91	0.0287	-5.28E-06	0.0309	-4.53E-04
9	7.951	2.332	0.0223	-4.45E-06	0.0223	3.64E-06

**Table 34. Continued**

Isochore	$P'$ (MPa)	$\rho^*$ (kmol/m <sup>3</sup> )	Analytical Derivatives		Numerical Derivatives	
			(dP/dT) (MPa/K)	(d <sup>2</sup> P/dT <sup>2</sup> ) (MPa/K <sup>2</sup> )	(dP/dT) (MPa/K)	(d <sup>2</sup> P/dT <sup>2</sup> ) (MPa/K <sup>2</sup> )
T = 430 K						
3	191.487	21.267	0.6526	-3.33E-04	0.6562	2.73E-04
4	143.714	19.333	0.5267	-1.54E-04	0.5272	-2.54E-04
8	10.182	2.91	0.0286	-5.05E-06	0.0286	1.56E-07
9	8.175	2.332	0.0222	-4.43E-06	0.0223	-1.43E-05
T = 440 K						
3	198.062	21.267	0.6493	-3.31E-04	0.6535	-8.14E-04
4	148.974	19.333	0.5252	-1.51E-04	0.5246	-2.84E-04
8	10.468	2.91	0.0286	-4.82E-06	0.0286	-5.43E-06
9	8.396	2.332	0.0222	-4.42E-06	0.0222	-1.12E-06
T = 450 K						
3	204.556	21.267	0.646	-3.29E-04	N/A	N/A
4	154.205	19.333	0.5237	-1.48E-04	N/A	N/A
8	10.754	2.91	0.0285	-4.60E-06	N/A	N/A
9	8.618	2.332	0.0221	-4.41E-06	0.022	-9.61E-07

## APPENDIX E. EXPRESSION OF RESIDUAL HEAT CAPACITY

The heat capacity at constant volume (Eq. 41) and the residual heat capacity at constant volume (Eq. 42):

$$C_v = \left( \frac{\partial U}{\partial T} \right)_v \quad (41)$$

$$C_v^r = \left( \frac{\partial U^r}{\partial T} \right)_v \quad (42)$$

The residual internal energy, Helmholtz energy and entropy are defined as:

$$\frac{U^r}{RT} = \frac{A^r}{RT} + \frac{S^r}{R} \quad (43)$$

$$\frac{A^r}{RT} = \int_0^\rho (Z-1) \frac{d\rho}{\rho} \quad (44)$$

$$\frac{S^r}{R} = \int_0^\rho \left[ 1 - \frac{1}{\rho R} \left( \frac{\partial P}{\partial T} \right)_\rho \right] \frac{d\rho}{\rho} \quad (45)$$

$$U^r = \int_0^\rho \frac{1}{\rho} \left[ P - T \left( \frac{\partial P}{\partial T} \right)_\rho \right] \frac{d\rho}{\rho} \quad (46)$$

Replacing Eqs. 44 and 45 into Eq. 43, and taking the derivative with respect to temperature:

$$\left(\frac{\partial U^r}{\partial T}\right)_{1/\rho} = \int_0^\rho \left(\frac{\partial P}{\partial T}\right)_\rho \frac{d\rho}{\rho^2} - \int_0^\rho \left[ \left(\frac{\partial P}{\partial T}\right)_\rho + T \left(\frac{\partial^2 P}{\partial T^2}\right)_\rho \right] \frac{d\rho}{\rho^2} \quad (47)$$

Replacing Eq. 47 into Eq. 42:

$$C_v^r = -T \int_0^\rho \left(\frac{\partial^2 P}{\partial T^2}\right)_\rho \frac{d\rho}{\rho^2} \quad (48)$$

## APPENDIX F. REGRESSION RESULTS OF INTEGRAND FUNCTION

**Table 35.** Regression results of Eq. 35 for set 1

Coefficient		Standard Error	Lower 95%	Upper 95%	rms
<b>T = 220 K</b>					
c <sub>1</sub>	-2.56E-08	1.13E-09	-3.56E-08	-1.56E-08	
c <sub>2</sub>	7.33E-07	2.46E-08	4.73E-07	9.94E-07	2.86E-13
c <sub>3</sub>	-4.39E-06	3.81E-07	-5.54E-06	-3.23E-06	
<b>T = 230 K</b>					
c <sub>1</sub>	-1.71E-08	1.66E-09	-3.12E-08	-3.00E-09	
c <sub>2</sub>	4.95E-07	3.57E-08	1.24E-07	8.66E-07	6.61E-13
c <sub>3</sub>	-3.43E-06	5.26E-07	-5.09E-06	-1.76E-06	
<b>T = 240 K</b>					
c <sub>1</sub>	-1.57E-08	1.14E-09	-2.54E-08	-6.06E-09	
c <sub>2</sub>	4.36E-07	2.45E-08	1.81E-07	6.90E-07	3.11E-13
c <sub>3</sub>	-2.83E-06	3.61E-07	-3.97E-06	-1.68E-06	
<b>T = 250 K</b>					
c <sub>1</sub>	-1.43E-08	9.57E-10	-2.24E-08	-6.15E-09	
c <sub>2</sub>	3.90E-07	2.06E-08	1.75E-07	6.04E-07	2.20E-13
c <sub>3</sub>	-2.53E-06	3.04E-07	-3.49E-06	-1.57E-06	
<b>T = 260 K</b>					
c <sub>1</sub>	-1.33E-08	8.34E-10	-2.04E-08	-6.21E-09	
c <sub>2</sub>	3.59E-07	1.80E-08	1.72E-07	5.45E-07	1.67E-13
c <sub>3</sub>	-2.34E-06	2.65E-07	-3.18E-06	-1.51E-06	
<b>T = 270 K</b>					
c <sub>1</sub>	-1.26E-08	7.48E-10	-1.89E-08	-6.23E-09	
c <sub>2</sub>	3.37E-07	1.61E-08	1.69E-07	5.04E-07	1.34E-13
c <sub>3</sub>	-2.21E-06	2.37E-07	-2.96E-06	-1.46E-06	



**Table 35.** Continued

	Coefficient	Standard Error	Lower 95%	Upper 95%	rms
T = 280 K					
c <sub>1</sub>	-1.30E-08	4.25E-10	-1.66E-08	-9.41E-09	
c <sub>2</sub>	3.53E-07	9.14E-09	2.58E-07	4.48E-07	4.33E-14
c <sub>3</sub>	-2.36E-06	1.35E-07	-2.78E-06	-1.93E-06	
T = 290 K					
c <sub>1</sub>	-1.16E-08	6.42E-10	-1.71E-08	-6.16E-09	
c <sub>2</sub>	3.07E-07	1.38E-08	1.63E-07	4.51E-07	9.90E-14
c <sub>3</sub>	-2.03E-06	2.04E-07	-2.67E-06	-1.39E-06	
T = 300 K					
c <sub>1</sub>	-1.13E-08	6.10E-10	-1.64E-08	-6.08E-09	
c <sub>2</sub>	2.97E-07	1.31E-08	1.60E-07	4.33E-07	8.94E-14
c <sub>3</sub>	-1.96E-06	1.94E-07	-2.58E-06	-1.35E-06	

**Table 36.** Regression results of Eq. 35 for set 2

	Coefficient	Standard Error	Lower 95%	Upper 95%	rms
T = 310 K					
c <sub>1</sub>	-8.52E-09	9.32E-10	-2.25E-08	5.44E-09	
c <sub>2</sub>	2.26E-07	1.95E-08	-1.13E-07	5.65E-07	1.16E-13
c <sub>3</sub>	-1.77E-06	2.75E-07	-2.81E-06	-7.23E-07	
T = 320 K					
c <sub>1</sub>	-8.42E-09	8.98E-10	-2.19E-08	5.05E-09	
c <sub>2</sub>	2.23E-07	1.88E-08	-1.04E-07	5.50E-07	1.08E-13
c <sub>3</sub>	-1.73E-06	2.65E-07	-2.74E-06	-7.24E-07	
T = 330 K					
c <sub>1</sub>	-8.34E-09	8.75E-10	-2.15E-08	4.79E-09	
c <sub>2</sub>	2.20E-07	1.83E-08	-9.83E-08	5.39E-07	1.03E-13
c <sub>3</sub>	-1.70E-06	2.58E-07	-2.68E-06	-7.18E-07	

**Table 36. Continued**

	Coefficient	Standard Error	Lower 95%	Upper 95%	rms
T = 340 K					
c <sub>1</sub>	-8.28E-09	8.61E-10	-2.12E-08	4.63E-09	
c <sub>2</sub>	2.18E-07	1.80E-08	-9.53E-08	5.31E-07	9.94E-14
c <sub>3</sub>	-1.67E-06	2.54E-07	-2.64E-06	-7.06E-07	
T = 350 K					
c <sub>1</sub>	-8.22E-09	8.53E-10	-2.10E-08	4.57E-09	
c <sub>2</sub>	2.16E-07	1.79E-08	-9.42E-08	5.27E-07	9.76E-14
c <sub>3</sub>	-1.65E-06	2.52E-07	-2.60E-06	-6.90E-07	
T = 360 K					
c <sub>1</sub>	-8.18E-09	8.50E-10	-2.09E-08	4.57E-09	
c <sub>2</sub>	2.15E-07	1.78E-08	-9.48E-08	5.24E-07	9.69E-14
c <sub>3</sub>	-1.62E-06	2.51E-07	-2.58E-06	-6.71E-07	
T = 370 K					
c <sub>1</sub>	-8.13E-09	8.51E-10	-2.09E-08	4.62E-09	
c <sub>2</sub>	2.13E-07	1.78E-08	-9.65E-08	5.23E-07	9.71E-14
c <sub>3</sub>	-1.60E-06	2.51E-07	-2.56E-06	-6.49E-07	
T = 380 K					
c <sub>1</sub>	-3.72E-09	4.68E-10	-1.20E-08	4.51E-09	
c <sub>2</sub>	9.41E-08	9.81E-09	-1.11E-07	2.99E-07	2.41E-14
c <sub>3</sub>	-1.07E-06	1.49E-07	-1.77E-06	-3.55E-07	
T = 390 K					
c <sub>1</sub>	-3.70E-09	4.90E-10	-1.23E-08	4.92E-09	
c <sub>2</sub>	9.31E-08	1.03E-08	-1.21E-07	3.08E-07	2.65E-14
c <sub>3</sub>	-1.05E-06	1.56E-07	-1.79E-06	-3.05E-07	

**Table 37.** Regression results of Eq. 35 for set 3

	Coefficient	Standard Error	Lower 95%	Upper 95%	rms
T = 400 K					
c <sub>1</sub>	-1.70E-09	8.64E-10	-1.74E-08	1.40E-08	
c <sub>2</sub>	4.96E-08	1.72E-08	-3.25E-07	4.25E-07	3.03E-14
c <sub>3</sub>	-9.18E-07	2.27E-07	-2.15E-06	3.09E-07	
T = 410 K					
c <sub>1</sub>	-1.51E-09	9.12E-10	-1.81E-08	1.51E-08	
c <sub>2</sub>	4.43E-08	1.81E-08	-3.51E-07	4.40E-07	3.37E-14
c <sub>3</sub>	-8.83E-07	2.40E-07	-2.18E-06	4.12E-07	
T = 420 K					
c <sub>1</sub>	-1.46E-09	9.64E-10	-1.90E-08	1.61E-08	
c <sub>2</sub>	4.29E-08	1.92E-08	-3.76E-07	4.61E-07	3.77E-14
c <sub>3</sub>	-8.66E-07	2.53E-07	-2.24E-06	5.03E-07	
T = 430 K					
c <sub>1</sub>	-1.08E-08	8.23E-10	-4.96E-08	2.79E-08	
c <sub>2</sub>	2.57E-07	1.67E-08	-6.38E-07	1.15E-06	5.85E-15
c <sub>3</sub>	-1.30E-06	2.42E-07	-3.55E-06	9.45E-07	
T = 440 K					
c <sub>1</sub>	-1.11E-08	9.98E-10	-5.81E-08	3.58E-08	
c <sub>2</sub>	2.63E-07	2.02E-08	-8.21E-07	1.35E-06	8.60E-15
c <sub>3</sub>	-1.30E-06	2.93E-07	-4.03E-06	1.42E-06	
T = 450 K					
c <sub>1</sub>	-1.14E-08	1.17E-09	-6.63E-08	4.35E-08	
c <sub>2</sub>	2.68E-07	2.36E-08	-1.00E-06	1.54E-06	1.18E-14
c <sub>3</sub>	-1.30E-06	3.42E-07	-4.49E-06	1.88E-06	

## APPENDIX G. IDEAL GAS HEAT CAPACITY DIPPR PROJECT

$$C_v^{ig} = A + B \left[ \frac{C/T}{\sinh(C/T)} \right]^2 + D \left[ \frac{E/T}{\cosh(E/T)} \right]^2 \quad (49)$$

The ideal gas heat capacity ( $C_v^{ig}$ ) calculated with Eq. 49 has units of J/kmol-K. Temperature range: 298.1 – 1500 K (Methane) and 50 – 1500 K (Ethane and Propane) and maximum percentage of deviation: 0.1% (Methane) and 0.3% (Ethane and Propane). The parameters needed in Eq. 49 appear in Table G-1 for each substance.

**Table 38.** Parameters for Eq. 49

Parameter	Methane	Ethane	Propane
A	33298	44256	59474
B	79933	84737	126610
C	2086.9	872.24	844.31
D	41602	67130	86165
E	991.96	2430.4	2482.7

## APPENDIX H. RESIDUAL AND ABSOLUTE HEAT CAPACITY

**Table 39.** Residual and absolute heat capacity for set 1

Isochore	$P'$ (MPa)	$\rho^*$ (kmol/m <sup>3</sup> )	$(d^2P/dT^2) \cdot \rho^{-2}$ (MPa·m <sup>6</sup> /K <sup>2</sup> ·kmol <sup>2</sup> )	$C_v^r$	$C_v$ (kJ/kmol-K)	$C_v^{(GERG)}$ <small>EoS</small>
T = 220 K						
1	112.942	24.817	-1.74E-06	2.907	28.992	32.971
2	66.321	22.664	-9.83E-07	2.249	28.333	31.764
3	46.929	21.267	-4.63E-07	2.06	28.145	31.167
5	12.041	14.699	6.98E-07	2.704	28.789	31.115
6	8.08	10.242	5.69E-07	3.433	29.517	33.076
8	4.004	2.91	-1.51E-06	2.171	28.255	29.219
9	3.432	2.332	-3.28E-06	1.835	27.92	28.578
10	2.543	1.63	-3.69E-06	1.367	27.451	27.791
T = 230 K						
1	124.133	24.817	-1.70E-06	4.502	30.782	33.101
2	74.941	22.664	-1.01E-06	3.855	30.136	31.9
3	54.138	21.267	-5.81E-07	3.6	29.88	31.292
5	15.007	14.699	2.59E-07	3.438	29.718	30.763
6	9.629	10.242	1.60E-07	3.504	29.784	31.899
7	6.918	5.897	-2.20E-06	2.935	29.216	31.219
8	4.31	2.91	-1.44E-06	1.843	28.124	28.962
9	3.641	2.332	-1.30E-06	1.545	27.825	28.427
10	2.702	1.63	-3.69E-06	1.139	27.42	27.761
T = 240 K						
1	135.191	24.817	-1.67E-06	3.839	30.346	33.264
2	83.506	22.664	-1.02E-06	3.144	29.651	32.071
3	61.316	21.267	-6.53E-07	2.863	29.37	31.455
5	17.975	14.699	8.54E-08	2.662	29.168	30.601
6	11.186	10.242	7.83E-08	2.81	29.317	31.308
7	7.653	5.897	-1.07E-06	2.438	28.944	30.702
8	4.618	2.91	-1.38E-06	1.561	28.068	28.832
9	3.868	2.332	-1.01E-06	1.313	27.82	28.378
10	2.856	1.63	-3.10E-06	0.972	27.479	27.807

**Table 39.** Continued

Isochore	$P'$ (MPa)	$\rho^*$ (kmol/m <sup>3</sup> )	$(d^2P/dT^2) \cdot \rho^{-2}$ (MPa · m <sup>6</sup> /K <sup>2</sup> · kmol <sup>2</sup> )	$C_v^r$	$C_v$ (kJ/kmol-K)	$C_v^{(GERG)}$ <i>EoS</i> )
T = 250 K						
1	146.157	24.817	-1.64E-06	3.907	30.671	33.46
2	92.003	22.664	-1.03E-06	3.187	29.951	32.277
3	68.488	21.267	-7.00E-07	2.884	29.648	31.656
5	20.947	14.699	3.44E-09	2.563	29.327	30.566
6	12.75	10.242	5.22E-08	2.654	29.418	30.985
7	8.372	5.897	-9.33E-07	2.284	29.048	30.397
8	4.918	2.91	-1.32E-06	1.459	28.223	28.805
9	4.099	2.332	-9.26E-07	1.227	27.991	28.413
10	3.014	1.63	-2.72E-06	0.908	27.672	27.918
T = 260 K						
1	157.011	24.817	-1.62E-06	4.018	31.072	33.69
2	100.439	22.664	-1.03E-06	3.276	30.33	32.517
3	75.309	21.267	-7.30E-07	2.956	30.009	31.894
5	23.921	14.699	-4.01E-08	2.544	29.598	30.626
6	14.318	10.242	4.13E-08	2.59	29.643	30.826
7	9.092	5.897	-8.94E-07	2.209	29.263	30.242
8	5.218	2.91	-1.27E-06	1.407	28.461	28.863
9	4.331	2.332	-8.93E-07	1.183	28.236	28.522
10	3.166	1.63	-2.46E-06	0.875	27.928	28.087
T = 270 K						
1	168.125	24.817	-1.59E-06	4.129	31.504	33.953
2	108.796	22.664	-1.03E-06	3.365	30.74	32.791
3	83.088	21.267	-7.49E-07	3.031	30.405	32.167
5	26.888	14.699	-6.54E-08	2.551	29.926	30.762
6	15.876	10.242	3.60E-08	2.563	29.938	30.788
7	9.819	5.897	-8.76E-07	2.172	29.546	30.206
8	5.525	2.91	-1.21E-06	1.38	28.755	28.995
9	4.564	2.332	-8.76E-07	1.159	28.534	28.694
10	3.32	1.63	-2.28E-06	0.857	28.232	28.308

**Table 39.** Continued

Isochore	$P'$ (MPa)	$\rho^*$ (kmol/m <sup>3</sup> )	$(d^2P/dT^2) \cdot \rho^{-2}$ (MPa · m <sup>6</sup> /K <sup>2</sup> · kmol <sup>2</sup> )	$C_v^r$	$C_v$ (kJ/kmol-K)	$C_v^{(GERG)}$ <i>EoS</i> )
T = 280 K						
1	178.88	24.817	-1.57E-06	4.474	32.201	34.249
2	117.143	22.664	-1.02E-06	3.685	31.411	33.098
3	90.161	21.267	-7.62E-07	3.342	31.068	32.475
5	29.861	14.699	-8.10E-08	2.867	30.594	30.962
6	17.442	10.242	3.31E-08	2.873	30.6	30.847
7	10.517	5.897	-8.65E-07	2.42	30.147	30.267
8	5.817	2.91	-1.16E-06	1.531	29.258	29.19
9	4.793	2.332	-1.45E-06	1.285	29.012	28.922
10	3.475	1.63	-2.14E-06	0.949	28.676	28.576
T = 290 K						
1	189.51	24.817	-1.55E-06	4.337	32.446	34.576
2	125.417	22.664	-1.02E-06	3.533	31.642	33.437
3	97.209	21.267	-7.70E-07	3.173	31.282	32.815
5	32.832	14.699	-9.11E-08	2.596	30.705	31.217
6	19.007	10.242	3.14E-08	2.564	30.673	30.987
7	11.228	5.897	-8.57E-07	2.153	30.262	30.409
8	6.109	2.91	-1.11E-06	1.364	29.473	29.441
9	5.02	2.332	-8.59E-07	1.145	29.254	29.199
10	3.626	1.63	-2.04E-06	0.846	28.955	28.887
T = 300 K						
1	199.871	24.817	-1.53E-06	4.434	32.955	34.933
2	133.775	22.664	-1.01E-06	3.612	32.132	33.806
3	104.212	21.267	-7.74E-07	3.241	31.761	33.185
5	35.793	14.699	-9.80E-08	2.626	31.146	31.52
6	20.567	10.242	3.04E-08	2.579	31.099	31.197
7	11.925	5.897	-8.50E-07	2.16	30.68	30.621
8	6.402	2.91	-1.06E-06	1.366	29.886	29.74
9	5.247	2.332	-8.54E-07	1.147	29.667	29.521
10	3.777	1.63	-1.96E-06	0.848	29.368	29.237

**Table 40.** Residual and absolute heat capacity for set 2

Isochore	$P'$ (MPa)	$\rho^*$ (kmol/m <sup>3</sup> )	$(d^2P/dT^2) \cdot \rho^{-2}$ (MPa · m <sup>6</sup> /K <sup>2</sup> · kmol <sup>2</sup> )	$C_v^r$	$C_v$ (kJ/kmol-K)	$C_v^{(GERG)}$ <i>EoS</i>
T = 310 K						
2	141.875	22.664	-1.00E-06	4.654	33.612	34.203
3	110.777	21.267	-7.76E-07	4.26	33.218	33.585
4	79.253	19.333	-6.31E-07	3.847	32.806	32.879
7	12.645	5.897	-8.43E-07	2.193	31.151	30.891
8	6.701	2.91	-1.02E-06	1.32	30.278	30.083
9	5.477	2.332	-8.49E-07	1.099	30.057	29.883
10	3.929	1.63	-1.90E-06	0.804	29.763	29.622
T = 320 K						
2	149.998	22.664	-9.95E-07	4.689	34.111	34.626
3	117.681	21.267	-7.77E-07	4.288	33.71	34.011
4	84.729	19.333	-5.99E-07	3.868	33.291	33.302
7	13.35	5.897	-8.38E-07	2.211	31.633	31.212
8	6.995	2.91	-9.74E-07	1.332	30.755	30.465
9	5.704	2.332	-8.46E-07	1.11	30.532	30.28
10	4.076	1.63	-1.85E-06	0.812	30.235	30.039
T = 330 K						
2	158.073	22.664	-9.88E-07	4.724	34.634	35.073
3	124.567	21.267	-7.76E-07	4.316	34.225	34.462
4	90.19	19.333	-5.71E-07	3.89	33.799	33.752
7	14.056	5.897	-8.32E-07	2.232	32.142	31.577
8	7.288	2.91	-9.33E-07	1.347	31.257	30.881
9	5.931	2.332	-8.42E-07	1.122	31.032	30.71
10	4.208	1.63	-1.81E-06	0.822	30.731	30.486
T = 340 K						
2	166.119	22.664	-9.79E-07	4.76	35.178	35.543
3	131.394	21.267	-7.74E-07	4.344	34.762	34.935
4	95.626	19.333	-5.47E-07	3.911	34.33	34.225
7	14.756	5.897	-8.27E-07	2.256	32.674	31.981
8	7.58	2.91	-8.93E-07	1.363	31.782	31.327
9	6.157	2.332	-8.39E-07	1.136	31.555	31.167
10	4.381	1.63	-1.78E-06	0.832	31.251	30.959



**Table 40. Continued**

Isochore	$P'$ (MPa)	$\rho^*$ (kmol/m <sup>3</sup> )	$(d^2P/dT^2) \cdot \rho^{-2}$ (MPa · m <sup>6</sup> /K <sup>2</sup> · kmol <sup>2</sup> )	$C_v^r$	$C_v$ (kJ/kmol-K)	$C_v^{(GERG)}$ <i>EoS</i> )
T = 350 K						
2	174.109	22.664	-9.71E-07	4.795	35.742	36.033
3	138.193	21.267	-7.71E-07	4.372	35.319	35.429
4	101.041	19.333	-5.25E-07	3.933	34.88	34.719
7	15.446	5.897	-8.21E-07	2.28	33.227	32.417
8	7.871	2.91	-8.54E-07	1.381	32.328	31.8
9	6.383	2.332	-8.36E-07	1.151	32.098	31.651
10	4.534	1.63	-1.75E-06	0.843	31.79	31.455
T = 360 K						
2	182.052	22.664	-9.63E-07	4.831	36.324	36.541
3	144.973	21.267	-7.68E-07	4.401	35.894	35.941
4	106.435	19.333	-5.05E-07	3.956	35.449	35.232
7	16.127	5.897	-8.16E-07	2.306	33.799	32.882
8	8.131	2.91	-8.17E-07	1.399	32.892	32.297
9	6.609	2.332	-8.33E-07	1.166	32.659	32.156
10	4.685	1.63	-1.72E-06	0.855	32.348	31.972
T = 370 K						
2	189.943	22.664	-9.55E-07	4.867	36.922	37.065
3	151.746	21.267	-7.64E-07	4.43	36.485	36.47
4	111.816	19.333	-4.88E-07	3.979	36.034	35.762
7	16.815	5.897	-8.11E-07	2.333	34.388	33.372
8	8.455	2.91	-7.82E-07	1.417	33.472	32.815
9	6.833	2.332	-8.30E-07	1.182	33.237	32.682
10	4.828	1.63	-1.70E-06	0.867	32.922	32.508
T = 380 K						
2	197.792	22.664	-9.46E-07	5.481	38.112	37.604
3	158.47	21.267	-7.60E-07	5.059	37.69	37.012
4	117.171	19.333	-4.72E-07	4.551	37.182	36.307
7	17.498	5.897	-8.06E-07	1.862	34.492	33.884
8	8.744	2.91	-7.48E-07	1.038	33.669	33.351
9	7.058	2.332	-8.28E-07	0.853	33.484	33.225

**Table 40.** Continued

Isochore	$P'$	$\rho^*$	$(d^2P/dT^2) \cdot \rho^{-2}$	$C_v^r$	$C_v$	$C_v^{(GERG)}$
	(MPa)	(kmol/m <sup>3</sup> )	(MPa·m <sup>6</sup> /K <sup>2</sup> ·kmol <sup>2</sup> )		(kJ/kmol-K)	<i>EoS</i> )
T = 390 K						
2	205.593	22.664	-9.38E-07	5.481	38.7	38.155
3	165.166	21.267	-7.56E-07	5.059	38.278	37.568
4	122.508	19.333	-4.58E-07	4.551	37.77	36.864
7	18.18	5.897	-8.01E-07	1.862	35.08	34.415
8	9.033	2.91	-7.15E-07	1.038	34.257	33.904
9	7.282	2.332	-8.25E-07	0.853	34.072	33.784

**Table 41.** Residual and absolute heat capacity for set 3

Isochore	$P'$	$\rho^*$	$(d^2P/dT^2) \cdot \rho^{-2}$	$C_v^r$	$C_v$	$C_v^{(GERG)}$
	(MPa)	(kmol/m <sup>3</sup> )	(MPa·m <sup>6</sup> /K <sup>2</sup> ·kmol <sup>2</sup> )		(kJ/kmol-K)	<i>EoS</i> )
T = 400 K						
3	171.827	21.267	-7.51E-07	5.51	39.328	38.134
4	127.83	19.333	-4.45E-07	5.036	38.853	37.434
7	18.857	5.897	-7.96E-07	1.868	35.685	34.963
8	9.321	2.91	-6.84E-07	0.99	34.808	34.47
9	7.505	2.332	-8.39E-07	0.806	34.623	34.355
T = 410 K						
3	178.322	21.267	-7.47E-07	5.579	40.004	38.71
4	133.144	19.333	-4.34E-07	5.098	39.523	38.012
7	19.542	5.897	-7.91E-07	1.862	36.287	35.523
8	9.564	2.91	-6.53E-07	0.982	35.407	35.048
9	7.728	2.332	-8.20E-07	0.798	35.223	34.938
T = 420 K						
3	184.939	21.267	-7.42E-07	5.636	40.676	39.294
4	138.429	19.333	-4.23E-07	5.149	40.19	38.6
7	20.223	5.897	-7.86E-07	1.874	36.915	36.096
8	9.895	2.91	-6.24E-07	0.987	36.028	35.636
9	7.951	2.332	-8.17E-07	0.802	35.843	35.531

**Table 41. Continued**

Isochore	$P'$ (MPa)	$\rho^*$ (kmol/m <sup>3</sup> )	$(d^2P/dT^2) \cdot \rho^{-2}$ (MPa · m <sup>6</sup> /K <sup>2</sup> · kmol <sup>2</sup> )	$C_v^r$	$C_v$ (kJ/kmol-K)	$C_v^{(GERG)}$ <i>EoS</i> )
T = 430 K						
3	191.487	21.267	-7.37E-07	1.924	37.587	39.885
4	143.714	19.333	-4.13E-07	1.453	37.115	39.193
8	10.182	2.91	-5.96E-07	1.203	36.866	36.232
9	8.175	2.332	-8.15E-07	1.028	36.69	36.132
T = 440 K						
3	198.062	21.267	-7.32E-07	1.756	38.046	40.481
4	148.974	19.333	-4.04E-07	1.28	37.57	39.793
8	10.468	2.91	-5.69E-07	1.22	37.51	36.836
9	8.396	2.332	-8.12E-07	1.045	37.334	36.739
T = 450 K						
3	204.556	21.267	-7.27E-07	1.594	38.514	41.081
4	154.205	19.333	-3.96E-07	1.113	38.034	40.397
8	10.754	2.91	-5.43E-07	1.237	38.158	37.446
9	8.618	2.332	-8.10E-07	1.061	37.981	37.352

## APPENDIX I. INTEGRAND FUNCTION OF NUMERICAL DERIVATIVES

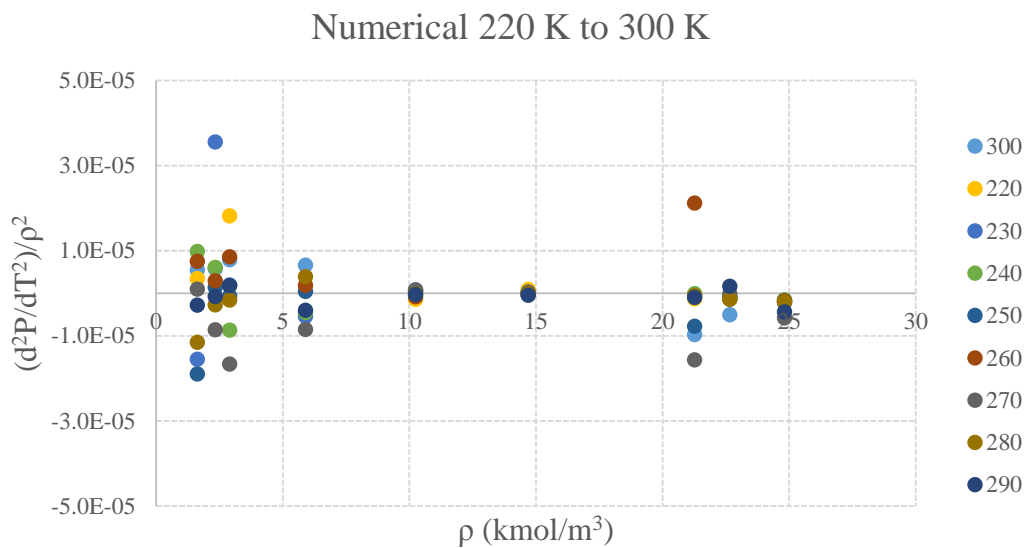


**Figure 55.** Integrand function of Eq. 34 for subset 1 using numerical derivatives

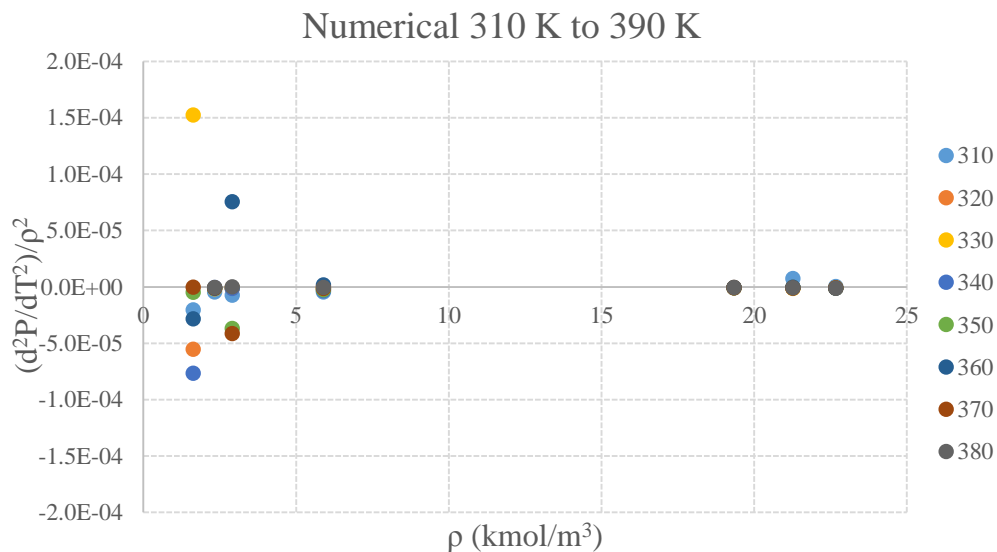


**Figure 56.** Integrand function of Eq. 34 for subset 2 using numerical derivatives

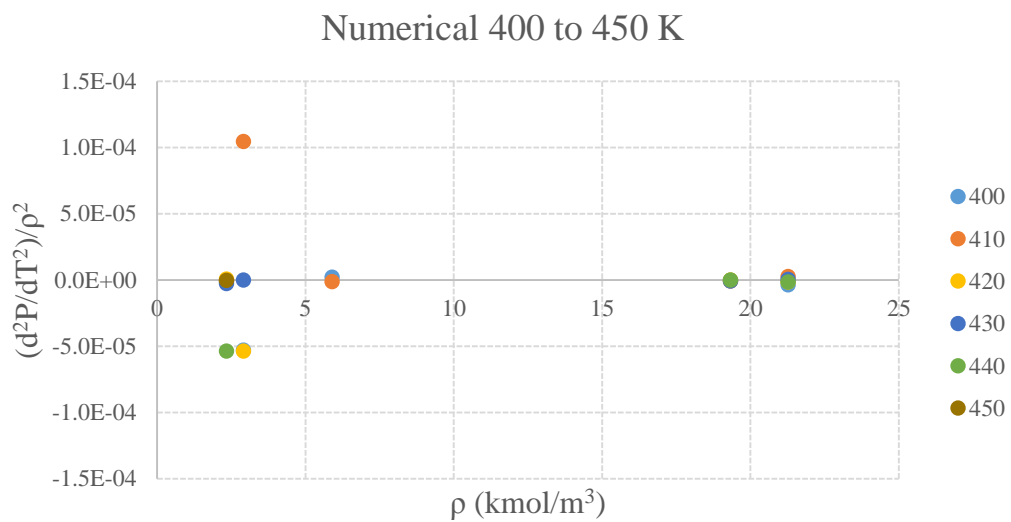


**Figure 57.** Integrand function of Eq. 34 for subset 3 using numerical derivatives

## APPENDIX J. MATLAB CODE

Code for fitting truly isochoric data and determining numerical and analytical derivatives. Example (Isochore 3):

```
function ISO31
clc
clear
format long
x_all=[];
residual_all=[];
ppredicted_all=[];
s_all = []
devCoef_all=[]
first_derivative=[];
second_derivative=[];
dp_all = [];
dpp_all = [];
dev_all = [];

% p = xlsread('isochore.xlsx', 3, 'L6:L37')
Y = xlsread('isochore.xlsx', 3, 'F6:F37')
p = xlsread('isochore.xlsx', 3, 'AJ6:AJ30')
T = xlsread('isochore.xlsx', 3, 'AI6:AI30')
h = xlsread('isochore.xlsx', 3, 'S6:S34')
w = xlsread('isochore.xlsx', 3, 'P6:P35')

%numerical derivatives
%w number of data for numerical derivatives

n = size (w)

for i = 2:(n(1)-1)

    c = w(i);
    a = w(i+1);
    b = w(i-1);
    l = h(i);

    di = ((a)-(b))./(2.*l);
    dii = ((a)-2.*(c)+(b))/(l.^(2));

    first_derivative=[first_derivative;di];
    second_derivative=[second_derivative;dii];
```

```

end

x0 = [1,1,1,1,1,1];    % Starting guess at the solution

options=optimset('TolFun',1E-20,'TolX',1E-
20,'MaxFunEvals',40000,'MaxIter',40000,'Algorithm','levenberg-
marquardt' );

[x,resnorm,residual] =
lsqnonlin(@functiongoal,x0,[],[],options,p,T);
% Invoke optimizer

hold on
plot(T, residual,'or')
ppredicted = (x(1)+x(2).*T+x(3).*T.^2)./(x(4)+x(5).*T+x(6).*T.^2)
dp = (((-x(1)-x(2).*Y-
x(3).*Y.^2).*x(5)+2.*x(6).*Y))+(x(4)+x(5).*Y+x(6).*Y.^2).*x(2)
+2.*x(3).*Y))./(x(4)+x(5).*Y+x(6).*Y.^2).^2);
dpp = (((x(4)+x(5).*Y+x(6).*Y.^2).^2).*x(6).*(-x(1)-x(2).*Y-
x(3).*Y.^2)+2.*x(3).*x(4)+x(5).*Y+x(6).*Y.^2))-
((2.*x(5)+2.*x(6).*Y).*x(4)+x(5).*Y+x(6).*Y.^2)).*((x(5)+2.*x(6)
).*Y).*(-x(1)-x(2).*Y-
x(3).*Y.^2)+(x(4)+x(5).*Y+x(6).*Y.^2).*x(2)+2.*x(3).*Y)))./(x(
4)+x(5).*Y+x(6).*Y.^2).^4);

dev_fit = ((p-ppredicted)./p).*100

% x_all is a a variable that save all the coefficients

x_all=[x_all;x];
residual_all=[residual_all;residual];
ppredicted_all = [ppredicted_all;ppredicted];
dp_all = [dp_all;dp];
dpp_all = [dpp_all;dpp];
dev_all = [dev_all,dev_fit];

disp('Coefficients values')
disp(x)
disp('Resnorm=')
disp(resnorm)

%Coefficients errors
n=size(p);
m=size(x0);

rms=sum((ppredicted-p).^2)./(n(1)-m(2));

% this derivative changes with the form of the fit

```

```

dX=[ 1./(x(4)+x(5).*T+x(6).*T.^2), T./(x(4)+x(5).*T+x(6).*T.^2),
T.^2./(x(4)+x(5).*T+x(6).*T.^2), (-x(1)-x(2).*T-
x(3).*T.^2)./(x(4)^2), (-x(1)-x(2).*T-
x(3).*T.^2)./(T.*(x(5)^2)), (-x(1)-x(2).*T-
x(3).*T.^2)./(T.^2.*(x(6)^2))];

```

```

%Matrix A
for k=1:m(2)
    for ii=1:n(1)
        A(ii,k)=dX(ii,k);
        At(k,ii)=dX(ii,k);
    end
end

E=(At*A).^(-1);

for k=1:m(2)
    s(k)=(rms*E(k,k)).^(1/2);
    devCoef(k)=(tinv(0.95,(n(1)-m(2))))*s(k);
end

s_all = [s_all;s];
devCoef_all=[devCoef_all;devCoef];

```

```
save ISO31
```

```

function f = functiongoal(x,p,T)
f = (p)-((x(1)+x(2).*T+x(3).*T.^2)./(x(4)+x(5).*T+x(6).*T.^2));

```

Code for determining residual and absolute heat capacity (Example: T = 280K)

```

function Temp280c
clc
clear
format long
x_all=[];
residual_all=[];
ypredicted_all=[];
integral_all=[];
s_all = []
devCoef_all=[]
Heatcapacity=[];
confidence=[];
P11=[];

```



```

P12=[];

y = xlsread('isotherm.xlsx', 7, 'K4:K12')
r = xlsread('isotherm.xlsx', 7, 'F4:F12')
T = xlsread('isotherm.xlsx', 7, 'C4:C12')

fitresults = fit(r,y,'poly2')
ci = confint(fitresults,0.95)
confidence=[confidence;ci];

p11= predint(fitresults,r,0.95,'observation','off');
p12= predint(fitresults,r,0.95,'function','on');
P11=[P11,p11];
P12=[P12,p12];

plot(fitresults,r,y),hold on, plot(r,p12);
x0 = [0,0,0]; % Starting guess at the solution

options=optimset('TolFun',1E-20,'TolX',1E-
20,'MaxFunEvals',40000,'MaxIter',40000,'Algorithm','levenberg-
marquardt' );

[x,resnorm,residual] =
lsqnonlin(@functiongoal,x0,[],[],options,y,r);
% Invoke optimizer

hold on
plot(r, residual,'or')
ypredicted = x(1).*r.^2+x(2).*r+x(3);
integral = x(3).*r+(x(2)/2).*r.^2+(x(1)/3).*r.^3

% x_all is a a variable that save all the coefficients

x_all=[x_all;x];
residual_all=[residual_all;residual];
ypredicted_all = [ypredicted_all;ypredicted];
integral_all = [integral_all;integral];

disp('Coefficients values')
disp(x)
disp('Resnorm=')
disp(resnorm)

%Cv residual calculation
n = size (T)

for i = 1:n(1)

```

```

Cv = T(i).*-1000.*integral(i);

Heatcapacity=[Heatcapacity;Cv];

end

%Coefficients errors
n=size(y);
m=size(x0);

rms=sum((ypredicted-y).^2)./(n(1)-m(2));

% this derivative changes with the form of the fit
dX=[r.^2, r, ones(n,1)];

%Matrix A
for k=1:m(2)
    for ii=1:n(1)
        A(ii,k)=dX(ii,k);
        At(k,ii)=dX(ii,k);
    end
end

E=(At*A).^(-1);

for k=1:m(2)
    s(k)=(rms*E(k,k)).^(1/2);
    devCoef(k)=(tinv(0.95,(n(1)-m(2))))*s(k);
end

s_all = [s_all;s];
devCoef_all=[devCoef_all;devCoef];

save Temp280c

function f = functiongoal(x,y,r)
f = (y)-(x(1).*r.^2+x(2).*r+x(3));

```